

### Abstract

A meridian scanning photometer was designed for investigating the time and space variations of auroral luminosity. With the aid of the quick-scan auroral photometer data of more than 300 clear night hours recorded at Syowa Station, Antarctica (geomagnetic lat. 69.6°S, long. 77.1°E), the following problems are studied: (1) space and time variation of auroral displays, (2) magnetic field variations associated with the space-time auroral displays, (3) relationships among auroras, magnetic field disturbance, magnetic pulsations, VLF hiss, VLF chorus and CNA during the course of substorms.

Various kinds of morphological evidence obtained through the above investigations show that a polar substorm consists of the breakup phase and the post-breakup phase. The breakup phase is characterized by a sudden intensification of auroral arc(s) or band(s) and a rapid poleward movement of the intensified aurora(s) with speed of about 1 km/s (Breakup type aurora). The post-breakup phase is defined as diffused auroras or rays which still remain after the intense breakup type aurora(s) have passed away polewards (Post-breakup type aurora). Generally, the post-breakup aurora(s) move towards the equator side.

A breakup type aurora is accompanied by a sharp pulsative geomagnetic disturbance (Breakup magnetic disturbance), while a post-breakup type aurora by a gradual negative bay-shape disturbance (Post-breakup magnetic disturbance). It seems that the sharp pulsative disturbance moves polewards together with the moving breakup aurora, while the gradual negative bay stays with the associated post-breakup aurora(s). Thus, the auroral electrojet can also be classified into AEJ-1, which is an intense and narrow electrojet moving together with the breakup aurora, and AEJ-2, which is a comparatively broad and weak electrojet associated with the post-breakup aurora(s). The auroral breakup phase is accompanied not only by a sharp pulsative geomagnetic disturbance but also by VLF hiss emissions, ULF emissions of PiB type and a sharp CNA phenomenon, while the post-breakup aurora is accompanied by a gradual geomagnetic bay, a gradual, weak CNA, VLF chorus emissions and ULF emissions of PiC type.

With reference to the space-time variations in auroras associated with geomagnetic perturbations at Syowa Station, an overall physical picture of dynamic auroral behaviors over the entire polar region is given, as a conclusion.

## 1. Introduction

The auroras may be described as visible glows of varying shape, size and color and their behaviors seem infinitely variable in their details, but there is nevertheless a certain regularity.

Up to the IGY-period, most of knowledge of the auroras was obtained from studies made with optical observations at many polar observatories throughout the world. HEPPNER (1954) has determined, on the basis of visual observations at College, Alaska, the diurnal pattern of the auroral and magnetic variations; namely, homogeneous or rayed arcs and positive magnetic disturbances in the evening hours, active auroral forms and large negative magnetic disturbances near midnight, and diffused or pulsating arcs or patches and negative magnetic disturbance in the morning hours. During the IGY-period, the picture of the entire sky observable from one station was photographed every minute by the all-sky camera equipment. Detailed morphological studies of auroras were carried out by DAVIS (1962) and AKASOFU (1964) using the all-sky camera records obtained at many stations distributed over the polar region. The present knowledge of the auroral displays has been greatly developed by their works. DAVIS has made the systematic studies of the auroral motions and the associated magnetic variations, while AKASOFU has established a world-wide pattern of auroral activity and the associated magnetic disturbance. This pattern has been called the auroral and magnetic substorm.

Syowa Station ( $69^{\circ}00'S$ ,  $39^{\circ}35'E$ ) is located at lat.  $69.6^{\circ}S$  and long.  $77.1^{\circ}E$  in the geomagnetic coordinates. Therefore, Syowa is one of the most suitable stations for the auroral observations. The observations for the upper atmosphere physics research in 1967-68 at Syowa covered the following items:

(a) Aurora: All-sky camera, auroral photometer for rapid variation of  $\lambda$  4278 Å, meridian scanning photometer (4278 Å), VHF auroral radar.

(b) Geomagnetism: 3-component flux-gate magnetometer, 3-component induction magnetometer, absolute magnetometer.

(c) Ionosphere: Vertical ionosonde ( $f=400\text{ kHz}\sim 15\text{ MHz}$ ), riometer ( $f=10, 20, 30, 50$  and  $70\text{ MHz}$ ).

(d) VLF emission: Narrow band intensity recorder ( $f=0.75, 1, 2, 4, 8, 12, 32, 64$  and  $128\text{ kHz}$ ), chorus recorder ( $f=0.2\sim 4\text{ kHz}$ ).

Based on the data of the systematic ground observations at Syowa Station,

the following problems will be specifically studied: (1) space and time variation of auroral displays, (2) magnetic field variations associated with the space-time auroral displays, (3) relationships among auroras, magnetic field disturbance, magnetic pulsations, VLF hiss, VLF chorus and cosmic noise absorption during the course of substorms. Finally, taking the various kinds of morphological evidence obtained through these investigations into consideration, the characteristics of the polar substorm are reexamined and discussed.

## 2. Auroral Photometry along the Geomagnetic Meridian

In the present study, the meridian time-diagram of auroral luminosity (auroral diagram) derived from the chart records of the meridian scanning photometer is adopted as the basic data of the auroral space-time variations. Outline of the geomagnetic meridian scanning photometer and a practical method of making the meridian time-diagrams of auroral luminosity are discussed in this section.

### 2.1. Outline of instrument

A meridian scanning photometer was designed for observing the time and space variations of the auroral luminosity ( $\lambda$  4278 Å) (Fig. 1). A rotating mirror scans from the north to the south along a geomagnetic meridian. The scanning time of this photometer is 12 sec and the field of view is  $5^\circ$  along the meridian. In the auroral zone, it is desirable to measure the auroral luminosity from 0.1 kR to a few tens of kR in 4278 Å line (about 40-50 dB). Therefore, signals of the auroral luminosity are amplified by high, medium and low gain amplifiers and are separately registered on a 3-channel pen-recorder.

Since the scanning photometer can measure the intensity of aurora which take place at least between zenith angle  $\chi=80^\circ$  towards the north and  $\chi=80^\circ$  towards the south along a geomagnetic meridian, the photometer can observe

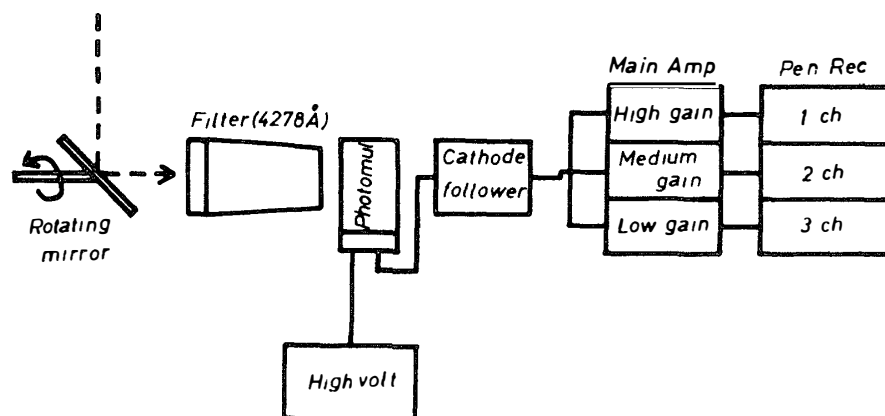


Fig. 1. Block diagram of the compositions of meridian scanning photometer

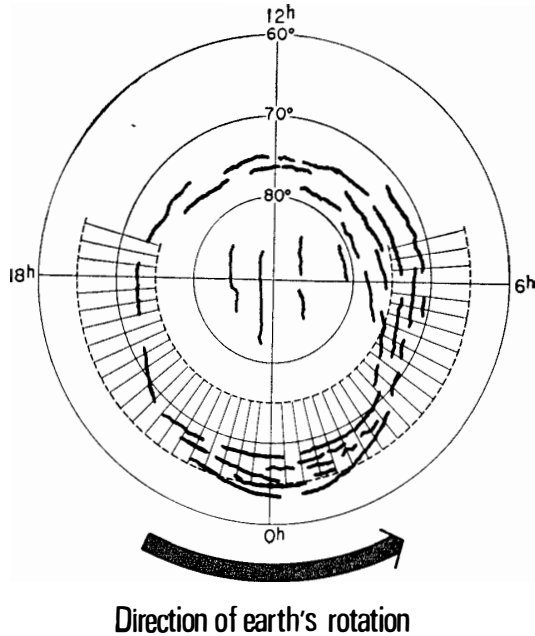


Fig. 2. Schematic illustration of the possible region in which the meridian scanning photometer, operating at Syowa Station ( $\Phi_m=69.6^\circ S$ ), can provide the data of the auroral occurrence. The geometry of the auroral oval under the moderately disturbed condition also is shown.

auroras occurring between  $\pm\Delta\varphi$  in latitude width from the observing point, where  $\Delta\varphi=80^\circ-\arcsin\left(0.985\frac{R}{R+h}\right)$  with  $R$ =earth's radius and  $h$ =average height of auroral emission. If  $h$  is assumed to be 120 km,  $\Delta\varphi$  becomes  $4.8^\circ$ , whence the photometer can observe auroras from 520 km north to 520 km south. Since the geometry of the auroral oval in the night side is located approximately at geomag. lat.  $70^\circ$  with the latitude width of  $10^\circ$  under the moderately disturbed condition (AKASOFU, 1968), the meridian scanning photometer, operating at Syowa Station ( $\Phi_m\cong 70^\circ$ ), can provide practically a continuous time sequence of the distribution of auroral intensity in the night side auroral oval (Fig. 2).

## 2.2. Meridian-time diagram of auroral luminosity (auroral diagram)

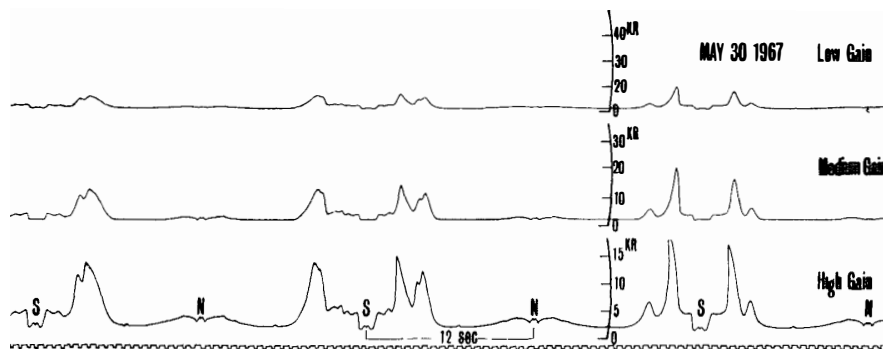


Fig. 3. Chart record obtained by the meridian scanning photometer. The square pulses at the bottom of the chart record indicate the zenith angle every ten degrees.

6 Constitution of Polar Substorm and Associated Phenomena in the Southern Polar Region

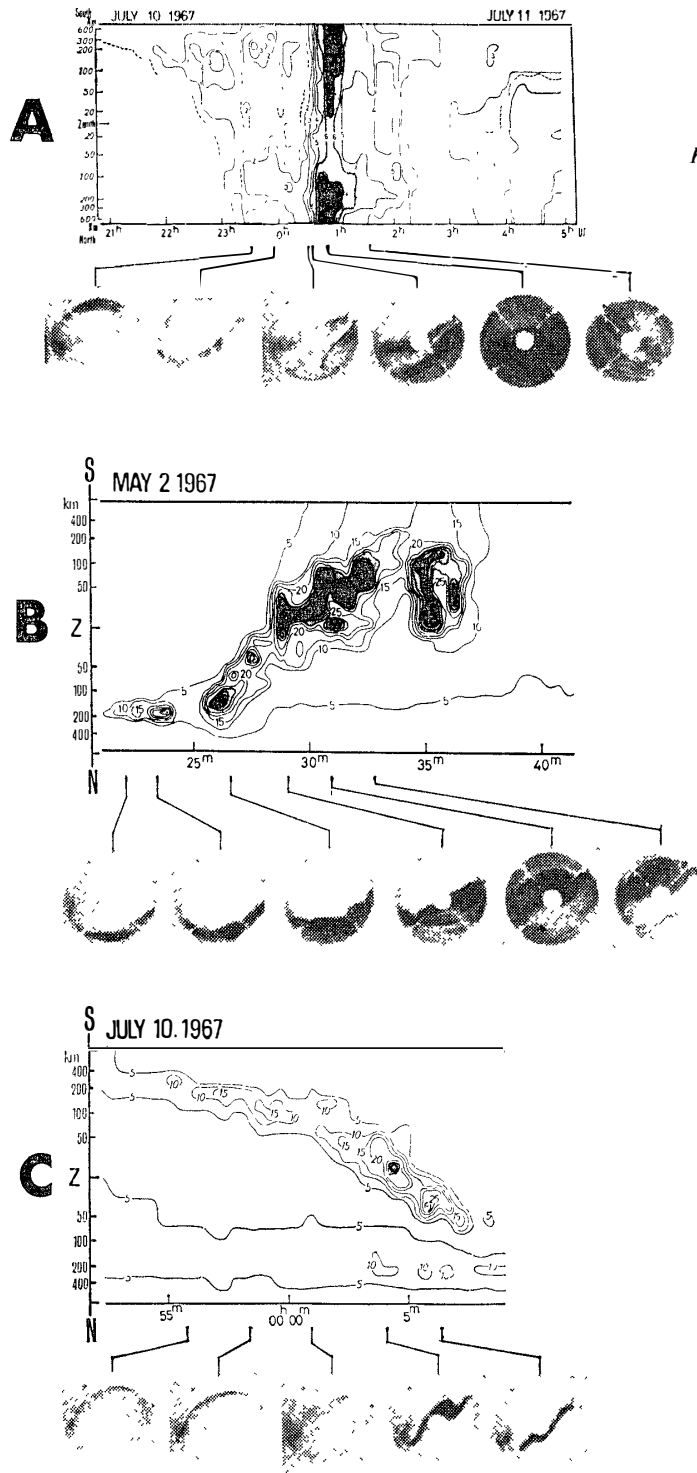


Fig. 4. The meridian-time diagrams of  $\lambda 4278\text{\AA}$  auroras (auroral diagrams) and simultaneous records of all-sky camera photographs of the auroras. The auroral diagram shown in the top (A) illustrates the gross characters of the auroral appearances through the night of July 10-11, 1967. But it is almost impossible to find out in the top figure the space-time variations of each auroral arc or band during the auroral substorm when auroras show very drastic changes in their luminosity and position. The auroral diagrams were drawn for the study of the characteristics in detail of the auroral dynamical display such as shown in the middle (B) and the bottom (C). The middle diagram shows the sudden brightening and the rapid poleward (southward in the southern hemisphere) movement of an auroral arc at the onset of an auroral substorm, and the bottom one illustrates the typical equatorward (northward) movements of the auroral arcs before the onset of the auroral substorm. The contours are  $1kR$  for the top and  $0.3kR$  for the middle and the bottom diagrams. Orientation of the all-sky camera photographs: top is the geomagnetic south (poleward) and bottom is the north (equatorward). Photographs are shown in negative.

Fig. 3 illustrates an example of the chart records obtained by the meridian scanning photometer. As mentioned above, signals of the auroral luminosity are separately registered on a pen-recorder with high, medium and low sensitivities. By this recording method, it is possible to make a reasonably accurate observation of the auroral luminosity in the intensity range from 0.1 kR to 10 kR.

In the chart record shown in Fig. 3, it is observed that the brightening of auroral arcs or bands occurred at the zenith angle ( $\chi$ ) of about  $75^\circ$  south from the observing point, and their luminosity changed very rapidly only for one minute. From these chart records of the scanning photometer, the meridian time-diagram of auroral luminosity can be derived. The intensity of auroral brightness is scaled for every  $9^\circ$  of the zenith angle (20 divisions from the south to north horizon). After arranging the scaled auroral intensities along a geomagnetic meridian (along the abscissa) as a function of time (along the ordinate), the iso-intensity contour lines of auroral brightness can be drawn. The diagrams, such as those shown in Fig. 4 for example, will be called the meridian-time diagram of auroral luminosity (auroral diagram). An important factor in this diagram is concerned with its high resolving power with respect to time, because the changes of auroral intensity and position are so rapid that even the scanning period of 12 sec becomes insufficient for some rapidly changing auroras.

### 3. Structure of Auroral Substorm

AKASOFU (1966) has pointed out that the first indication of the auroral substorm is a sudden brightening of the quiet arc lying in the midnight sector of the auroral oval. Within a few minutes after the onset of the auroral substorm, the rayed arcs suddenly become active and show rapid poleward motions; this phenomenon is a so-called "auroral breakup". After this activity, the auroras in the form of a diffused surface or rays still remain over the whole sky. This stage is often referred to the "post-breakup phase". The structure of an isolated

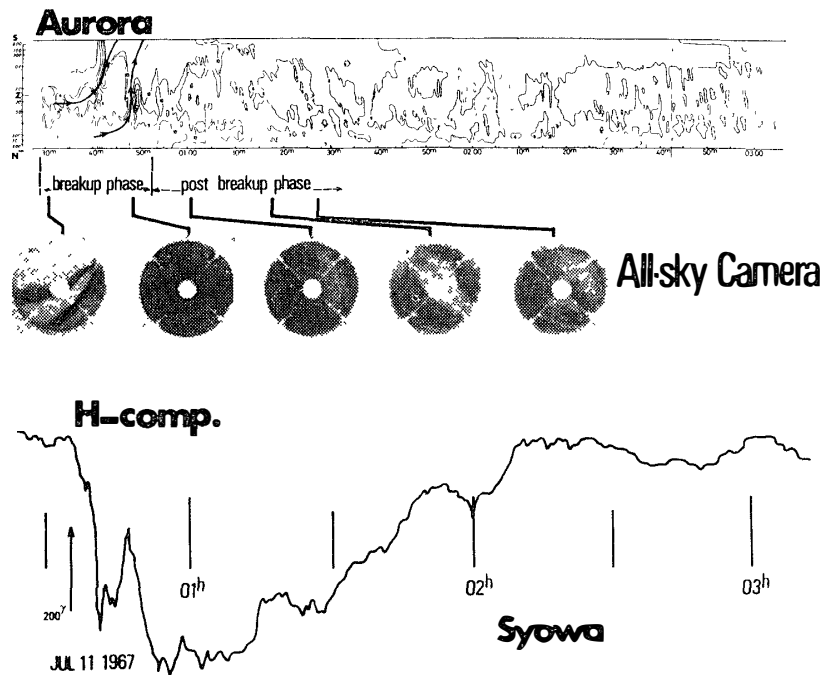


Fig. 5. The meridian time-diagram of  $\lambda 4278\text{\AA}$  aurora (top) during the auroral substorm on July 11, 1967 at Syowa Station. The simultaneous all-sky camera photographs (middle) and the magnetic H-component record (bottom) also are shown. In this example, the breakup phase of the auroral substorm would be from 00h30m to 00h52m and the post-breakup phase from 00h52m to about 03h00m. ●orientation of all-sky camera photographs: bottom is the geomagnetic north, and right is the west. Photographs are shown in negative. The contour in the auroral diagram is 1kR.

auroral substorm, recognized by the meridian-time diagram of auroral luminosity obtained at Syowa, is generally consistent with the view given by AKASOFU.

Fig. 5 shows the meridian-time diagram of auroral luminosity (top) together with the simultaneous all-sky camera photographs (middle) and magnetic record (bottom) during an auroral substorm observed on July 11, 1967 at Syowa Station. As seen in the auroral diagram, two arcs with the discrete structure showed sudden brightening at 00 h 30 m (UT)\* (see also all-sky camera photograph). After lying quiet and motionless for 10 min or so, the intense poleward side one of the two arcs began to move polewards at 00 h 40 m with the speed of about 1 km/s. The movement of this arc was accompanied by a sharp drop in the magnetic H-component. Thereafter, another discrete arc, lying quietly in the northern part (equator side) of the sky, suddenly began to move towards the pole at 00 h 46 m and within a few minutes after the beginning of its poleward

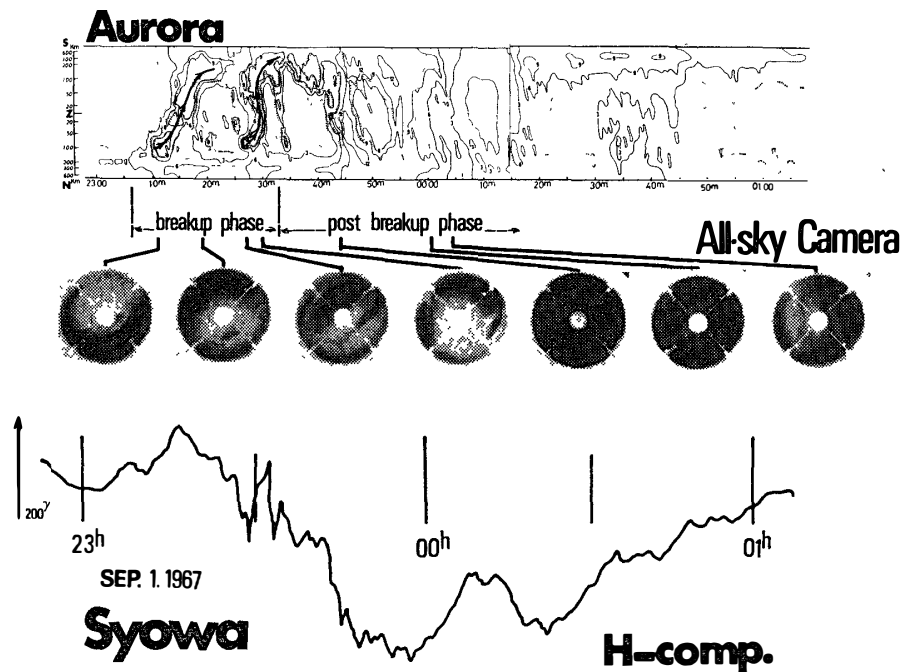


Fig. 6. The meridian-time diagram of  $\lambda 4278\text{\AA}$  auroras and simultaneous records of all-sky camera photographs of the auroras and the horizontal component of geomagnetic variation, observed at Syowa Station on September 1, 1967. In this example, the breakup phase of the auroral substorm would be from 23h06m to 23h33m and the post-breakup phase from 23h33m to about 01h00m. Orientation of all-sky camera photographs: bottom is the geomagnetic north and right is the west. Photographs are shown in negative. The contour in the auroral diagram is 1kR.

\* Universal time (UT) and Geomagnetic local time (Geomag. LT) are nearly the same at Syowa Station. Therefore, universal time (UT) is adopted in this paper.

movement, the active aurora spread and blanketed the whole sky of the observing station. At the same-time, a second sharp decrease was observable in the magnetic H-component. After these poleward travelings of the auroral arcs were over, the sky has been filled by comparatively weak auroras in the form of a diffused surface and rays. These non-discrete auroras were getting weaker and gradually moved equatorwards. The display lasted until 03 h 00 m. During this period, the magnetic H-component showed a gradual recovery.

The time-sequence of an auroral substorm illustrated in Fig. 6 is a similar example to that shown in Fig. 5. In this example, two rapid poleward travelings of the auroral arcs were observed successively at 23 h 10 m and 27 m on September 1, 1967. After the intense auroral arcs had passed away polewards, the auroras with strong brightness covered the whole sky and showed the movement towards the equator. This situation lasted for more than one hour and the auroral activities gradually diminished with time.

The above-mentioned characteristics of time sequence of an auroral substorm, illustrated in the typical examples of Figs. 5 and 6, are always the same for all auroral substorms which take place in the night sector. Namely, an auroral arc or band is suddenly intensified, and after 2 to 20 min the intense aurora moves polewards with an average speed of about 1 km/s. This phase of an auroral substorm may be called the breakup phase. The auroral activity which remains for a long time after the breakup phase and which moves equatorwards may be called the post-breakup phase of an auroral substorm. Frequently, poleward travelings of two or more auroral arcs or bands take place at the onset-time of an auroral substorm as shown in examples in Figs. 5 and 6.

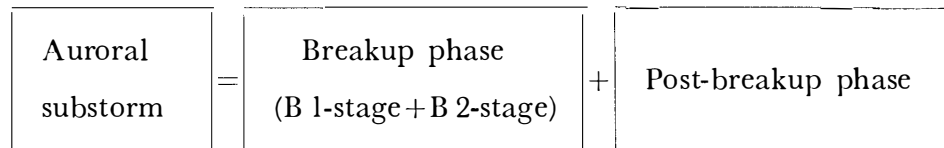
To continue the present study, it may be necessary to define the general characteristics of the breakup phase and post-breakup phase of an auroral substorm.

Breakup phase: An auroral arc or band with the discrete structure, lying quietly along the geomagnetic east-west direction, is suddenly intensified and 2-20 min later the auroral arc begins to move rapidly towards the pole with increasing brightness. The auroral arc or band which shows a rapid poleward traveling may be called the "breakup type aurora". The breakup type aurora can be divided into two stages: the pre-stage (B 1-stage) when the intensified aurora does not move along the geomagnetic meridian, and the main stage (B 2-stage) when the aurora moves polewards. In the period when one or more "breakup type auroras" are observable, the observing area is considered to be at "the breakup phase of an auroral substorm".

Post-breakup phase: Over the sky where a "breakup type aurora" has passed away polewards, the auroras in the forms of a diffused surface or rays still remain. These auroras generally move equatorwards with their activity diminishing with time. These auroras which show the equatorward movement may be called the "post-breakup type aurora". In the period when "post-breakup auroras" are observable, the observing area is considered to be at "the post-breakup phase of

an auroral substorm”.

According to the above definitions, the structure of an auroral substorm observed at a station in or near the auroral zone may be expressed by the following block diagram:



The distinct point in the above definition is that the breakup or post-breakup phase is not determined on the whole polar region, but is defined at each observing station or area. In other words, no auroral phenomena may be observable in some area when another area is subjected to the breakup phase of an auroral substorm; or some area has already entered the post-breakup phase while the breakup phase is still continuing in another area.

#### 4. Breakup Phase of Auroral Substorm

During the breakup phase of an auroral substorm, one or more intense auroral arcs exhibit rapid poleward movements. These poleward traveling arcs or bands are called the “breakup type aurora” in the present study. Some characteristics of the “breakup type aurora” and the associated magnetic variations are studied statistically, based on the auroral diagrams obtained at Syowa Station over a period of 300 h (most of them are given in JARE Sci. Rep., Series A, No. 8 by HIRASAWA and KAMINUMA, 1970).

##### 4.1. Characteristics of the breakup type aurora

Some characteristics of breakup type auroras are investigated through the statistical studies of 65 examples of the auroral substorms.

###### 4.1.1. Occurrence possibilities of breakup type aurora

As is shown in Fig. 7, the breakup type auroras are most frequently observed around midnight (from 23 h to 24 h Geomag. LT) at the typical auroral zone station, such as Syowa Station ( $\Phi_m=69.6^\circ$ ). It may also be noted that the occurrences of the breakup type auroras are less frequent in the morning than in the evening hours and no breakup auroras are observable after 02 h LT. This fact may indicate that the occurrences of the breakup type auroras are not symmetric with respect to the midnight sector, but are frequent along the evening side auroral oval.

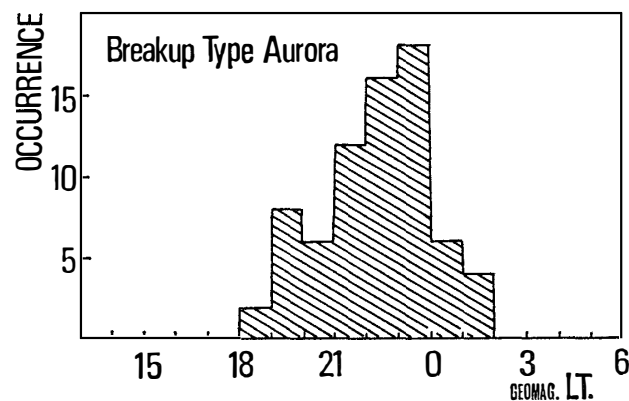


Fig. 7. Occurrence possibilities of the breakup type auroras at Syowa Station ( $\Phi_m=69.6^\circ S$ ).

#### 4.1.2. Duration of B1- and B2-stages of breakup type aurora

As is pointed out in the definition of the “breakup phase of an auroral substorm” (Section 3), the breakup type aurora can be divided into two stages, that is, the pre-stage (B1-stage) when the intensified auroral arc does not move and the main stage (B2-stage) when the aurora moves polewards. In the case of the breakup type auroral events shown in Fig. 5, the periods of B1- and B2-stages of the poleward side breakup aurora are from 00 h 30 m to 40 m and from 00 h 40 m to 46 m respectively, and those of the equatorward side one are from 00 h 31 m to 46 m and from 00 h 46 m to 52 m, respectively. Fig. 8 illustrates that the duration of the B1-stage (pre-stage) of the breakup auroras ranges from 2 min to 25 min, and that the duration time is shortest around midnight and the longest at the dusk side. These statistical results show that the breakup type aurora is intensified simultaneously along the auroral oval especially in the dusk side, and that its poleward movement begins from the midnight sector, and propagates mainly towards the dusk, reaching 18 h LT meridian about 25 min later.

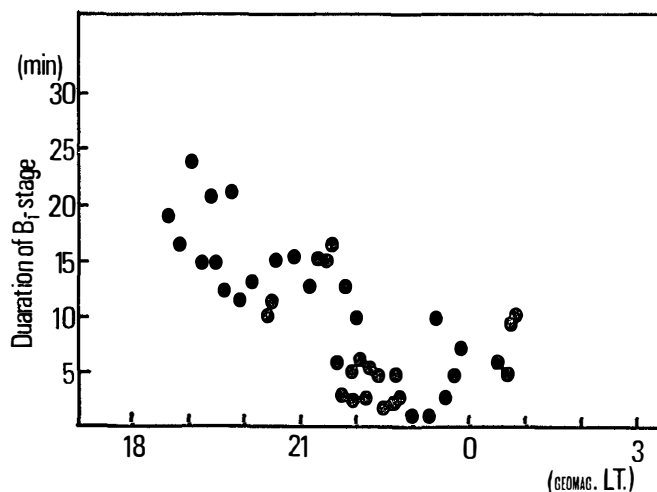


Fig. 8. Duration of B1-stage of the breakup type auroras, observed at Syowa Station.

It is practically impossible to get the exact duration of B2-stage (the poleward traveling stage) of the breakup type aurora, using data of a single observatory. When the breakup type aurora starts its poleward movement below the equatorward horizon or disappears out of the view of a observing point, we cannot find the beginning or the end time of B2-stage. However, as is mentioned before (Fig. 2), the meridian scanning photometer, operating at Syowa can cover practically most of the night side auroral oval under the moderate disturbed condition. Therefore, the duration time of B2-stage obtained at Syowa shown in Fig. 9 may not too much differ from the exact value. It would be concluded thus that the duration time of B2-stage with respect to the geomagnetic meridian ranges from 5 min to 30 min, the median value being about 10 min.

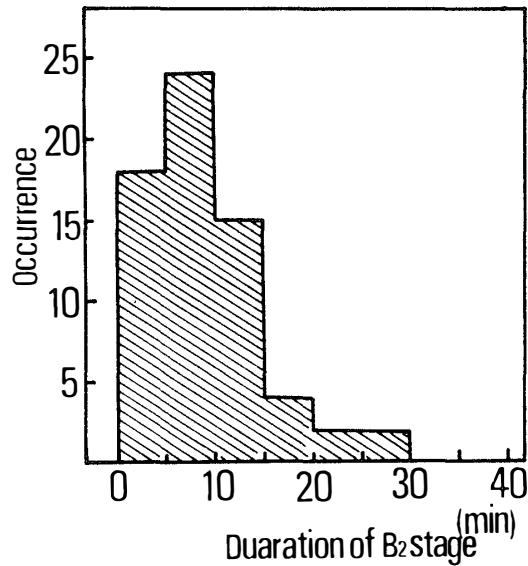


Fig. 9. Duration of B2-stage of the breakup type aurora, observed at Syowa Station.

4.1.3. Speed of poleward movement of the breakup type aurora

Breakup type auroras move towards the pole with a great speed during their B2-stage. The speed of the poleward motion is statistically investigated. As is shown in Fig. 10, the speed ranges mostly from 0.5 to 1.5 km/s, the median value being about 1.0 km/s.

A further discussion on the characteristics of the breakup type aurora is given in Section 8.2.

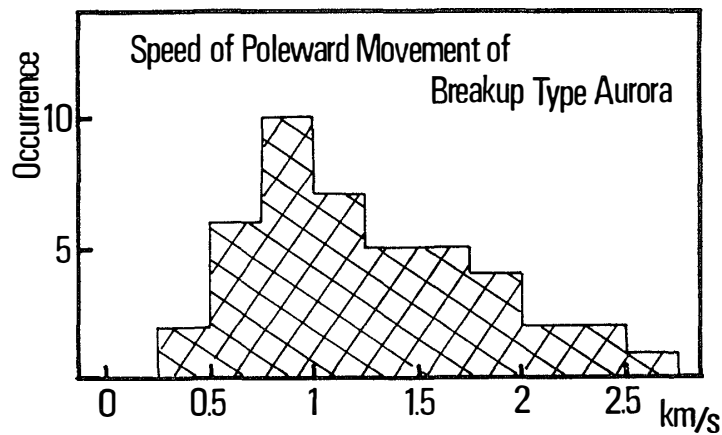


Fig 10 Histogram of the speed of poleward movement of the breakup type aurora, observed at Syowa Station,

#### 4.2. Magnetic variations associated with the breakup type aurora

The intense auroras are associated with a particular type of geomagnetic disturbances. These disturbances, generally referred to as magnetic substorms or geomagnetic bays, are confined to the region around the auroral breakup area. The general correlation in time and position of auroras and magnetic variations has been made by many research workers (HEPPNER, 1954; AKASOFU, 1960; DAVIS, 1962; OGUTI, 1963). An attempt will be made in this paper to find a more detailed correlation between the auroral space-time variations during the breakup type aurora events and the horizontal magnetic disturbances. The critical discussion of the electric current system which produces magnetic disturbances also will be given based on the analyzed results as well as the existing theories.

4.2.1. *Rotation of magnetic horizontal vectors associated with the poleward movement of breakup type aurora*

(a) Substorm on June 8, 1967

The meridian-time diagram of aurora shown in the middle of Fig. 11 illustrates that an auroral arc suddenly began to brighten near the zenith of Syowa Station at about 20 h 00 m on June 8, 1967 and was lying motionless along the

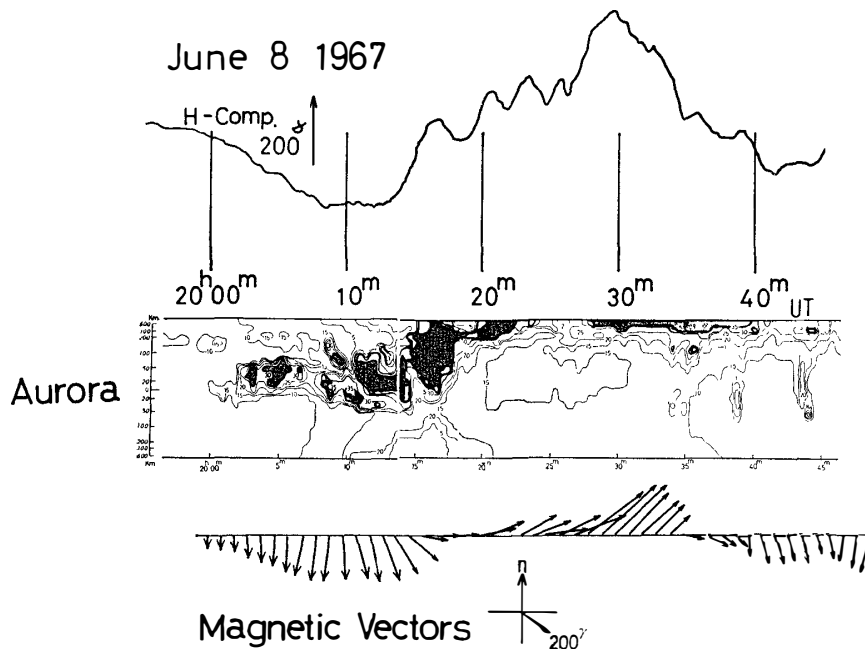


Fig. 11. Example of characteristics of the horizontal disturbing vectors during the magnetic substorm observed at Syowa Station on June 8, 1967 and the simultaneous meridian-time diagram of  $\lambda 4278\text{\AA}$  aurora. From top to bottom: (1) Horizontal component of the magnetogram. (2) Meridian-time diagram of  $\lambda 4278\text{\AA}$  aurora. Contour; "5" corresponds to 1.5kR. (3) Horizontal magnetic disturbance vectors.

geomagnetic meridian until 10 h 12 m (B1-stage of breakup type aurora). During this B1-stage, the geomagnetic H-component gradually decreased and the magnetic vectors were directed towards the south, indicating that the direction of the overhead current was westward. Thereafter, the arc began to show a rapid poleward movement with speed of about 1.2 km/s from 10 h 12 m. Geomagnetic horizontal vectors changed their direction and showed a counterclockwise rotation (south→east→north) in association with this poleward traveling of the intense arc. The arc passed away out of the view of Syowa Station at about 20 h 25 m. It is considered that another breakup type aurora took place around 20 h 27 m in the poleward side area about 600 km distant from Syowa Station. The simultaneous horizontal disturbance vectors moved toward the north and began to show a counterclockwise rotation. After the breakup phase of the auroral substorm was over around 20 h 40 m, the magnetic vectors returned to the initial stage and were directed to the south (westward overhead current).

(b) Substorm on May 2, 1967

The breakup type aurora illustrated in Fig. 12 is a similar example to that shown in Fig. 11. In this example of May 2, 1967, the period of the B1- and B2-stages of the breakup type aurora appear to be from 20 h 14 m to 26 m and

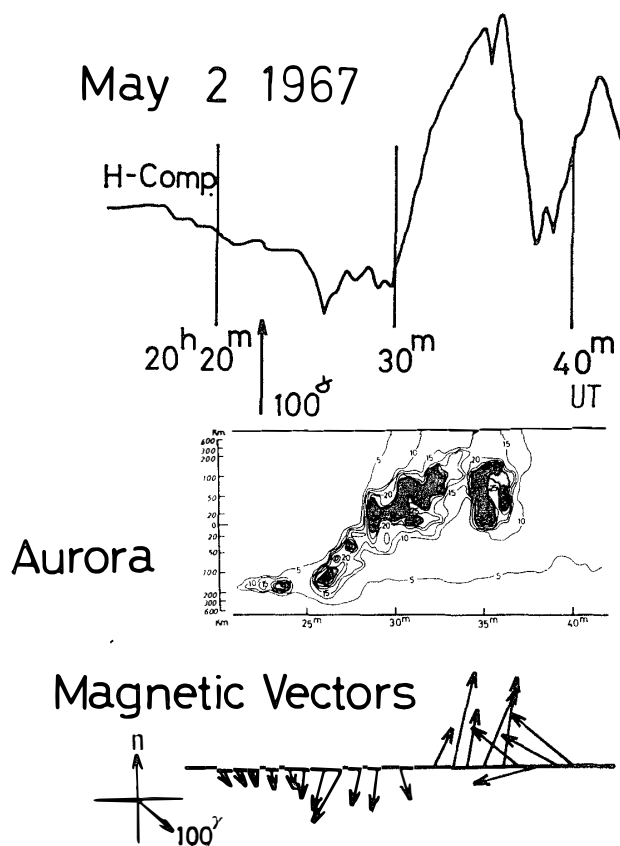


Fig. 12. Example of characteristics of the horizontal disturbing vectors during the magnetic substorm observed at Syowa Station on May 2, 1967, and the simultaneous meridian-time diagram of  $\lambda 4278\text{\AA}$  aurora. From top to bottom: (1) Horizontal component of the magnetogram. (2) Meridian-time diagram of  $\lambda 4278\text{\AA}$  aurora. Contour; "5" corresponds to 1.5kR. (3) Horizontal magnetic disturbance vectors.

from 20 h 26 m to 36 m, respectively. During the B1-stage, the magnetic horizontal vectors pointed towards the south (westward overhead current), while the magnitude of magnetic vectors increased and their direction rotated counterclockwise in association with the poleward movement of the breakup auroras during the B2-stage.

(c) Substorm on Sept. 29, 1967

In an example of the auroral substorm shown in Fig. 13, two breakup type auroras occurred successively at 21 h 30 m and 21 h 55 m during the breakup phase of the auroral substorm observed on Sept. 29, 1967. The periods of the B2-stages of each breakup aurora while the auroras moved rapidly towards the pole are approximately from 21 h 35 m to 39 m and from 21 h 55 m to 22 h 00 m, respectively. During the B2-stage, the horizontal disturbance vectors rotated counterclockwise with increasing magnitude in both cases.

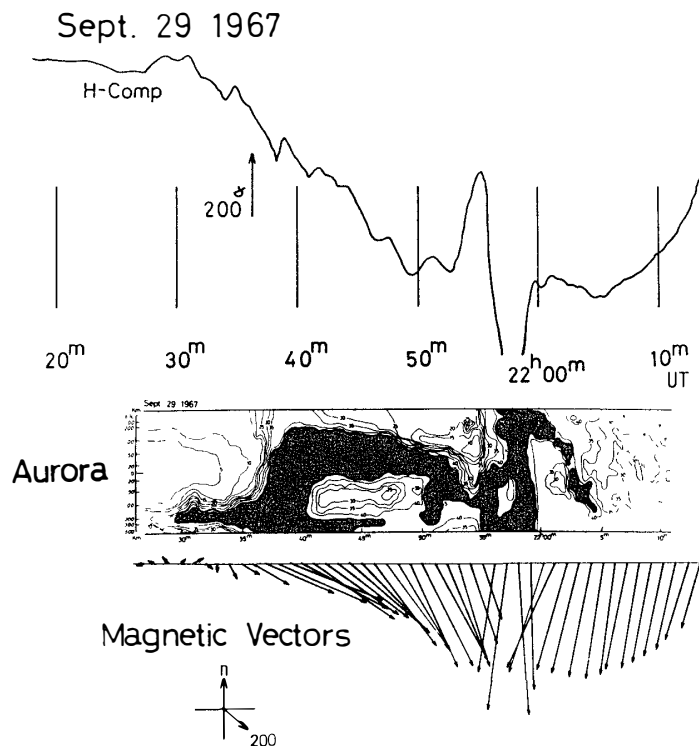


Fig. 13. Example of characteristics of the horizontal disturbing vectors during the magnetic substorm observed at Syowa Station on September 29, 1967 and the simultaneous meridian-time diagram of  $\lambda 4278\text{\AA}$  aurora. From top to bottom: (1) Horizontal component of the magnetogram. (2) Meridian-time diagram of  $\lambda 4278\text{\AA}$  aurora. Contour; "5" corresponds to 2.5kR. (3) Horizontal magnetic disturbance vectors.

## (d) Substorm on June 2, 1967

The horizontal disturbance vector (original vectors) changed its direction largely during the B2-stage (23 h 30 m–35 m on June 2, 1967 in Fig. 14) of the breakup type aurora observed around the midnight sector, but its rotation sense is rather obscure. The duration of B2-stage of this breakup type aurora is about 5 min (from 23 h 30 m to 35 m). Therefore, it may be natural to consider that the poleward expansion of the breakup type aurora had a larger effect on the short period component of the geomagnetic disturbance (less than 5 min in period) than on the longer period one. For the purpose of emphasizing this characteristic, changes of the horizontal geomagnetic disturbances are decomposed into the short period component (less than 5 min in period) and the longer period one (larger than 5 min in period) by the numerical filtering technique. As is shown in Fig. 14, the horizontal disturbance vector of the short period component (high frequency), which contains the larger effect of the breakup type aurora, rotates clockwise (north→east→south) during the B2-stage of breakup aurora, being similar to the examples shown in Figs. 11, 12 and 13.

On the other hand, the horizontal disturbing vector of the long period component (low frequency one) keeps its direction toward the south almost invariably, and the variation of its magnitude is consistent with the increase and decrease of the total auroral activities shown in the auroral diagram.

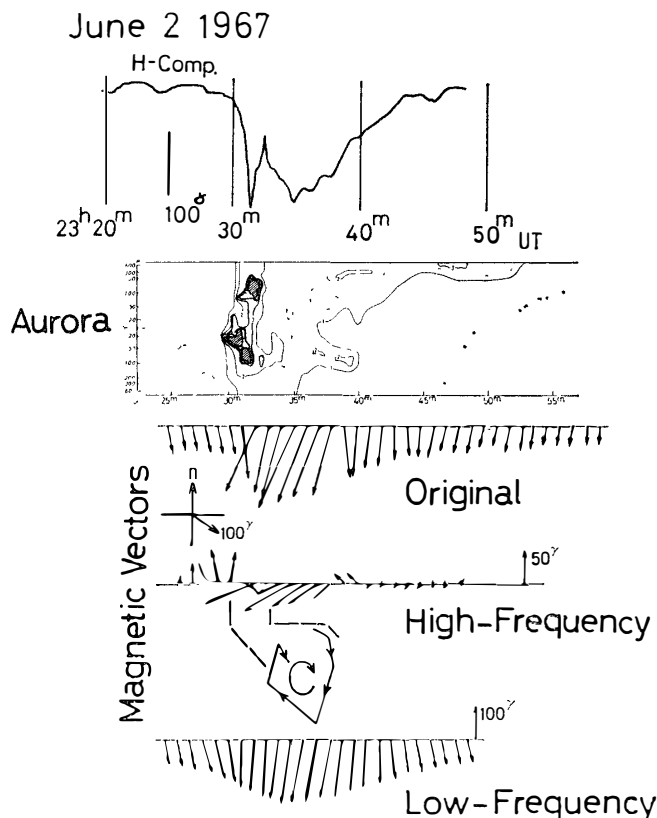


Fig. 14. Example of characteristics of the horizontal disturbing vectors during magnetic substorm observed at Syowa Station on June 2, 1967, and the simultaneous meridian-time diagram of  $\lambda 4278\text{\AA}$  aurora. From top to bottom: (1) Horizontal component of the original magnetogram. (2) Meridian-time diagram of  $\lambda 4278\text{\AA}$  aurora. Contour, "1" corresponds to 1kR. (3) Original horizontal disturbance vectors. (4) Horizontal disturbance vectors of the high frequency component (Period  $\leq 5\text{min}$ ). (5) Vector diagram of (4). (6) Horizontal disturbance vectors of the low frequency component (Period  $> 5\text{min}$ ).

(e) Substorm on May 25, 1967

The auroral diagram of Fig. 15 shows the auroral breakup occurred from the northward side (equatorward side) of Syowa Station. The breakup type aurora passed over the zenith of Syowa at 21 h 22 m and moved away polewards. This is a typical breakup type aurora event observed during the severe magnetic storm of May 25, 1967. The period of the B1-stage of this breakup aurora was from 21 h 04 m to 20 m, while the duration of B2-stage was about 10 min in the period from 21 h 20 m to 30 m. Therefore, changes of the horizontal geomagnetic disturbances are decomposed into the shorter period component

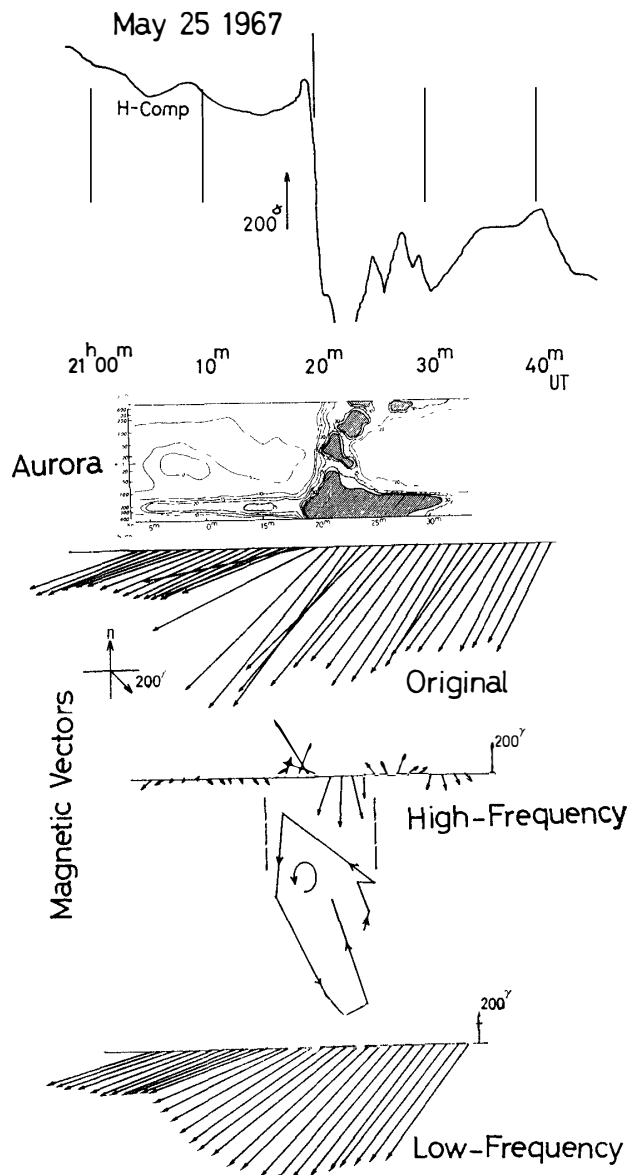


Fig. 15. Example of characteristics of the horizontal disturbing vectors during the magnetic substorm observed at Syowa Station on May 25, 1967, and the simultaneous meridian-time diagram of  $\lambda 4278\text{\AA}$  aurora. From top to bottom: (1) Horizontal component of the original magnetogram. (2) Meridian-time diagram of  $\lambda 4278\text{\AA}$  aurora. Contour; "5" corresponds to  $5kR$ . (3) Original horizontal disturbance vectors. (4) Horizontal disturbance vectors of the high frequency component (Period  $\leq 10\text{min}$ ). (5) Vector diagram of (4). (6) Horizontal disturbance vectors of the low frequency component (Period  $> 10\text{min}$ ).

(less 10 min in period) and the longer period component (longer than 10 min in period) by the same filtering technique as in the case of Fig. 14. As is clearly seen in Fig. 15, the horizontal magnetic vector of the short period component (high frequency) shows the clear counterclockwise rotation, being associated with a rapid poleward movement of the breakup type aurora. On the other hand, the horizontal disturbing vector of the longer period component (low frequency) keeps its direction approximately towards the invariant direction of the magnetic south through the B1- and B2-stages of the breakup auroras.

(f) Substorm on July 11, 1967

As shown in the auroral diagram in Fig. 16, two breakup type auroras

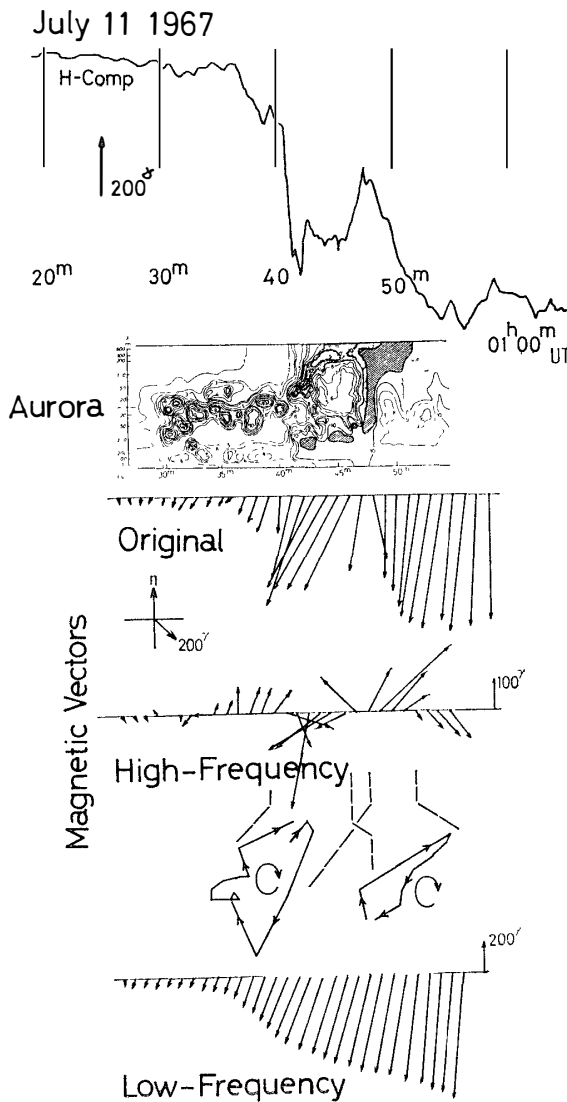


Fig. 16. Example of characteristics of the horizontal disturbing vectors during the magnetic substorm observed at Syowa Station on July 11, 1967, and the simultaneous meridian-time diagram of  $\lambda 4278\text{\AA}$  aurora. From top to bottom: (1) Horizontal component of the original magnetogram. (2) Meridian-time diagram of  $\lambda 4278\text{\AA}$  aurora. Contour, "1" corresponds to 1kR. (3) Original horizontal disturbance vectors. (4) Horizontal disturbance vectors of the high frequency component (Period  $\leq 5\text{min}$ ). (5) Vector diagram of (4). (6) Horizontal disturbance vectors of the low frequency component (Period  $> 5\text{min}$ ).

were suddenly intensified at about 00 h 30 m, and then the intense poleward side arc began to move polewards at about 00 h 40 m while the equatorward side one began to move also polewards at about 00 h 48 m. The duration of the B2-stage of the both breakup type auroras is about 5 min (from 00 h 40 m to 46 m for the poleward side arc and from 00 h 46 m to 52 m for the equatorward side one). It may be considered therefore that the short period component (less than 5 min in period) of the horizontal disturbing vector contains the effect of the auroral poleward movements to a greater extent than does the long period one (longer than 5 min in period). As is shown in Fig. 16, the

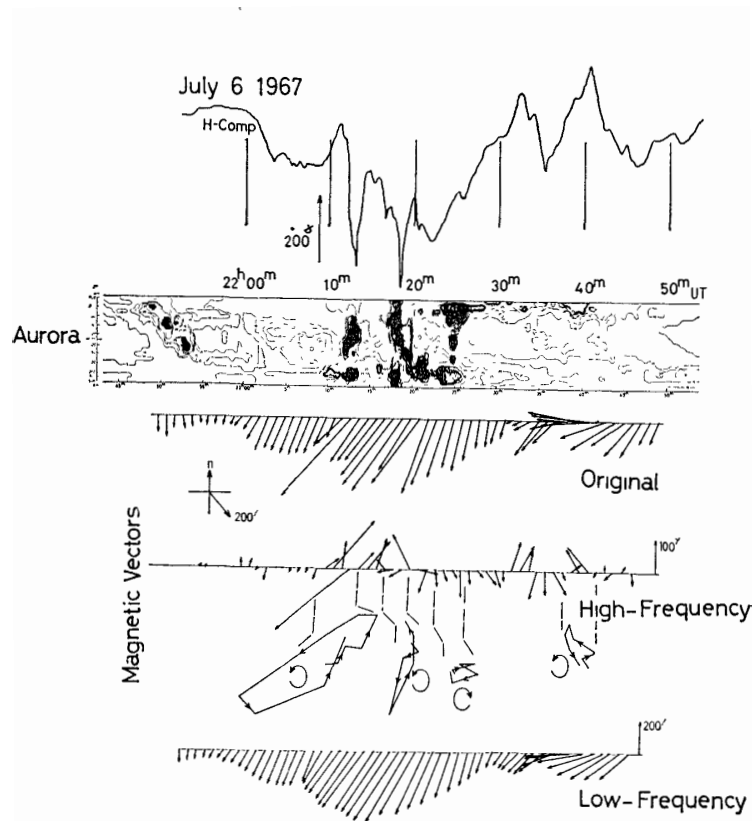


Fig. 17. Example of characteristics of the horizontal disturbing vectors during the magnetic substorm observed at Syowa Station on July 6, 1967, and the simultaneous meridian-time diagram of  $\lambda 4278\text{\AA}$  aurora. From top to bottom: (1) Horizontal component of the original magnetogram. (2) Meridian-time diagram of  $\lambda 4278\text{\AA}$  aurora. Contour; "5" corresponds to 1.5kR. (3) Original horizontal disturbance vectors. (4) Horizontal disturbance vectors of the high frequency component (Period  $\leq 5$ min). (5) Vector diagram of (4). (6) Horizontal disturbance vectors of the low frequency component (Period  $> 5$ min).

horizontal disturbance vector of the short period component rotates clockwise at the B2-stages of the both breakup type auroras, while that of the long period component keeps its direction (magnetic south) almost invariable.

(g) Substorm on July 6, 1967

The auroral diagram shown in Fig. 17 illustrates that four breakup type auroras took place successively during the breakup phase of an auroral substorm observed at Syowa Station on July 6, 1967. The first breakup aurora was observed in the period between 22 h 10 m and 14 m, the second one between 22 h 12 m and 20 m, the third one between 22 h 23 m and 26 m and the last one occurred at about 300–400 km pole side from Syowa Station in the period between 22 h 36 m and 41 m. The duration of all breakup type aurora was about 5 min or so. Therefore, for the purpose of investigating the effect on the magnetic disturbance of these breakup type auroras, the horizontal disturbance vector was decomposed into the shorter and the longer period components, and the rotation sense of the shorter period component, associated with the breakup auroras, was investigated. The rotation senses of the magnetic vector were counterclockwise for the first, second and last breakup type auroras, while its rotation sense is clockwise only for the third breakup one.

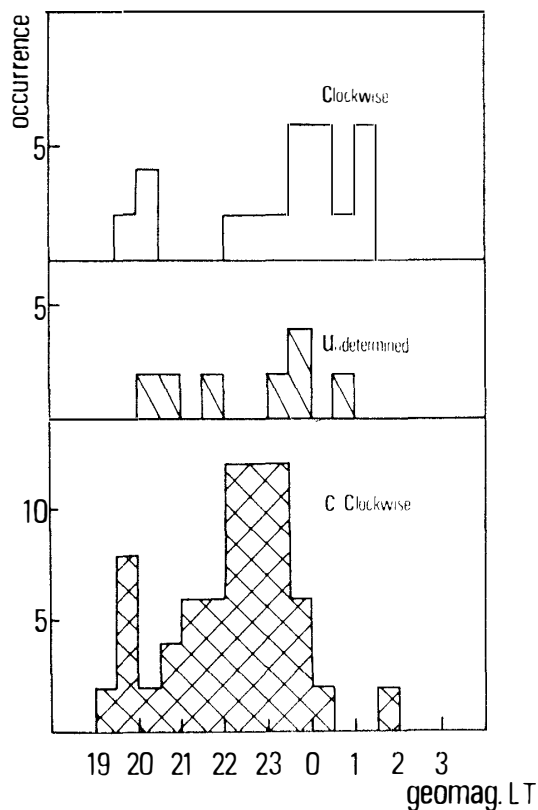


Fig. 18. Histogram showing the dependence of geomagnetic local time of clockwise and counterclockwise rotations of the magnetic horizontal disturbance vectors associated with the poleward movements of the breakup type auroras.

4.2.2. *Clockwise and counterclockwise rotations of magnetic horizontal disturbance vectors associated with poleward movements of breakup type auroras*

As has been illustrated in the examples from Fig. 11 to Fig. 17, the geomagnetic horizontal disturbing vector clearly shows the rotation with the increase of its magnitude when the breakup type aurora moves towards the pole (in the B2-stage of the breakup type aurora). Fig. 18 shows the histograms to represent the statistical dependence of the sense of rotation of the horizontal disturbance vector upon the geomagnetic local time. As seen in this figure, the counterclockwise rotation is clearly dominant in the dusk while the clockwise rotation is rather dominant in the dawn.

4.2.3. *Electric-current pattern associated with breakup type aurora*

The electric-current pattern which produces magnetic disturbances associated with auroras is called the “auroral electrojet (AEJ)”. Two kinds of basic electric-current patterns for AEJ have been postulated (FUKUSHIMA, 1971); the first is the ionospheric current pattern which has a westward current along the active auroras and its return current flow (two-dimensional current pattern) (CHAPMAN, 1935; VESTINE and CHAPMAN, 1938; SILSBEE and VESTINE, 1942; FUKUSHIMA, 1953). The second consists of the field-aligned current in the magnetosphere and of an east-west current segment in the ionosphere (three-dimensional current pattern) (BIRKELAND, 1908; ALFVÉN, 1939, 1940; ATKINSON, 1967; AKASOFU *et al.*, 1969). The schematic diagrams to show these two basic current patterns are given in Fig. 19, viewed from the south geomagnetic pole a few earth radii above the ionosphere.

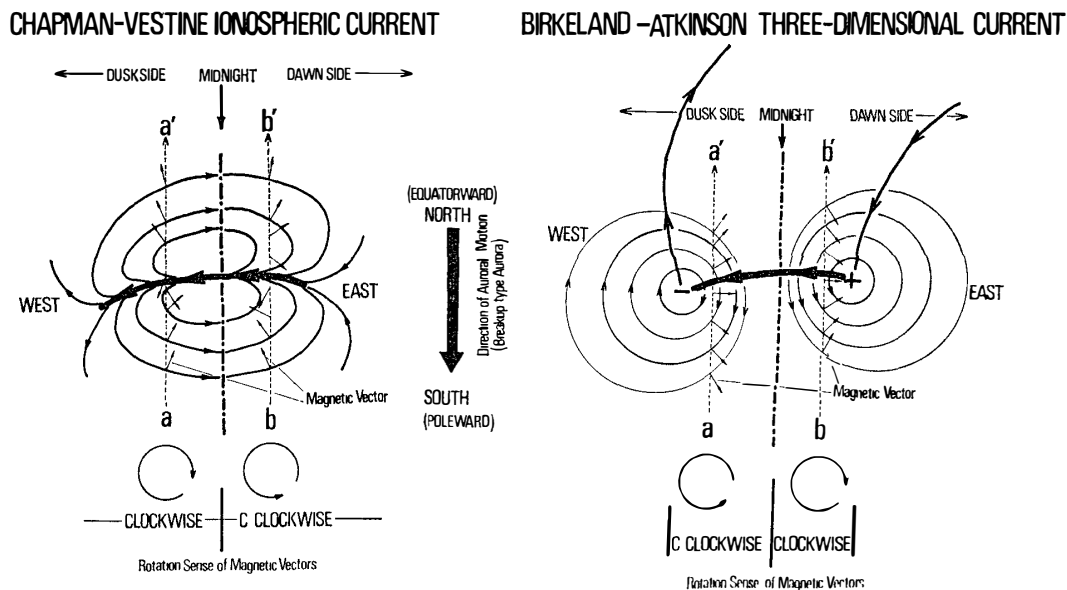


Fig. 19. Schematic illustration of the two-dimensional ionospheric current pattern (left) and the three-dimensional current pattern (right) for the auroral electrojet associated with the breakup type aurora.

It seems very likely that the rotation of the short period horizontal disturbance vectors are due to the poleward motion of the electrical current through the breakup type aurora. Now, an attempt will be made to examine which of the two basic current patterns is favorable for interpreting the observed rotation sense of the horizontal disturbance vectors (Fig. 18).

(a) Case of two-dimensional ionospheric current pattern (CHAPMAN-VESTINE ionospheric current)

It is assumed that the two-dimensional ionospheric current pattern, such as shown schematically on the left of Fig. 19, occurs in the midnight sector associated with the breakup type aurora and this current pattern moves toward the pole. In such a condition, the rotation sense of the magnetic horizontal vector is clockwise in the dusk and counterclockwise in the dawn side as is indicated in the figure. This tendency is inconsistent with the observed result in Fig. 18. Therefore, it is difficult for the current pattern of this type to stand consistently for the geomagnetic disturbances associated with the breakup type auroras.

(b) Case of the three-dimensional current pattern (BIRKELAND-ATKINSON three-dimensional current)

The right-hand side figure in Fig. 19 shows the three-dimensional current pattern which consists of the incoming and outgoing field aligned currents and the strong horizontal westward electrojet flowing through the breakup type aurora. It is assumed that the ionospheric Hall current predominates around the eastern (counterclockwise current flow surrounding the positive charge accumulation) and the western edge (clockwise current flow surrounding negative accumulation) of the breakup type aurora (ATKINSON, 1967). When the auroral electrojet of this type moves polewards and passes through the zenith of an observing point from the equator side to the pole side, a horizontal magnetic disturbance vector due to the ionospheric Hall current rotate counterclockwise between the middle and the western edge of the electrojet and clockwise between the middle and eastern edge of the electrojet. On the other hand, the horizontal magnetic disturbance on the ground caused by the ionospheric westward electrojet (Pedersen current) is always southwards throughout the period of the poleward motion of the electrojet, and it may contribute considerably to the steady southward magnetic disturbance of the long period component. Since the breakup type auroras appear mostly around 23 h in local time, the dusk side and dawn side may statistically be covered mostly by the western half and the eastern half respectively of the breakup type electrojet. Thus, the statistical characteristics of the dominant counterclockwise rotation in the dusk sector and the dominant clockwise rotation in the dawn sector of the short period horizontal magnetic disturbance vector can naturally be explained by the three-dimensional current pattern, such as schematically illustrated on the right-hand side of Fig. 19.

If the breakup type aurora is associated with the three-dimensional current flow and the ionospheric Hall current caused by the charge accumulation around

the eastern and western edge of the aurora is well dominant, what kinds of other phenomena could be expected? As is clearly seen in the right hand figure of Fig. 19, in the western half of the electrojet (dusk side), the magnetic vectors due to the Hall current point towards the magnetic north (H-component  $\rightarrow$  positive) on the equator side of the westward current flow along the aurora, while those on the pole side of the westward current flow point to the south (H-component  $\rightarrow$  negative). On the other hand, in the case of the two-dimensional current flow, the return current is symmetric with respect to the westward current jet. Therefore, the magnetic vectors have the northward direction (H-component  $\rightarrow$  positive) on the equator side as well as on the pole side of the westward electrojet (see the left hand figure of Fig. 19).

The auroral diagram in Fig. 20 A illustrates that auroras were brightening on the pole side of the station and began to increase in luminosity at 22 h 35 m on July 6, 1967. They showed the maximum at 22 h 39 m and were gradually restored to the former state. Associated with this auroral display, the geomagnetic horizontal intensity ( $\vec{H}$ ) began to increase at 22 h 35 m and attained the maximum value at 22 h 40 m. Similar correlations between the aurora and the geomagnetic field variations in the dusk side are shown in Fig. 20B and C.

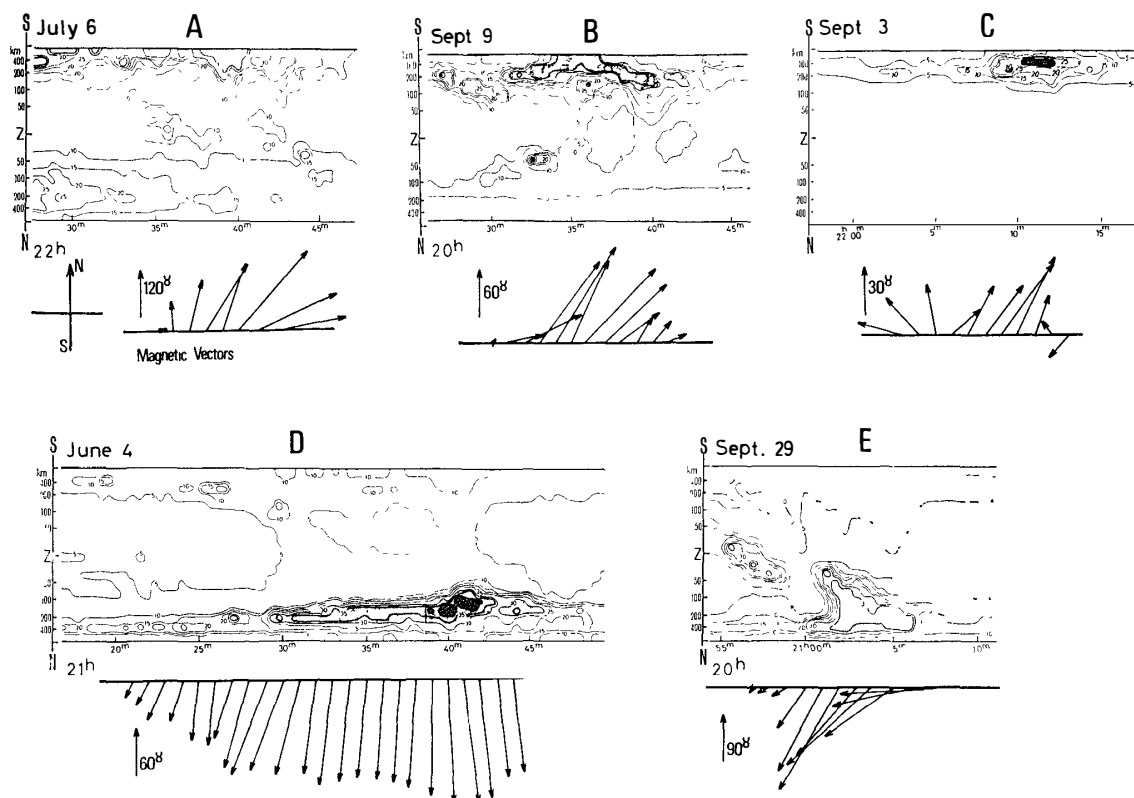


Fig. 20. Geomagnetic field variations associated with the poleward and the equatorward auroral brightening in the dusk hours.

We may conclude here that, when the breakup type aurora occurs in the dusk on the polar side of the observing station, the H-component value increases with a close correlation to the auroral activity.

On the other hand, when the auroras show brightening on the equator side of the observing station in the dusk, the H-value decreases with increasing activation of the aurora, as is illustrated in Fig. 20D and E.

Though the current flow patterns through the magnetosphere and the ionosphere during the breakup phase of a substorm would be, in fact, very complicated because of their superposition, mutual interference and space-time variation, it would be concluded based upon all the observed facts mentioned above that the basic current pattern associated with the breakup type auroras would be the three-dimensional current flow, such as shown in the right hand figure of Fig. 19.

### 5. Post-Breakup Phase of Auroral Substorm

During the post-breakup phase of an auroral substorm, the auroras in the form of a diffused surface or rays (post-breakup type auroras) still remain over the sky where “breakup type auroras” have passed away polewards. These auroras generally move equatorwards with their diminishing activity.

In the present section, the mutual relation between the “breakup” and “post-breakup type aurora” is examined based on the auroral and magnetic data obtained at Syowa Station and also on the simultaneous magnetograms from Mawson (73.1°S in geomag. lat., 102.9° in geomag. long.) and Plateau Station (77.2°S in geomag. lat., 52.5° in geomag. long.) which are located on the poleward side of Syowa (69.6°S in geomag. lat., 77.1° in geomag. long.) (Fig. 21). The magnetic variations during the post-breakup phase are also investigated in comparison with those during the breakup phase of an auroral substorm.

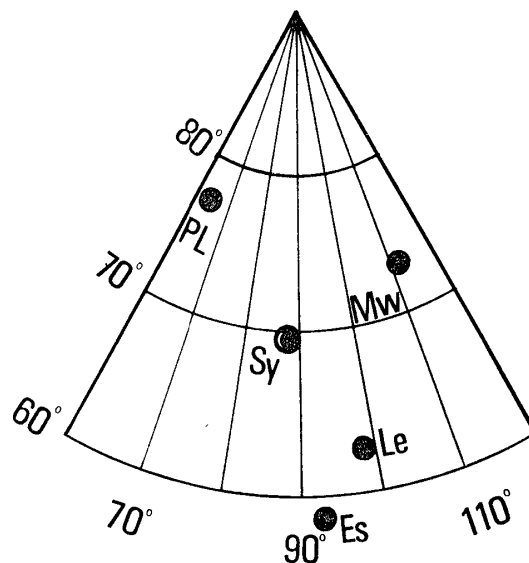


Fig. 21. Observatories whose magnetic and auroral data are used; Plateau (Pl), Mawson (Mw), Syowa (Sy), Lerwick (Le) and Eskdalemuir (Es).

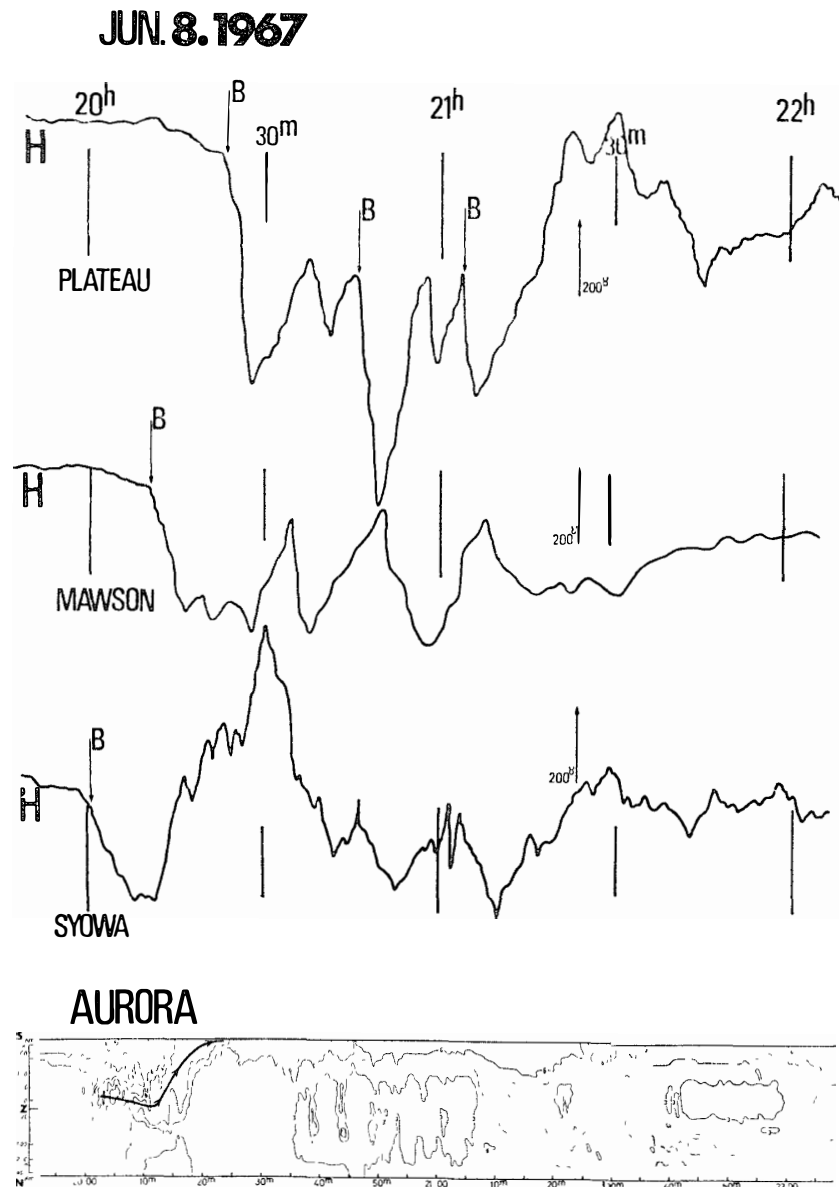


Fig. 22. Example of the poleward movement of the breakup type aurora and the associated magnetic variation on June 8, 1967. From top to bottom: (1) Horizontal component at Plateau Station (geomag. lat.  $77.2^{\circ}\text{S}$ , long.  $52.5^{\circ}$ ). (2) Horizontal component at Mawson (geomag. lat.  $73.1^{\circ}\text{S}$ , long.  $102.9^{\circ}$ ). (3) Horizontal component at Syowa Station (geomag. lat.  $69.6^{\circ}\text{S}$ , long.  $77.1^{\circ}$ ). (4) Meridian time diagram of  $\lambda 4278\text{\AA}$  aurora obtained at Syowa Station. Contour; "1" corresponds to 1kR.

## 5.1. Mutual relation between the breakup and the post-breakup type aurora

### 5.1.1. Substorm on June 8, 1967

In Fig. 22, simultaneous magnetograms (H-component) obtained at Mawson and Plateau Station, are shown together with the magnetogram and the meridian diagram of auroral luminosity obtained at Syowa Station. The auroral diagram shown in the bottom of Fig. 22 illustrates that a typical breakup type aurora was observed in the period from 20 h 00 m to 25 m of June 8, 1967. During this period, Syowa Station was in the breakup phase of the auroral substorm. This breakup type aurora began to move towards the pole around 20 h 10 m. The magnetic H-component at Mawson showed a sudden decrease around 20 h 12 m, being associated with the poleward movement of the breakup type aurora. The breakup phase at Mawson seems to begin about 10 min later than the beginning of the breakup phase at Syowa Station. This intense aurora traveled further towards pole at a high speed and disappeared from the view of Syowa around 20 h 25 m. At that time, the magnetogram at Plateau Station begins to show a sharp decrease in the H-component and Plateau Station seems to enter into the breakup phase of the auroral substorm about 25 min later than that of Syowa. As has been illustrated above, the area which is in the breakup phase of an auroral substorm rapidly moves towards the pole, associated with the poleward movement of the breakup type aurora.

The auroral diagram of Fig. 22 shows also that the sky was filled by the comparatively weak auroras after the poleward traveling auroral arc had disappeared from the view of Syowa. These auroras were getting weaker and gradually moved equatorwards. The display lasted for about 2 hours. This period is the post-breakup phase of an auroral substorm at Syowa.

When we investigated what would happen in the pole side during the post-breakup phase of Syowa, the magnetic variations of Plateau Station, which is located about 700 km poleward from Syowa, showed successive sudden drops in H-component, indicating that at least three breakups of auroras occurred successively at about 20 h 25 m, 20 h 50 m and 21 h 05 m. From this fact, it would be reasonably concluded that the post-breakup type auroras, which are produced by the successive breakup events in the higher latitudes, expand towards the equator and remain for a long period in the post-breakup phase in the lower latitudes.

### 5.1.2. Substorm on Sept. 1, 1967

The poleward movements of the breakup type auroras illustrated in Fig. 23, are similar to those shown in Fig. 22. As is seen in the auroral diagram in the bottom of Fig. 23, the two rapid poleward travelings of the auroral arcs were observed successively at 23 h 10 m and 27 m. The first breakup type aurora disappeared around 23 h 20 m within the view of Syowa Station, while the second one moved further toward the pole and caused a sudden decrease of magnetic H-component (the onset of substorm) around 23 h 37 m at Mawson and around 23 h 43 m at Plateau Station about 16 min later than that of Syowa.

After the breakup type auroras have passed away polewards, the sky is

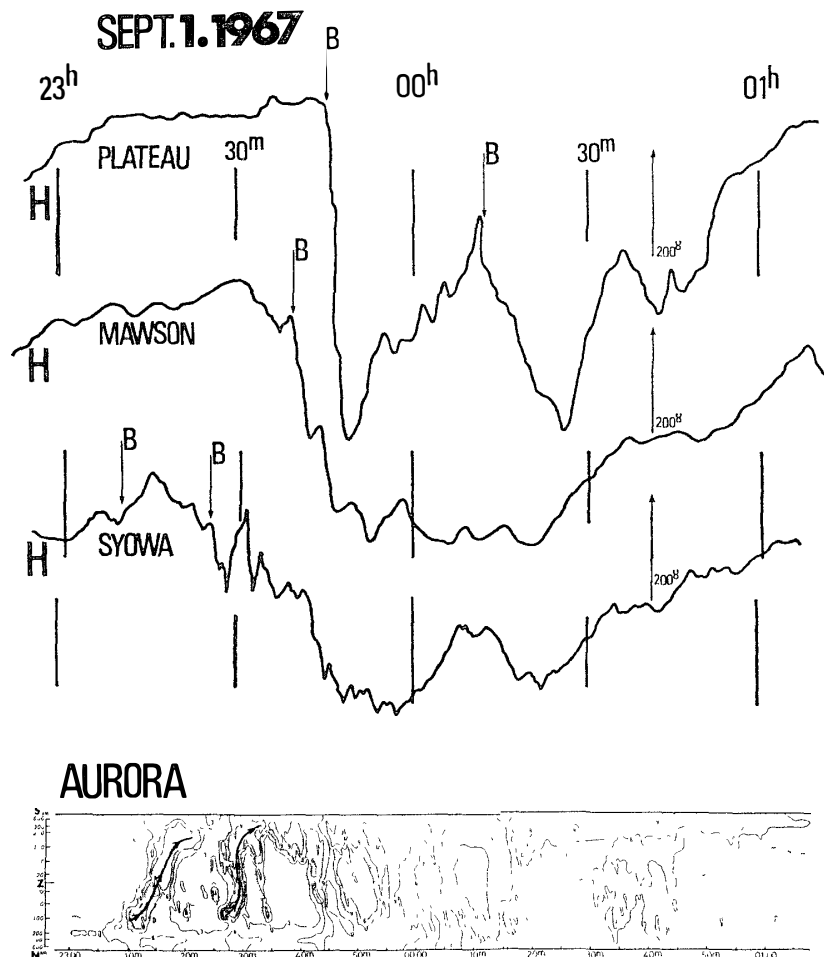


Fig. 23. Example of the poleward movement of the breakup type aurora and the associated magnetic variation on Sept. 1, 1967. From top to bottom: (1) Horizontal component at Plateau Station (geomag. lat.  $77.2^{\circ}\text{S}$ , long.  $52.5^{\circ}$ ). (2) Horizontal component at Mawson (geomag. lat.  $73.1^{\circ}\text{S}$ , long.  $102.9^{\circ}$ ). (3) Horizontal component at Syowa Station (geomag. lat.  $69.6^{\circ}\text{S}$ , long.  $77.1^{\circ}$ ). (4) Meridian-time diagram of  $4278\text{\AA}$  aurora obtained at Syowa Station. Contour: "1" corresponds to  $1\text{kR}$ .

filled by the post-breakup type auroras of intense brightness which are produced by the intense breakup auroras. These post-breakup auroras exhibit rapid equatorward movements in the period from 23 h 35 m to 00 h 10 m. The auroral activities became weak, falling to less than 1 kR, around 00 h 10 m of Sept. 2, but they were intensified again from 00 h 16 m. Meanwhile, at the pole side of Syowa, a sharp decrease is found in the magnetic H-component of Plateau Station at 00 h 11 m. This is about 5 min earlier than the reintensifications

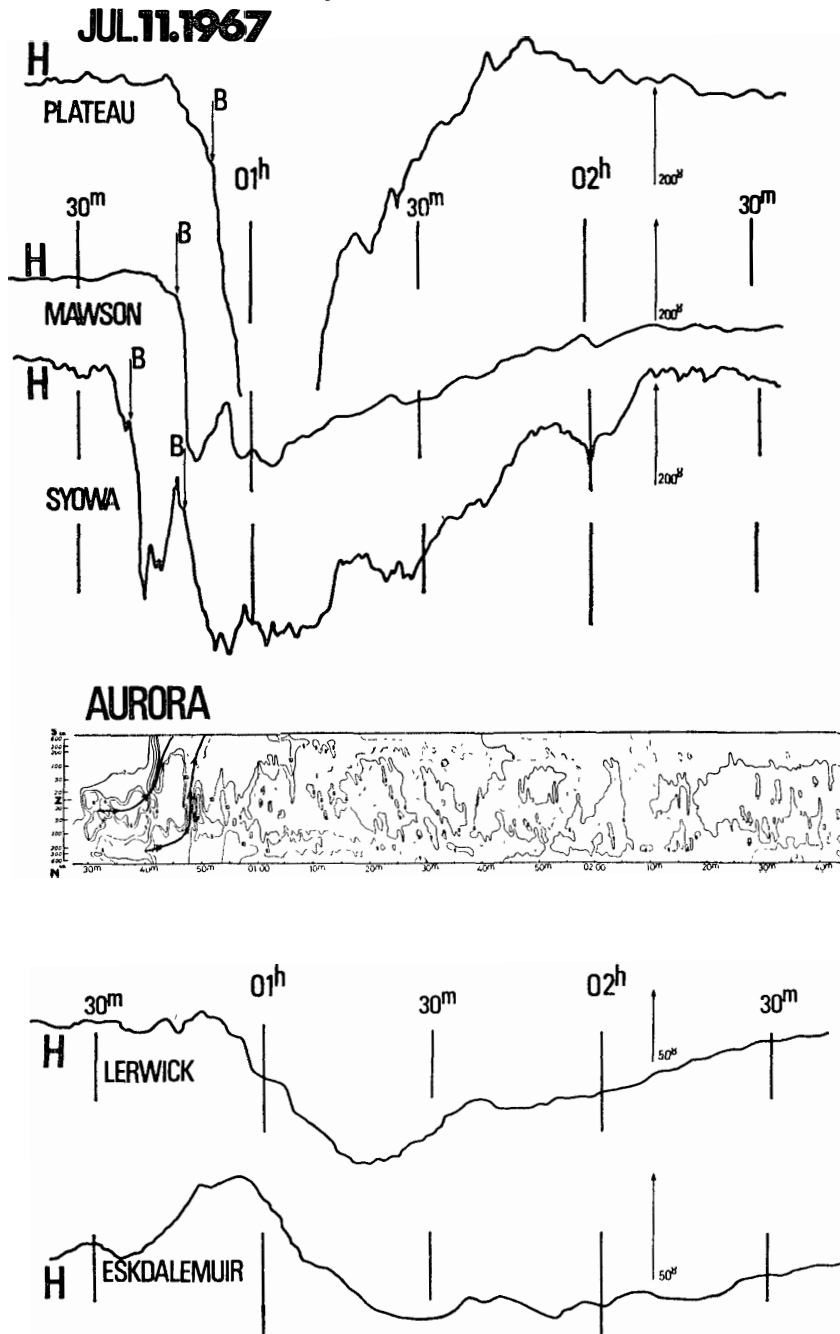


Fig. 24. Example of the poleward movement of the breakup type aurora and the equatorward expansion of the post-breakup type aurora on July 11, 1967. From top to bottom: (1) Horizontal component at Plateau Station (geomag. lat.  $-77.2^\circ$ , long.  $52.5^\circ$ ). (2) Horizontal component at Mawson (geomag. lat.  $-73.1^\circ$ , long.  $102.2^\circ$ ). (3) Horizontal component at Syowa Station (geomag. lat.  $-69.6^\circ$ S, long.  $77.1^\circ$ ). (4) Meridian-time diagram of  $\lambda 4278\text{\AA}$  aurora obtained at Syowa Station. Contour; "1" corresponds to 1kR. (5) Horizontal component at Lerwick (geomag. lat.  $62.5^\circ$ N, long.  $88.6^\circ$ ). (6) Horizontal component at Eskdalemuir (geomag. lat.  $58.5^\circ$  N, long.  $82.9^\circ$ ).

of the auroral activities at Syowa, indicating that the intensification of the post-breakup type aurora in the period from 00 h 16 m to about 01 h 00 m resulted from the auroral breakup event in the higher latitudes.

### 5.1.3. Substorm on July 11, 1967

In this example (Fig. 24), magnetograms (H-component) of Lerwick (geomag. lat. 62.5°; long. 88.6°) and Eskdalemuir (geomag. lat. 58.5°; long. 82.9°), which are located at the equatorward side of Syowa along nearly the same longitude in the northern hemisphere, are shown together with those of Plateau, Mawson and Syowa Station (cf. Fig. 21).

In the auroral diagram shown in the middle of Fig. 24, the successive poleward movements of two breakup auroras were observed during the breakup phase of an auroral substorm (from 00 h 30 m to 52 m). These breakup auroras traveled further towards the pole, and caused a sharp drop in H-component (the breakup of the auroral substorm) around 00 h 45 m at Mawson and around 00 h 54 m at Plateau Station. After these breakup auroras had passed away polewards, the sky was blanketed by the post-breakup type auroras with the comparatively weak luminosity, which gradually moved equatorwards.

In this case, the magnetic H-components of the lower latitude stations showed the maximum decrease around 01 h 20 m at Lerwick and around 01 h 30 m at Eskdalemuir, while the H-component of Syowa attained the maximum decrease (the maximum stage of magnetic substorm) around 01 h 00 m. Namely, the maximum stage of magnetic bay-disturbance in the lower latitude was found a few tens of minutes later than that in the higher. This fact may indicate that the region of the post-breakup type auroras expands towards the equator with time at the speed of about 0.8 km/s.

According to the examples shown in Figs. 22, 23 and 24, it is clearly recognized that the "post-breakup type aurora" is closely related to the breakup event. The "post-breakup type aurora" appears over the sky where "breakup type aurora" has passed away poleward and the intensification of the former's activity in the lower latitudes corresponds to the latter in the higher latitudes. One may say therefore that the "breakup type aurora" and the "post-breakup type one" form a pair event.

The top of the left side figures in Fig. 51 represents a composition of an elemental auroral substorm which consists of the "breakup type aurora" on the poleward side border and the "post-breakup type aurora" expanding equatorwards from the edge of the "breakup type aurora". In actual cases, two or more elemental auroral substorms often appear in the midnight sector of the auroral oval, as schematically illustrated at the bottom of the left side of Fig. 51.

## 5.2. Magnetic variations associated with post-breakup type aurora

In Section 4.2., magnetic disturbances associated with the breakup type aurora during the breakup phase of the auroral substorm (breakup magnetic disturbance) were clarified and it is concluded that the geomagnetic horizontal

disturbing vectors change their directions considerably and show the definite rotation with an increase of their magnitude when the breakup type aurora moves towards the pole.

In this section, the magnetic disturbances during the post-breakup phase (post-breakup magnetic disturbance) will be studied, in comparison with the breakup magnetic disturbance.

5.2.1. Substorm on June 8, 1967

As seen in the auroral diagram in the top of Fig. 25, the typical breakup type aurora was observed during the breakup phase at Syowa Station. During this phase, the magnetic H-component showed pulse-like variation and the (magnetic) horizontal disturbance vectors rotated counterclockwise, being associated

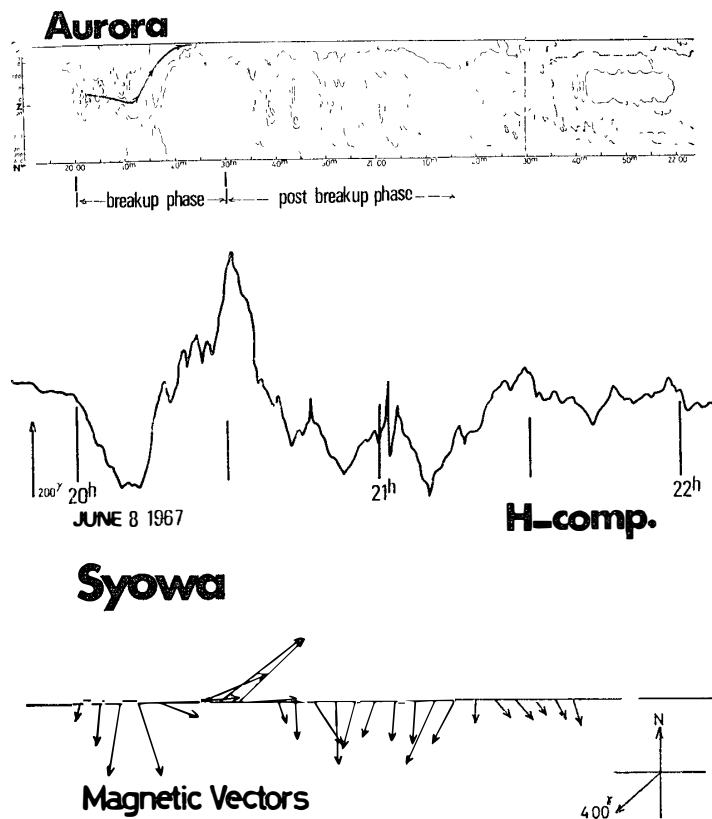


Fig. 25. Example of characteristics of the horizontal disturbing vectors during the post-breakup phase of the auroral substorm observed at Syowa Station on June 8, 1967 and the simultaneous meridian-time diagram of  $\lambda 4278\text{\AA}$  aurora. From top to bottom: (1) Meridian-time diagram of  $\lambda 4278\text{\AA}$  aurora. Contour; "I" corresponds to 1kR. (2) Horizontal component of the magnetogram. (3) Horizontal magnetic disturbance vectors.

with the poleward movement of the intense aurora (cf. Fig. 11).

After the breakup type aurora had passed away towards the pole, the post breakup phase at Syowa Station began and continued till about 22 h 00 m. During the period, the magnetic horizontal vectors did not change their directions unlike those during the breakup phase and they were directed towards the south (the westward overhead current).

#### 5.2.2. Substorm on July 11 and on Sept. 29, 1967

In the example of the auroral substorm shown in Fig. 26, two breakup type auroras occurred successively at 00 h 40 m and 00 h 46 m during the breakup phase on July 11, 1967. During the breakup phase, the magnetic horizontal vectors changed their directions considerably and their short period component rotated clockwise in association with the poleward movements of the both breakup type auroras, as has been illustrated in detail before (cf. Fig. 16). On the other hand, the magnetic vectors during the post-breakup phase point quasi-stationarily towards the south and their magnitudes were approximately in accord with the activities of the post-breakup type auroras. A similar example to this is shown also in Fig. 27.

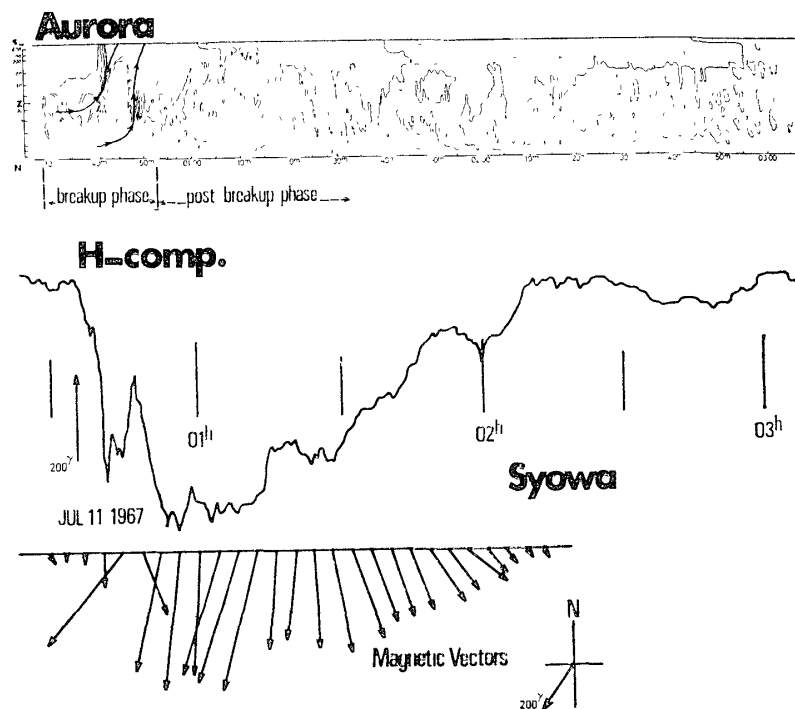


Fig. 26. Example of characteristics of the horizontal disturbing vectors during the post-breakup phase of the auroral substorm observed at Syowa Station on July 11, 1967 and the simultaneous meridian-time diagram of  $\lambda 4278\text{\AA}$  aurora. From top to bottom: (1) Meridian-time diagram of  $\lambda 4278\text{\AA}$  aurora. Contour; "1" corresponds to 1kR. (2) Horizontal component of the magnetogram. (3) Horizontal magnetic disturbance vectors.

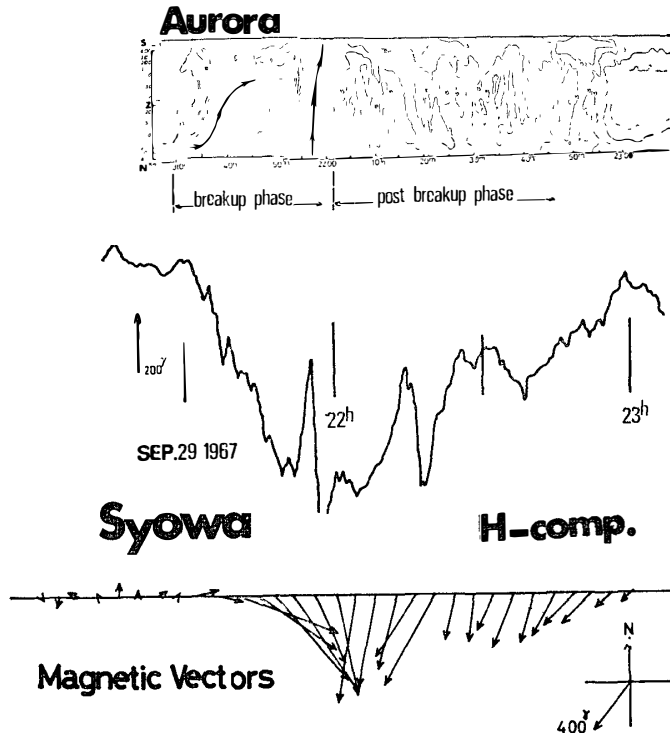


Fig. 27. Example of characteristics of the horizontal disturbing vectors during the post-breakup phase of the auroral substorm observed at Syowa Station on Sept. 29, 1967 and the simultaneous meridian-time diagram of  $\lambda 4278\text{\AA}$  aurora. From top to bottom: (1) Meridian-time diagram of  $\lambda 4278\text{\AA}$  aurora. Contour; "1" corresponds to 1kR. (2) Horizontal component of the magnetogram. (3) Horizontal magnetic disturbance vectors.

5.2.3. Substorm on May 25, 1967

The auroral diagram of Fig. 28 shows that the auroral breakup occurred in the northward side (equatorward side) of Syowa Station during the severe magnetic storms of May 25, 1967. The typical breakup type aurora passed over the zenith of Syowa at 21h 22m and moved away polewards. During the breakup phase at Syowa, the horizontal disturbance vectors changed their directions suddenly with increasing magnitude (cf. Fig. 15).

After the disappearance of the breakup type aurora out of the view of the observing station, the high active zone of the auroras was present at the equatorward side of Syowa Station. The equatorward movements towards the high active zone of the auroras were observed during the post-breakup phase of the auroral substorm. During the post-breakup phase, the magnetic H-component showed gradual variation, while the pulse-like variation during the breakup phase, and the magnetic horizontal disturbing vectors whose magnitudes were approximately in proportion to the auroral activities pointed towards the south.

The above-mentioned characteristics of the magnetic disturbances associated with the post-breakup type auroras (post-breakup magnetic disturbance) are always the same for all substorms which take place in the night sector. The post-breakup magnetic disturbances show the gradual variations as compared with the breakup magnetic disturbances. The magnetic horizontal vectors, whose magnitudes are approximately proportional to the activities of the post-breakup type auroras, do not change their directions in comparison with those during the breakup phase, and pointed quasi-stationarily towards the magnetic south (the westward overhead current).

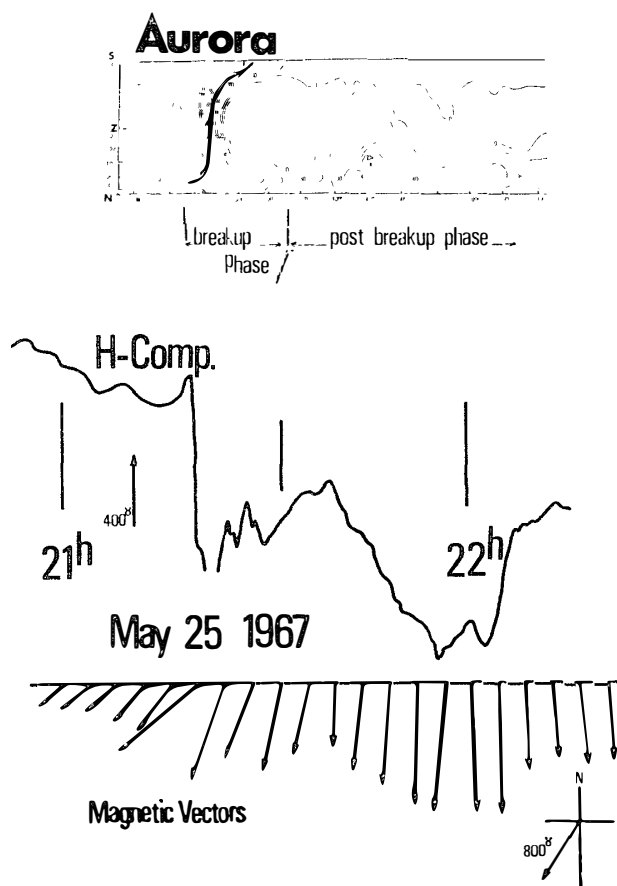


Fig. 28. Example of characteristics of the horizontal disturbing vectors during the post-breakup phase of the auroral substorm observed at Syowa Station on May 25, 1967 and the simultaneous meridian-time diagram of  $\lambda 4278 \text{ \AA}$  aurora. From top to bottom: (1) Meridian-time diagram of  $\lambda 4278 \text{ \AA}$  aurora. Contour; "1" corresponds to 1kR. (2) Horizontal component of the magnetogram. (3) Horizontal magnetic disturbance vectors.

### 5.3. Space relation between the breakup and the post-breakup magnetic disturbances

Fig. 29 shows an example that an active region of the post-breakup type auroras expanded towards the equator side after the breakup event in the pole side and caused the post-breakup magnetic disturbance in the lower latitudes. As seen in the auroral diagram shown at the middle of Fig. 29, the intensification of the auroral brightness was observable around 22 h 20 m of July 5, 1967 near the pole side horizon of Syowa. At the same time, the magnetic H-component of Plateau Station, which is located at the pole side of Syowa, showed pulsative variations and the magnetic vectors rotated obviously counterclockwise. Judging from the characteristics of the magnetic variations associated with the

breakup type auroras mentioned before (cf. Section 4.2.), it may be certain that breakup event occurred around 22 h 20 m in the pole side region (higher latitude region) of Syowa Station. After the breakup event in the higher latitudes, the active area of the post-breakup type auroras expanded towards the equator. Being associated with the equatorward expansion of the post-breakup type aurora, the magnetic disturbance was developed at Syowa and the magnetic

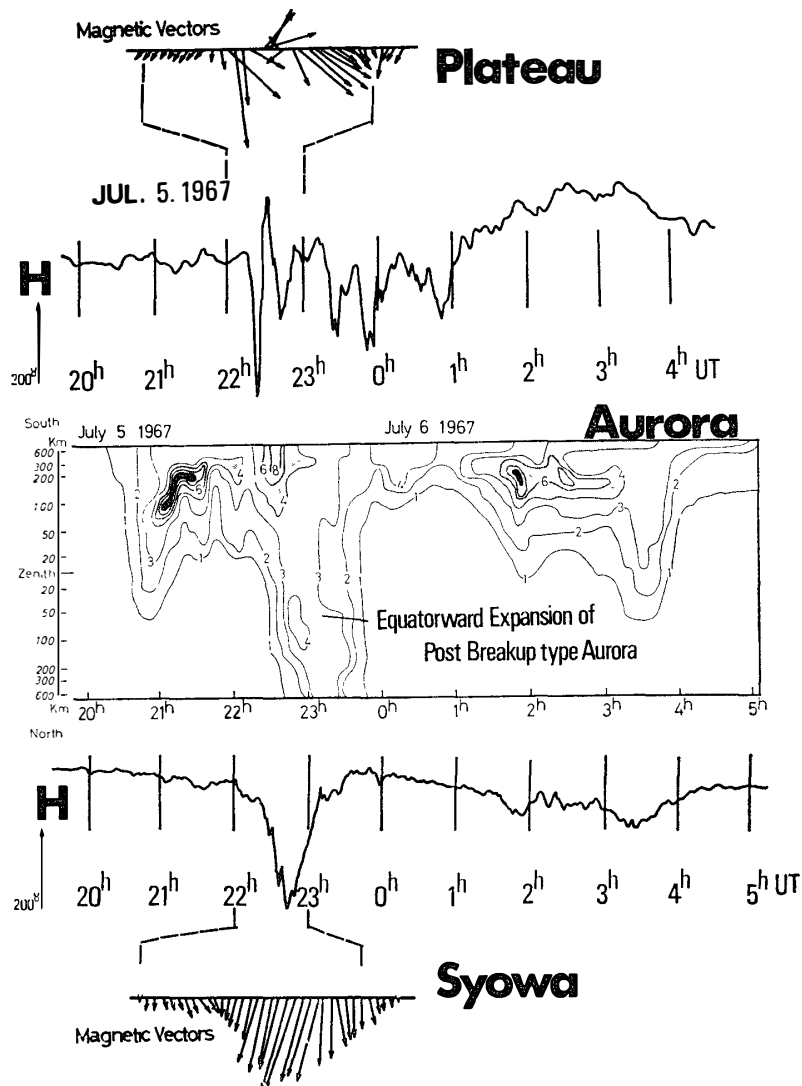


Fig. 29. Example of the equatorward expansion of the active area of the post-breakup type auroras and the associated magnetic variation. From top to bottom: (1) Magnetic horizontal disturbance vectors at Plateau Station. (2) Horizontal component at Plateau. (3) Meridian-time diagram of  $\lambda 4278\text{\AA}$  aurora obtained at Syowa Station. Contour; "1" corresponds to 1kR. (4) Horizontal component at Syowa Station. (5) Magnetic horizontal disturbing vectors at Syowa Station.

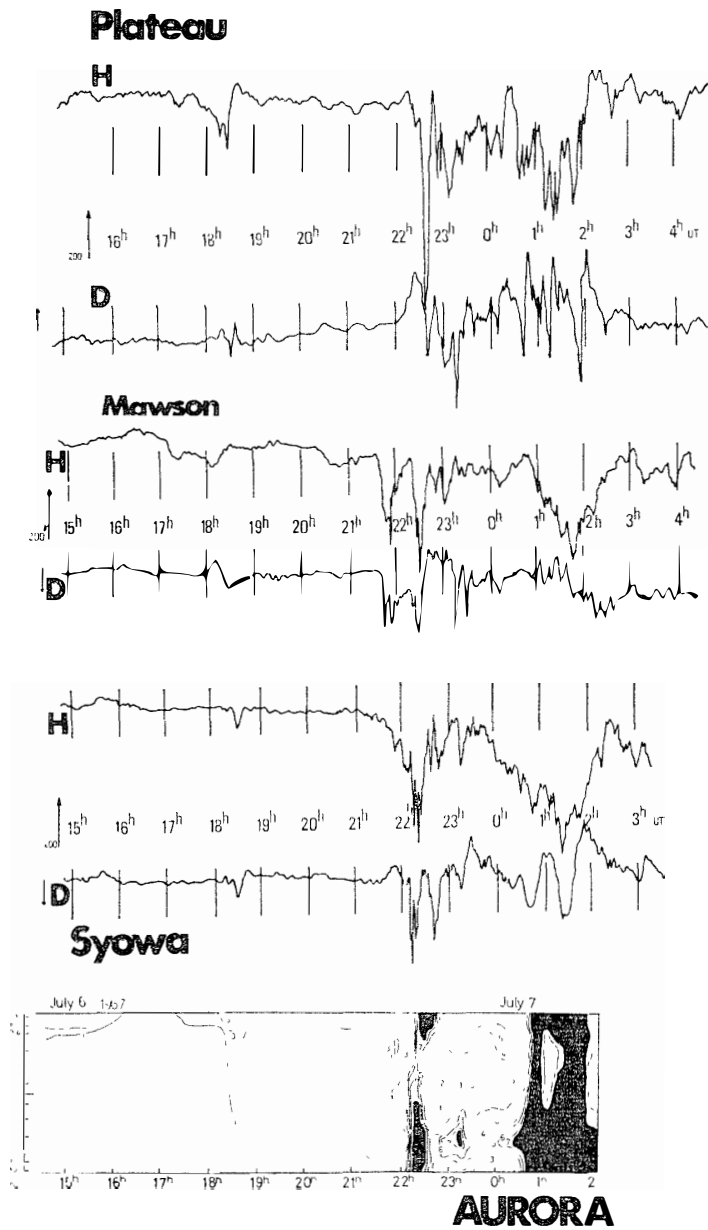


Fig. 30. Example of the relation between the breakup and the post-breakup magnetic disturbances on July 6-7, 1967. From top to bottom: (1) Magnetogram at Plateau Station (geomag. lat.  $77.2^{\circ}\text{S}$ , long.  $52.5^{\circ}$ ). (2) Magnetogram at Mawson (geomag. lat.  $73.1^{\circ}\text{S}$ , long.  $102.9^{\circ}$ ). (3) Magnetogram at Syowa Station (geomag. lat.  $69.6^{\circ}\text{S}$ , long.  $77.1^{\circ}$ ). (4) Meridian-time diagram of  $\lambda 4278\text{\AA}$  obtained at Syowa Station. Contour; "1" corresponds to 1kR.

vectors were directed towards the magnetic south without a rotation. Thus, it may be reasonable to consider that the magnetic disturbance at Syowa in this case was not accompanied by the breakup type auroras, but by the post-breakup type auroras (post-breakup magnetic disturbance).

Fig. 30 shows the auroral diagram obtained at Syowa Station on July 6 and 7, 1967 together with the simultaneous magnetograms at Plateau, Mawson and Syowa. It is found in the magnetic records of Syowa and Mawson that the breakup type magnetic disturbances were observable from 21 h to 23 h on July 6 and the post-breakup ones occurred during the early morning hours (00h~03h)

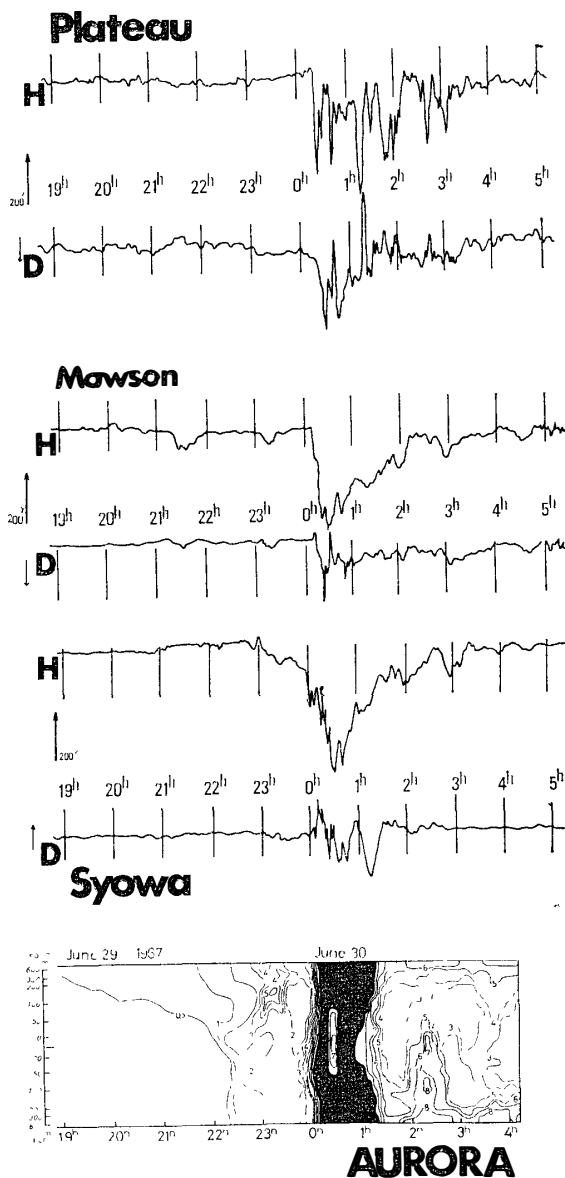


Fig. 31. Example of the relation between the breakup and the post-breakup magnetic disturbances on June 29-30, 1967. From top to bottom: (1) Magnetogram at Plateau Station (geomag. lat.  $77.2^{\circ}$ S, long.  $52.5^{\circ}$ ). (2) Magnetogram at Mawson (geomag. lat.  $73.1^{\circ}$ S, long.  $102.9^{\circ}$ ). (3) Magnetogram of Syowa Station (geomag. lat.  $69.6^{\circ}$ S, long.  $77.1^{\circ}$ ). (4) Meridian-time diagram of  $\lambda 4278\text{\AA}$  obtained at Syowa Station. Contour; "1" corresponds to 1kR.

on July 7 (cf. auroral diagrams shown in the paper by HIRASAWA and KAMINUMA, 1970). During the period when the post-breakup magnetic disturbances were taking place at Mawson and Syowa, the magnetic records at Plateau, which is located in their poleward side, exhibited three successive pulsative variations in both H- and D-components. These corresponding H- and D-components variations had nearly the same amplitude but their phases are clearly different between the two. This fact may indicate that the magnetic horizontal vectors rotated for each pulsative variation. It may be concluded from these facts that the successive breakup magnetic disturbances occurred in association with the poleward traveling of the intense breakup type auroras near Plateau Station in the period from 00h to 03h on July 7. Thus, it may reasonably be considered that the breakup magnetic disturbances were observable in the polar side area when the post-breakup ones occurred in a certain polar region.

The auroral diagram and the simultaneous magnetograms illustrated in Fig. 31 are similar to those shown in Fig. 30. In this example of June 29-30, 1967, it is also found that the pulsative magnetic variations occurred repeatedly at a higher latitude station, Plateau, while the magnetic disturbance at lower latitude stations, Mawson and Syowa, are to be the bay-shape without such large fluctuations.

Judging from the above mentioned facts, it may be concluded that the post-breakup magnetic disturbances are closely related to the breakup ones in the higher latitudes and that the pulsative or the bay-shape magnetic disturbances with a sharp drop is caused by the poleward traveling of the breakup type auroras, while the bay disturbances with the gradual decrease are originated in the equatorward expansions of post-breakup type auroras which results in the breakup event in the higher latitudes.

## 6. Auroral Appearances Preceding the Onset of Auroral Breakup

The diurnal tendency of the auroral appearance in the polar region has been investigated in detail by many research workers. When we observe auroras at a station located at a geomagnetic latitude,  $\Phi_m=70^\circ\sim 65^\circ$  (in the so-called auroral zone), the auroral glows appear above the poleward horizon of the observing station in the evening hours (18 h $\sim$ 20 h LT). As the nighttime progresses, the auroral glows become the homogeneous arcs or bands. Towards the local midnight, the active region of the aurora shifts towards the low latitudes and various types of the aurora are observable (HEPPNER, 1954).

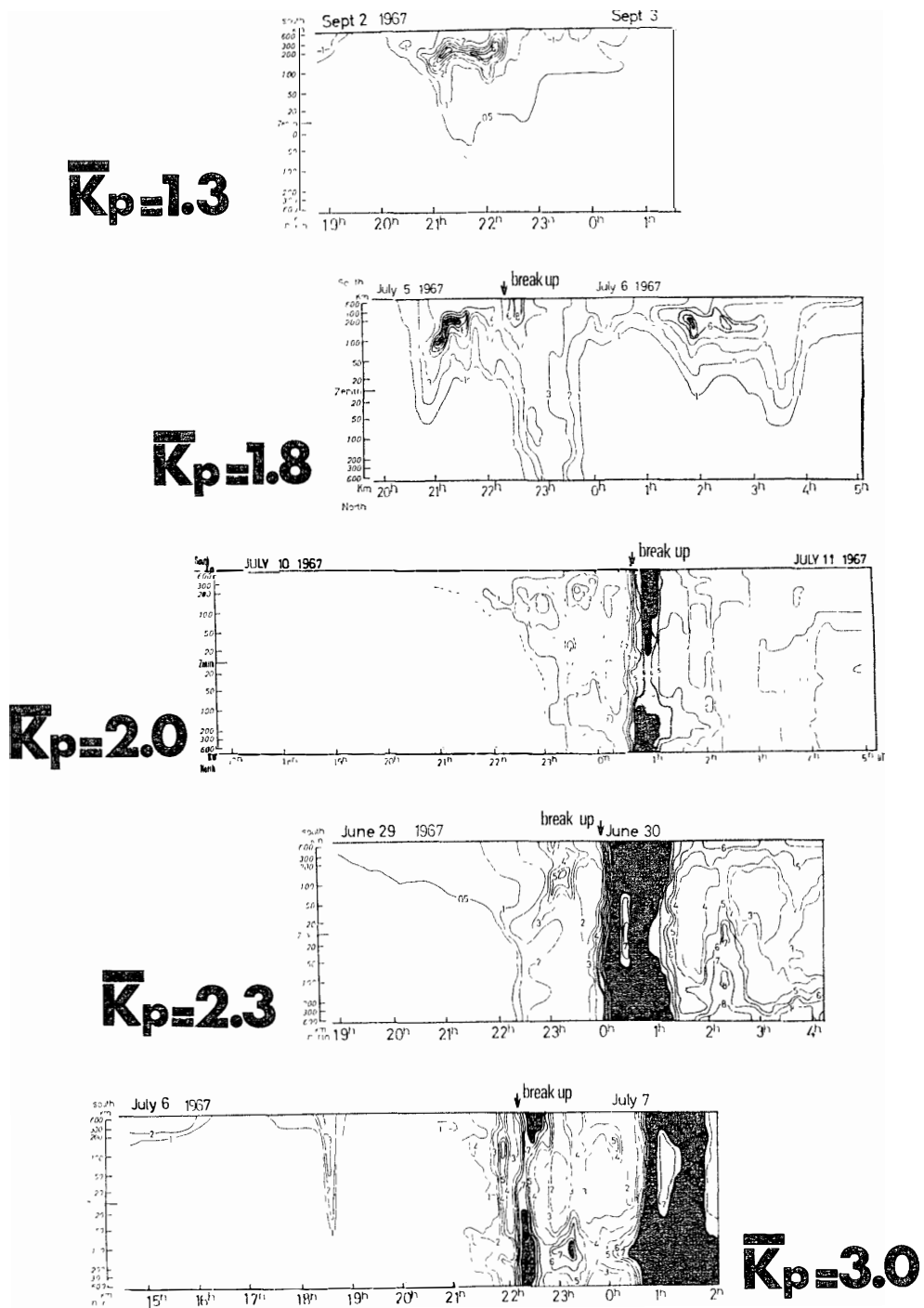
A similar diurnal tendency is found also in the meridian-time diagram of auroral luminosity obtained at Syowa Station. In the middle diagram of Fig. 32A (on July 10 $\sim$ 11, 1967), faint auroras appear on the pole side of Syowa Station at 20 h $\sim$ 21 h. They spread towards the equator, cover the zenith of the observing station at 22 h 30 m and reach up to the north horizon at about 23 h. After 23 h, the auroras are visible from the north to the south of the station. Between 00 h 40 m and 02 h 00 m, an auroral substorm occurs. Within several minutes after the onset of a storm, the active auroras with an intense luminosity spread and blanket the sky. A similar diurnal tendency is found also in the other data shown in Fig. 32A and B.

It should also be noted in the auroral diagrams shown in Fig. 32 that the auroral agitations with the intensity of about several kR (in 4278 Å) in luminosity were observable, preceding the onset of auroral breakup (the onset time of auroral breakups at Syowa Station is indicated by the arrow marks in each diagram). In other words, it is extremely rare for the auroral breakup event to occur without any auroral appearances before it. In this section, let us examine the auroral behavior prior to the breakup phase.

### 6.1. Auroral agitations before breakup .

#### 6.1.1. Event on July 6, 1967

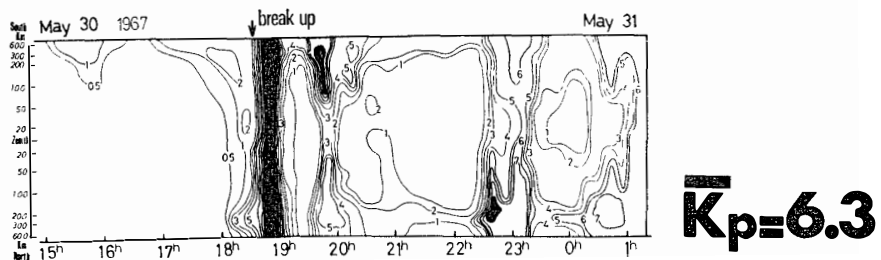
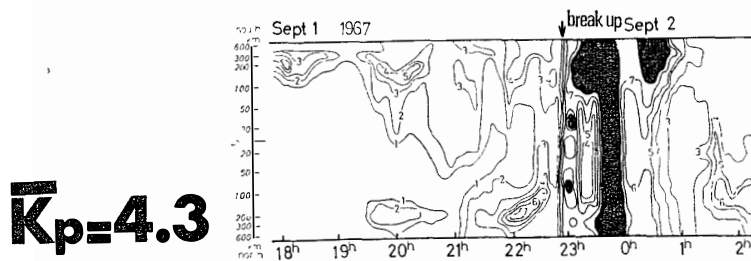
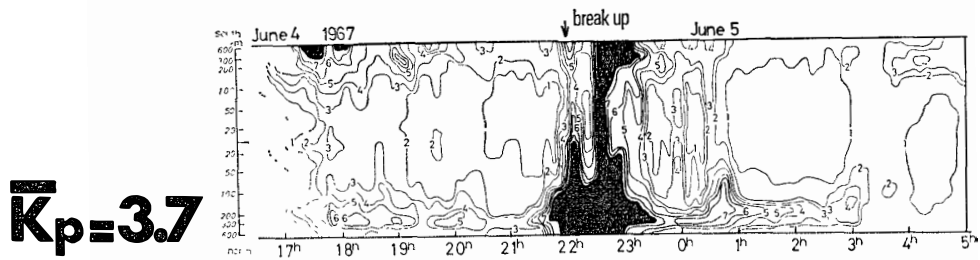
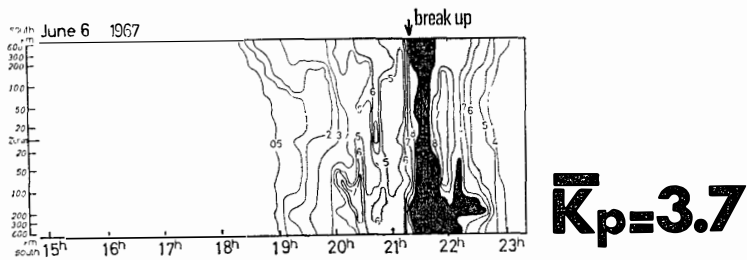
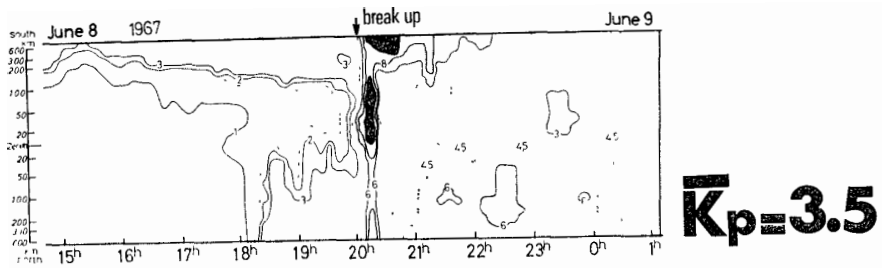
As seen in the auroral diagram shown in Fig. 33, a breakup type aurora brightened and its rapid poleward expansion occurred at 22 h 09 m on July 6, 1967. This is the onset of an auroral breakup at Syowa Station. Precedent to this breakup event, an increase of auroral activities was observed from about 21 h 40 m, and the definite equatorward motions of the auroral bands or arcs occurred in the period from 22 h 46 m to 55 m and from 22 h 01 m to 09 m.



(A)

Fig. 32A and B. The diurnal tendency of the diagrams obtained at Syowa order of the magnitudes of breakups at Syowa Station "1" corresponds to 1kR.

Auroral Appearances Preceding the Onset of Auroral Breakup



(B)

auroral appearances. The meridian-time auroral Station for the selected ten days are put in the the average  $K_p$  ( $\bar{K}_p$ ). The onset time of auroral was indicated by arrow in each diagram. Contour;

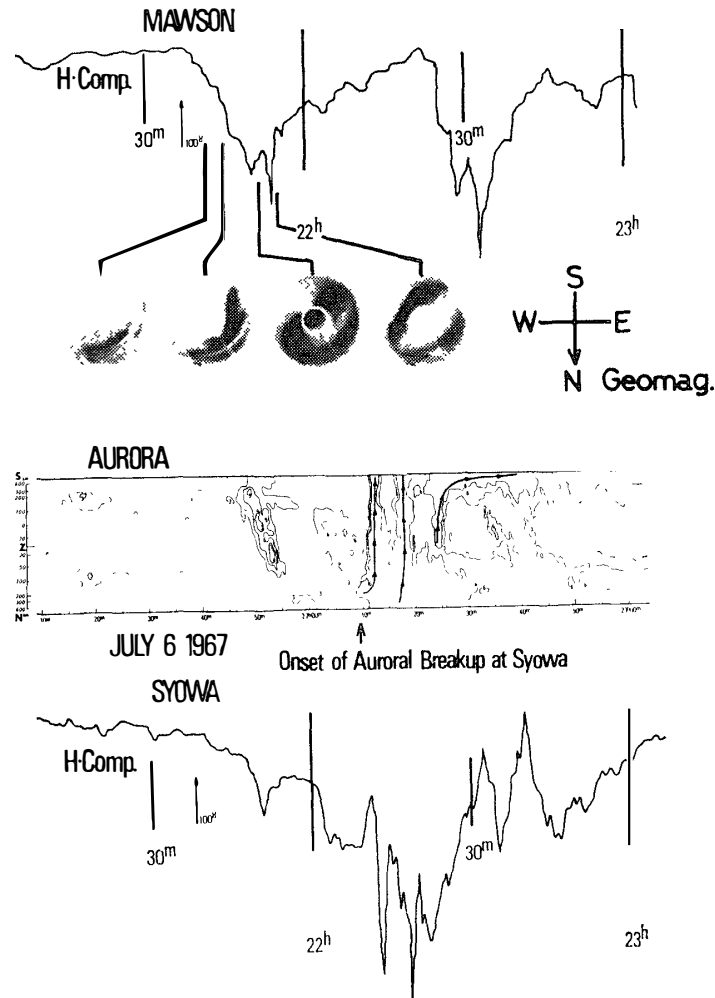


Fig. 33. Example of auroral activations before breakup on July 6, 1967. From top to bottom: (1) Magnetic H-component at Mawson (geomag. lat.  $73.1^{\circ}\text{S}$ , long.  $102.9^{\circ}$ ). (2) All-sky camera data at Mawson. (3) Meridian-time diagram of  $\lambda 4278\text{\AA}$  aurora obtained at Syowa Station (geomag. lat.  $69.6^{\circ}\text{S}$ , long.  $77.1^{\circ}$ ). Contour; "1" corresponds to  $1\text{kR}$ . (4) Magnetic H-component at Syowa Station.

These auroral displays are considered to be the auroral agitations before a breakup. Meanwhile, the magnetic H-component variation and the all-sky camera data observed at a higher latitude station, Mawson, exhibited the occurrence of the breakup event; a sharp drop of about  $350\gamma$  in the magnetic H-component and the poleward traveling of breakup type aurora. Judging from these observed facts, it would be reasonable to consider that the auroral agitations before the breakup at Syowa Station in this case are the results of equatorward expansion of the post-breakup type auroras produced by the breakup event in the higher latitudes.

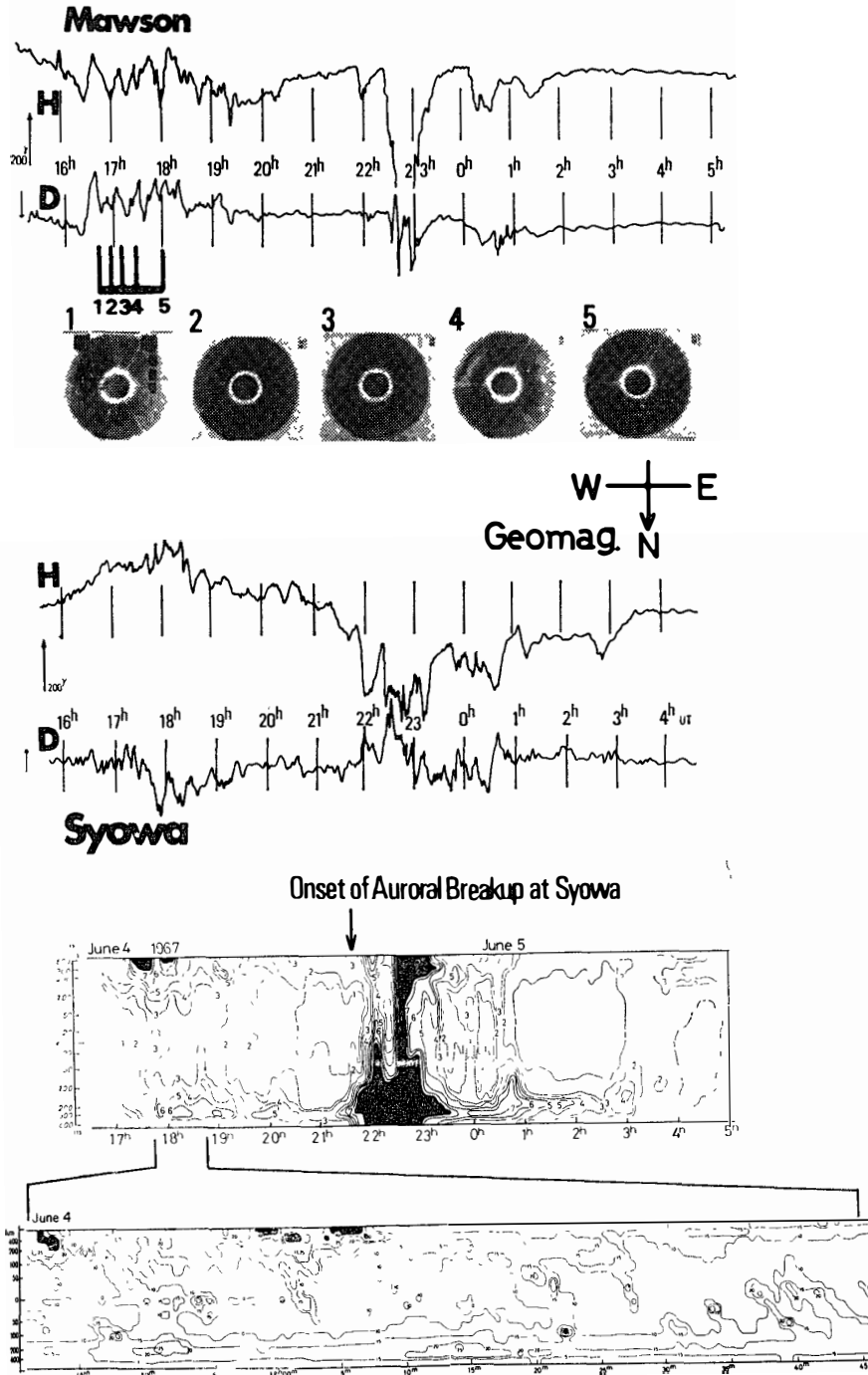


Fig. 34. Example of auroral activations before breakup on July 4-5, 1967. From top to bottom: (1) Magnetogram at Mawson (geomag. lat.  $73.1^{\circ}$ S, long.  $102.9^{\circ}$ ). (2) All-sky camera data at Mawson. (3) Magnetogram at Syowa Station (geomag. lat.  $69.6^{\circ}$ S, long.  $77.1^{\circ}$ ). (4) Meridian-time diagram obtained at Syowa Station. Contour; "1" corresponds to 1kR for the upper diagram and 0.3kR for the bottom one.

### 6.1.2. Event on July 4-5, 1967

The auroral diagram in Fig. 34 shows an occurrence of the auroral breakup event around 21 h 30 m on June 4, 1967 at Syowa Station. Precedent to this breakup, the auroral active region began to expand around 16 h 30 m towards the low latitude from the high latitudes, and the definite equatorward movements of auroral arcs or bands were observed especially from 17 h 30 m to 18 h 54 m, as seen in the bottom of Fig. 34. During the period when the activations of aurora were observable at Syowa (from 16 h 30 m to 20 h 00 m) prior to the breakup, the magnetic H-component at Mawson showed successive pulse-like disturbances with the amplitude of about 100-150  $\gamma$ , accompanied by the similar fluctuations in magnetic D-component. The all-sky camera data at Mawson during this period illustrate the blanketing over the sky of the intense auroras, corresponding to the magnetic pulse-like fluctuations. These may indicate the auroral breakups occurred successively around Mawson Station in the period from 16 h 30 m to 20 h 00 m. Therefore, the auroral agitations preceding the breakup at Syowa (around 21 h 30 m) is the equatorward expansion of post-breakup type auroras resulting from the breakup events in the higher latitudes.

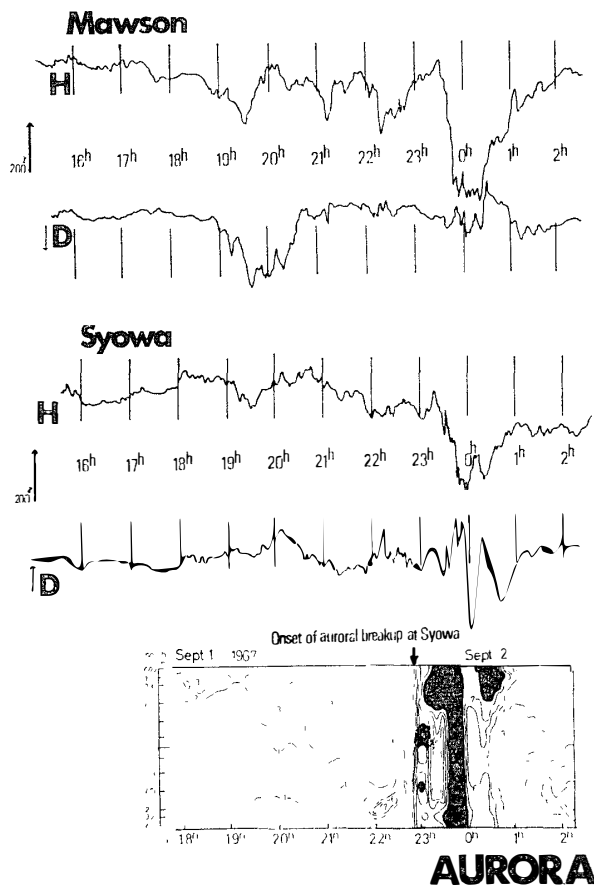


Fig. 35. Example of auroral activations before breakup on Sept. 1, 1967. From top to bottom: (1) Magnetogram at Mawson (geomag. lat.  $73.1^{\circ}\text{S}$ , long.  $102.9^{\circ}$ ). (2) Magnetogram at Syowa Station (geomag. lat.  $69.6^{\circ}\text{S}$ , long.  $77.1^{\circ}$ ). (3) Meridian-time diagram of  $\lambda 4278\text{\AA}$  obtained at Syowa Station. Contour; "1" corresponds to 1kR.

### 6.1.3. *Event of September 1, 1967*

The auroral diagram and the simultaneous magnetograms illustrated in Fig. 35 are similar to those shown in Fig. 34. In this example of September 1, 1967, an auroral active region with intensity of several kR ( $4278 \text{ \AA}$ ) began to expand towards the equator around 19 h and reached the equator side horizon of Syowa at 21 h, preceding the onset of the auroral breakup around 23 h at Syowa. In this period (from 19 h to 23 h), the magnetic variation at Mawson showed that successive bay-like disturbances with the amplitude of about  $200\gamma$  occurred during the period from 19 h to 20 h, from 21 h to 21 h 20 m and from 22 h to 23 h, respectively. Hence, the auroral agitations preceding the breakup at Syowa would also be the post-breakup type auroras produced by the breakup in the pole side of the observing station.

### 6.2: **Auroral display during the so-called growth phase of polar substorms**

Recent research works have revealed that the polar substorms have a significant growth phase when the energy for the substorm is stored in the magnetotail. The growth phase is characterized by various kinds of coherent event; the substorm is preceded by the southward turning of the solar wind magnetic field direction from the northward direction (IJIMA, 1968; ROSTOKER, 1968; HIRSHBERG and COLBURN, 1969; AUBRY *et al.*, 1970; IJIMA and NAGATA, 1970; ARNOLDY, 1971; KOKUBUN, 1971), an increase of the magnetic field in the magnetotail (FAIRFIELD and NESS, 1970; CAMIDGE and ROSTOKER, 1970; RUSSEL *et al.*, 1970; AUBRY and McPHERRON, 1971; IJIMA and NAGATA, 1971), a thinning of the plasma sheet at the distance of 18 Re (HONES *et al.*, 1971), an inward movement of the inner edge of plasma sheet (VASYLIUNAS, 1968), an enhancement of the polar two-vortex current system (DP-2 field) indicating a growth of the magnetospheric convection of low energy plasma (IJIMA, 1968; IJIMA *et al.*, 1968; IJIMA and NAGATA, 1970; KOKUBUN, 1971), a gradual enhancement of the polar westward current flow and the development of its associated magnetic variation (McPHERRON, 1970), a trigger bay-disturbance (ROSTOKER, 1968) and others.

On the other hand, from the viewpoint of the auroral display, AKASOFU (1968) concluded that there is no visible auroral indication of the growth phase of a polar substorm. It should also be noted, as illustrated previously, that the auroral activations before the breakup phase can not always be identified as a precursor phenomenon of a breakup of an isolated auroral substorm, but it may be identified as a part of the post-breakup type auroras of another auroral substorm which has broken up previously at a certain higher latitude. The question whether the auroral substorm takes place with some precursory auroral phenomenon or not should be regarded still pending.

In this section, this problem will be further investigated.

#### 6.2.1. *Event on July 10-11, 1967*

The auroral diagram obtained at Syowa is shown in Fig. 36 together with the simultaneous magnetic H-components at 15 polar stations in the southern (9 stations) and the northern (6 stations) hemispheres. It may be observed in the auroral diagram and the magnetic H-component at Syowa Station that an

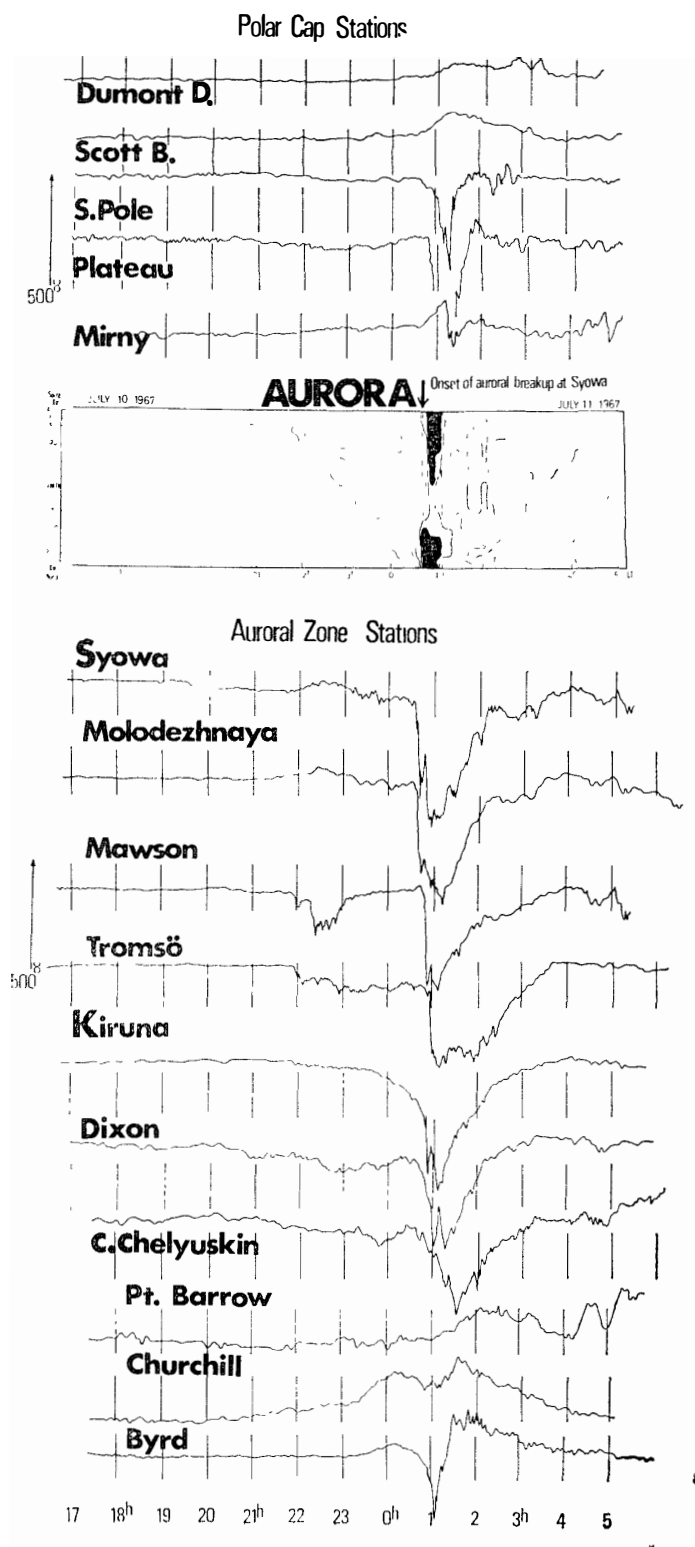


Fig. 36. Example of auroral activation before breakup on July 10-11, 1967. From top to bottom: (1) Magnetic H-components at polar cap stations, Dumont d'Urville Base (geomag. lat.  $-75.5^\circ$ , long.  $230.9^\circ$ ), Scott Base ( $-79.0^\circ$ ,  $294.4^\circ$ ), South Pole ( $-78.5^\circ$ ,  $0.3^\circ$ ), Plateau ( $-77.2^\circ$ ,  $52.5^\circ$ ), Mirny ( $-77.0^\circ$ ,  $146.8^\circ$ ). (2) Meridian-time diagram obtained at Syowa Station. Contour; "1" corresponds to  $1kR$ . (3) Magnetic H-components at auroral zone stations, Syowa Station (geomag. lat.  $-69.7^\circ$ , long.  $77.1^\circ$ ), Molodezhnaya ( $-69.5^\circ$ ,  $98.9^\circ$ ), Mawson ( $-73.1^\circ$ ,  $103.4^\circ$ ), Tromsö ( $67.0^\circ$ ,  $117.5^\circ$ ), Kiruna ( $65.3^\circ$ ,  $115.7^\circ$ ), Dixon ( $63.0^\circ$ ,  $161.4^\circ$ ), Cape Chelyuskin ( $65.9^\circ$ ,  $177.5^\circ$ ), Point Barrow ( $68.6^\circ$ ,  $241.2^\circ$ ), Churchill ( $68.6^\circ$ ,  $322.6^\circ$ ), Byrd Station ( $-70.6^\circ$ ,  $336.3^\circ$ ).

auroral breakup occurred at 00 h 40 m on July 11, 1967 (cf. Fig. 16). Preceding this breakup event, the activations of auroras were observed at the polar side of the observing station. They began to spread towards the equator from 22 h, covered the zenith of Syowa at 22 h 30 m and reached up to the northern horizon at about 23 h. During the period between 22 h 00 m and 00 h 40 m when the auroral activation before the breakup event are observable at Syowa, the magnetic disturbance with a rapid decrease of about 100~200  $\gamma$  amplitude occurred around 22 h-23 h at Mawson and Tromsø which are located at about 2 hours midnight side of Syowa Station. It seems very likely therefore that the auroral activation before the breakup at Syowa in this example is also part of the post-breakup type auroras of another auroral breakup in a certain area.

On the other hand, however, IJIMA and NAGATA (1971) have concluded from an investigation based on the data of PCM, AU, AL, Dst indices on the ground and the magnetotail magnetic field observed by the Explorer 33 that the period

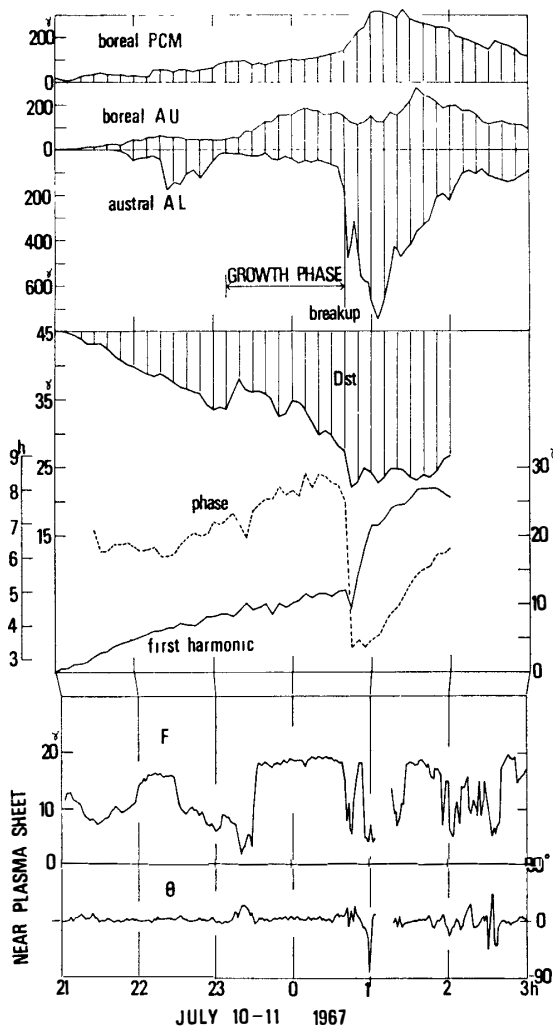


Fig. 37. Example of the growth phase of a polar substorm on July 10-11, 1967. From top to bottom: (1) Boreal PCM to represent the strength of DP2 field in the northern polar cap. (2) Boreal AU to represent the positive magnetic disturbances in the northern polar region. (3) Austral AL to represent the negative magnetic disturbances in the southern polar region. (4) Dst to represent the symmetric component of equatorial ring current. (5) Amplitude and phase of the first harmonic of asymmetric component of equatorial ring current, where phase=12h means the southward maximum of the asymmetric field at the midnight. (6) Tail magnetic field at the near-plasma sheet region in the distant tail by Explorer 33 (After IJIMA and NAGATA, 1971).

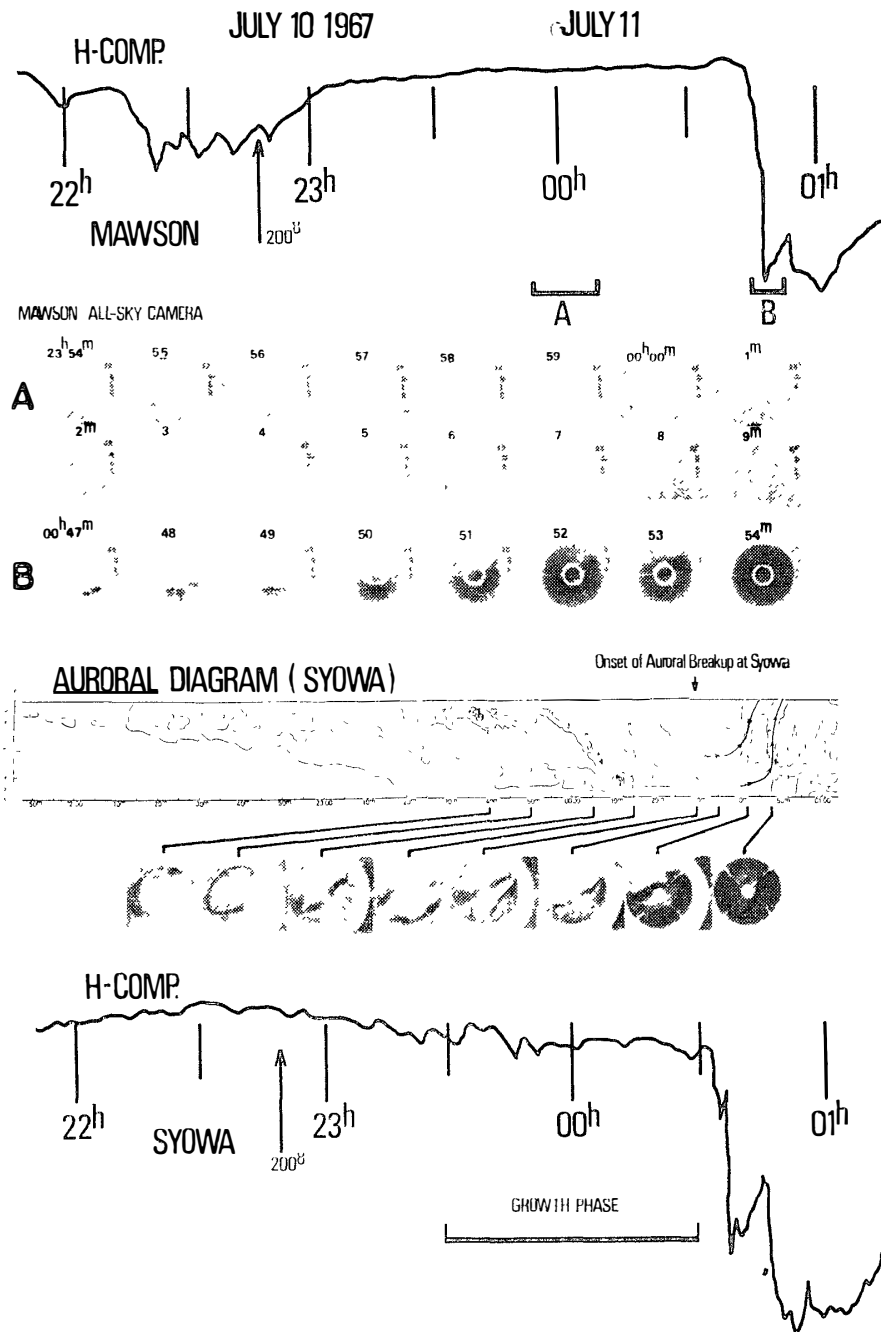


Fig. 38. Example of the auroral displays before an auroral breakup on July 11, 1967. From top to bottom: (1) Horizontal component at Mawson (geomag. lat.  $-73.1^{\circ}\text{S}$ , long.  $102.2^{\circ}$ ). (2) All-sky camera data obtained at Mawson (from 23h54m to 00h09m and from 00h47m to 54m). (3) Meridian-time diagram of  $4278\text{\AA}$  aurora obtained at Syowa Station (geomag. lat.  $69.6^{\circ}\text{S}$ , long.  $77.1^{\circ}$ ). Contour; "1" corresponds to  $1\text{ kR}$ . (4) All-sky camera data obtained at Syowa. (5) Horizontal component at Syowa.

between 23 h 30 m and 00 h 40 m on July 10–11, 1967, can be considered to be the growth phase for the subsequent typical auroral breakup observed at 00 h 40 m on July 11, while, from 22 h 30 m to 23 h 30 m, a weak substorm is seen on the ground and at the tail (As seen in the bottom of Fig. 37, the tail field magnitude collapsed in the period between 22 h 30 m and 23 h 30 m, but it recovered and augmented beyond the quiet value of several gammas at about 23 h 30 m. This condition lasted till 00 h 40 m on July 11 and the subsequent collapse of the tail field was associated with the main ground substorm). The purpose of the following study is to see what auroral displays are appearing in the southern polar region during IJIMA and NAGATA's growth phase of the polar substorm on July 10–11, 1967. Fig. 38 shows an enlarged auroral diagram (with respect to the ordinate, a function of time) at Syowa together with the simultaneous magnetic H-component and the all-sky camera data obtained at Syowa and Mawson Station. In the auroral diagram shown in the middle of Fig. 38, the auroras with the intensity of several kR began to appear around 22 h 10 m at the pole side of the observing station, Syowa, and this auroral activated area showed a gradual expansion toward the lower latitude. In this period (between 22 h 10 m and 23 h 00 m), a magnetic negative bay disturbance with amplitude of about  $200 \gamma$  was observed at a higher latitude station, Mawson. Therefore, we may conclude that the auroral appearance at Syowa in this interval was a part of the post-breakup type aurora which resulted from the breakup event in the higher latitude.

During IJIMA and NAGATA's growth phase (from 23 h 30 m on July 10 to 00 h 40 m on July 11), a discrete auroral arc suddenly brightened around 23 h 30 m at the pole side of Syowa and began to show the equatorward movement at 23 h 50 m, as shown in the auroral diagram. This auroral display is also seen in the simultaneous all-sky camera photographs obtained at Syowa. In this interval when the auroral arc showed its equatorward movement around Syowa (from 23 h 50 m to 00 h 10 m), no visual auroras are observable at the higher latitude station, Mawson, as is illustrated by the all-sky camera data, and no marked rapid magnetic disturbance occurred at the 15 polar cap and auroral zone stations shown in Fig. 36. It may be reasonably considered, therefore, that a discrete auroral arc observed at Syowa in the period between 23 h 30 m and 00 h 10 m is not a part of the post-breakup type auroras, but it is the aurora owing to the growth mechanism of a polar substorm.

## 7. Geophysical Phenomena Associated with Auroral and Magnetic Substorm

In this section, we shall examine the occurrence tendencies of polar upper atmospheric phenomena, such as geomagnetic pulsations, VLF emissions and cosmic noise absorptions (CNA) from the viewpoint that a polar substorm consists of the breakup and the post-breakup phases.

### 7.1. General characteristics of geophysical phenomena

It has been noted that the geomagnetic pulsations of Pi type are associated with the auroral and magnetic substorms. The wave forms of irregular pulsations associated with the breakup phase of a polar substorm are clearly different from those during the post-breakup phase, as already pointed out by HEACOCK (1967). According to HEACOCK's terminology, Pi bursts (PiB) are observed in the breakup phase, while PiC pulsations are emitted in the post-breakup phase (cf. Fig. 39).

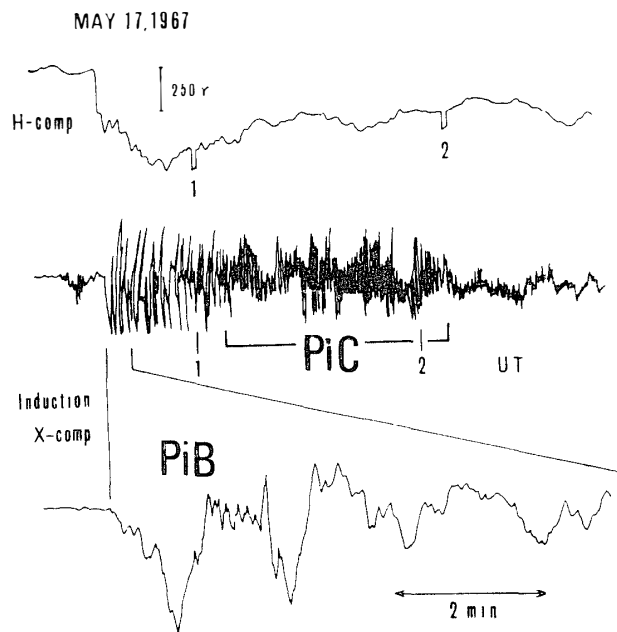


Fig. 39. Example of PiB and PiC geomagnetic pulsations observed at Syowa Station.

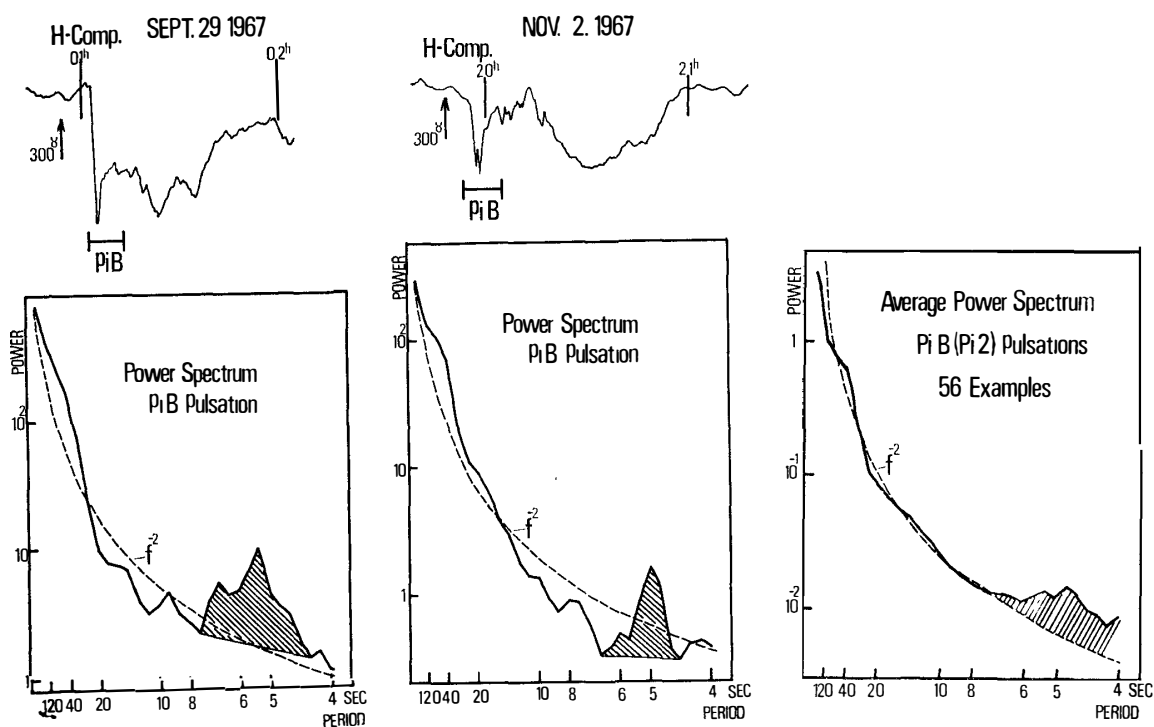


Fig. 40. Typical examples of the power spectrum of PiB geomagnetic pulsations observed at Syowa Station. The dotted line represents the spectrum of  $f^{-2}$ .

Fig. 41. Average power spectrum of 56 examples of PiB geomagnetic pulsations observed at Syowa Station. The dotted line represents the spectrum of  $f^{-2}$ .

Two examples of the dynamic spectrum of PiB pulsations are shown in Fig. 40. Their spectra are of nearly a random noise type which is expressed as proportional to  $f^{-2}$ , where  $f$  represents frequency. However, there is a dominant spectral peak around 5 sec in period superimposed on a falling spectrum of  $f^{-2}$ . Such a spectral form of PiB pulsations is also confirmed by the average power spectrum of 56 examples of PiB pulsations shown in Fig. 41. On the other hand, the individual and average spectra of PiC pulsations illustrated in Figs. 42 and 43, suggest a difference in characteristics between the dynamic spectrum of PiC and that of PiB pulsations; Namely, the spectrum of PiC also is approximately a random noise type as  $f^{-2}$ , similar to that of PiB, but the dominant spectral peak in PiC is found around 10~8 sec in period which is about twice longer than that of PiB. It has also been noted that PiC pulsations have a good correlation with the auroral pulsations (CHAMBELL, 1960) and a one-to-one correspondence is found between PiC and X-Ray fluctuations (McPHERRON *et al.*, 1968).

It has already been established (WATTS, 1957; ELLIS, 1957, 1959; MOROZUMI, 1965, 1967; HARANG *et al.*, 1967; KAMINUMA and HIRASAWA, 1969) that the atmospheric radio noise at kilocycle frequencies is closely associated with strong auroras

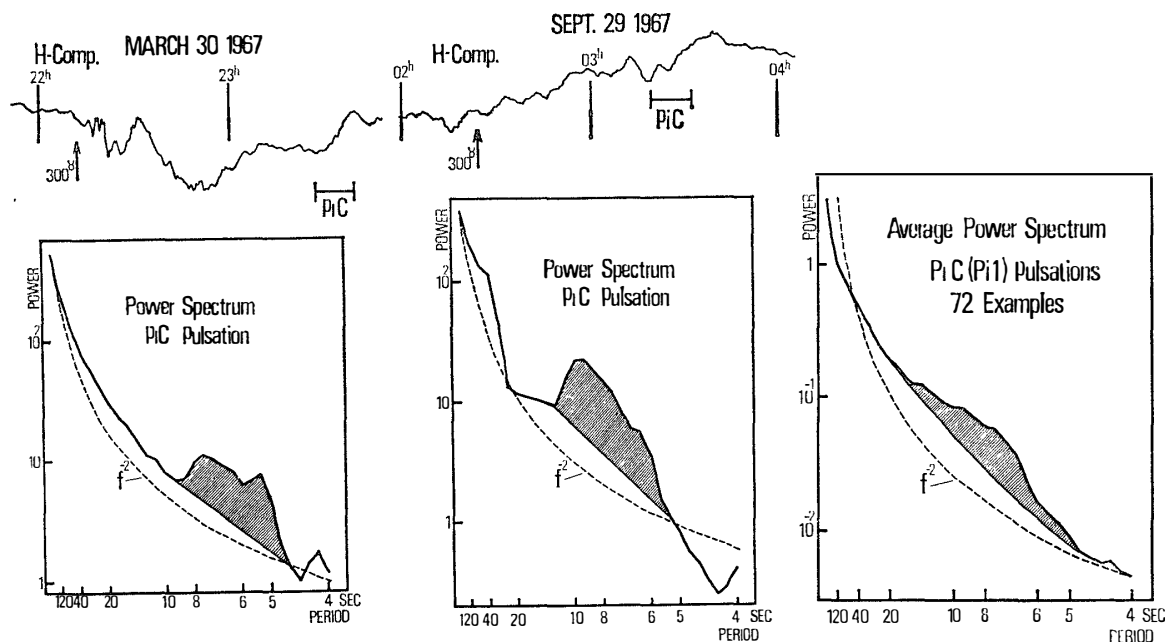


Fig. 42. Typical examples of the power spectrum of PiC geomagnetic pulsations observed at Syowa Station. The dotted line represents the spectrum of  $f^{-2}$ .

Fig. 43. Average power spectrum of 72 examples of PiC geomagnetic pulsations observed at Syowa Station. The dotted line represents the spectrum of  $f^{-2}$ .

(auroral hiss) (cf. Fig. 44 A and B). Fig. 45 represents an example of the VLF auroral hiss (2kHz and 4kHz bands) whose strong emissions are associated with the typical breakup type aurora event observed on June 8, 1957 at Syowa Station. In this example, a beautiful one-to-one correspondence is observed between the intensifications of the auroral hiss emissions and the luminosity fluctuations of the breakup aurora. The diurnal variation in occurrence of the auroral hiss of frequency of 12 kHz is investigated and illustrated in Fig. 46. This diagram shows that the auroral hiss is most frequently observed around midnight ( $\sim 22$ h LT) at a typical auroral zone station, such as Syowa. It is noted that this diurnal tendency agrees well with that of the breakup type auroras illustrated in Fig. 7. These results may indicate that the auroral VLF hiss is certainly caused by the precipitating electrons associated with the breakup type auroras.

As for the VLF chorus observed at Syowa Station, an extensive report has already been published (KOKUBUN *et al.*, 1969), dealing mostly with the polar chorus which is emitted in the daytime sector in high latitudes. However, the post-breakup auroras in the night sector also are almost always accompanied by the chorus type VLF emission. This type of VLF chorus has been noted by MOROZUMI (1965) and MOROZUMI and HELLIWELL (1966), and its characteristics have recently been studied in detail by HAYASHI and KOKUBUN (1971), it being called the auroral chorus. The dynamic spectrum of the auroral chorus consists of fine

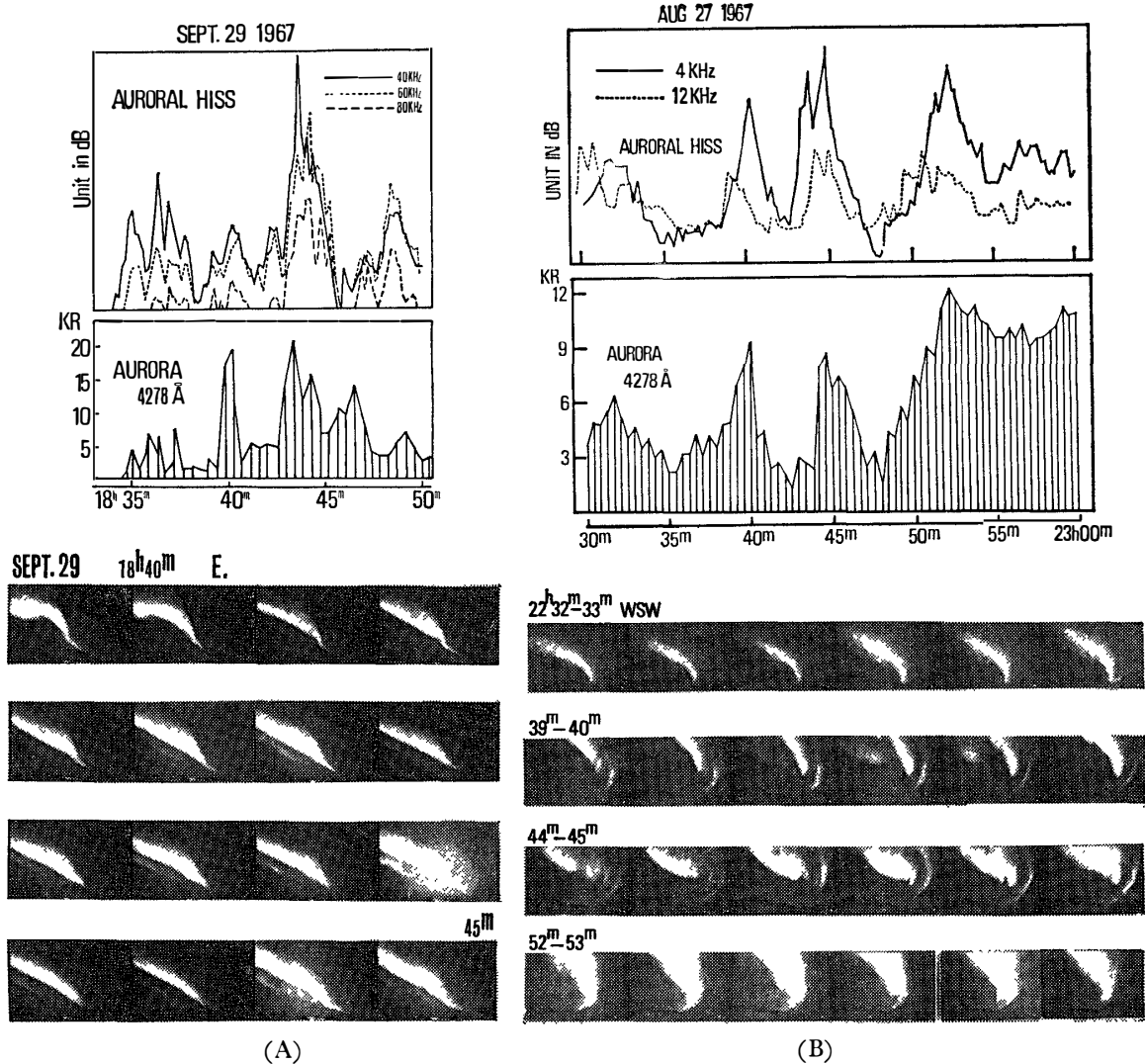


Fig. 44 A and B. Correlation between the intensity of auroral hiss and the luminosity of the auroral arc obtained at Syowa Station. The form of the arc is also shown. E (geomagnetic east) and WSW (west-south-west) indicate camera direction.

discrete-risers of 0.1~0.3 sec in duration and a very weak hiss background. These risers appear in the form of a group of several seconds in duration, and such groups take place intermittently at an interval from several to ten seconds.

The breakup type aurora is associated simultaneously with a sharp cosmic noise absorption (CNA) phenomenon also, as shown in Figs. 47 A and B. The post-breakup phase also is accompanied by the CNA phenomena of smaller magnitude, and each intensification in the post-breakup aurora and the post-breakup magnetic disturbance corresponds to a peak of CNA. Studies on the auroral CNA phenomena have been made in some detail by many research workers (e.g. LITTLE and LEINBACH, 1958; HOLT and OMHOLT, 1962) and their results have been well



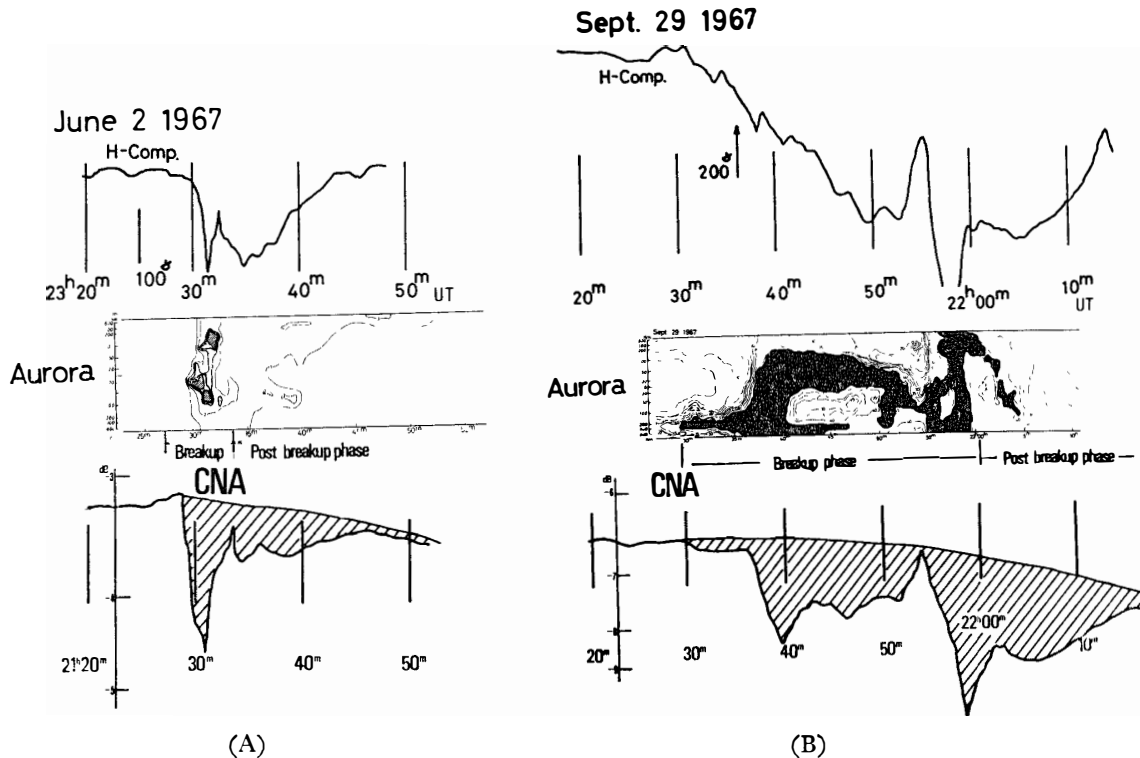


Fig. 47 A and B. Examples of cosmic noise absorption (CNA) associated with the breakup type aurora.

summarized by AKASOFU (1968) under the subject of "ionospheric substorm". The present result about the auroral CNA has nearly the same characteristics as those in AKASOFU's works.

(The details of characteristics of the polar geophysical phenomena associated with the auroral substorm obtained in the present study are discussed in another report which will be published in the near future).

## 7.2. Occurrences of geophysical phenomena in the course of a polar substorm

Simultaneous data of the magnetogram (H-component), the meridian-time auroral diagram, CNA, VLF hiss (4kHz and 12kHz bands), VLF chorus (750Hz band), geomagnetic micropulsations and auroral luminosity variations in zenith on July 11, 1967 are summarized in Fig. 48 for the purpose of correlating the occurrence characteristics of various polar upper atmospheric phenomena in the course of an auroral and magnetic substorm. The diagram of this kind will be called "correlation chart of polar geophysical phenomena" (The chart for the selected 6 nights are given in Appendix of this report). In the auroral diagram in the second of Fig. 48, we find the successive poleward movements of two breakup auroras during the breakup phase of an auroral substorm (from 00h 30 m to 52 m). Corresponding to these breakup auroral events, the sharp variations of the magnetic

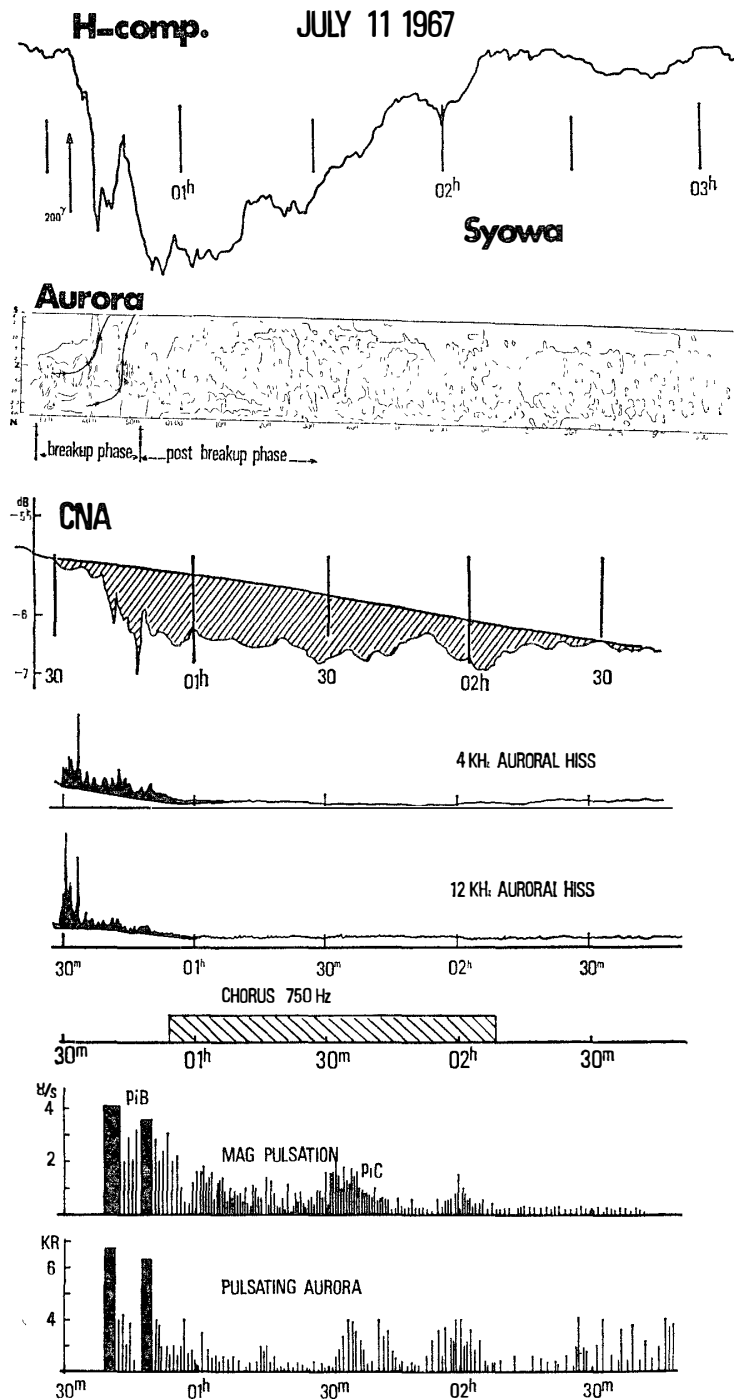


Fig. 48. Example of auroral and magnetic substorm and associated phenomena from top to bottom: (1) Horizontal component of magnetogram. (2) Meridian-time diagram of  $\lambda$  4278Å auroras. (3) CNA. (4) Intensity of VLF hiss emission ( $f=4\text{kHz}$ ). (5) Intensity of VLF hiss emissions ( $f=12\text{kHz}$ ). (6) Intensity of VLF chorus emission ( $f=750\text{Hz}$ ). (7) Amplitude of geomagnetic pulsations. (8) Amplitude of auroral pulsation in the zenith (All observed at Syowa Station).

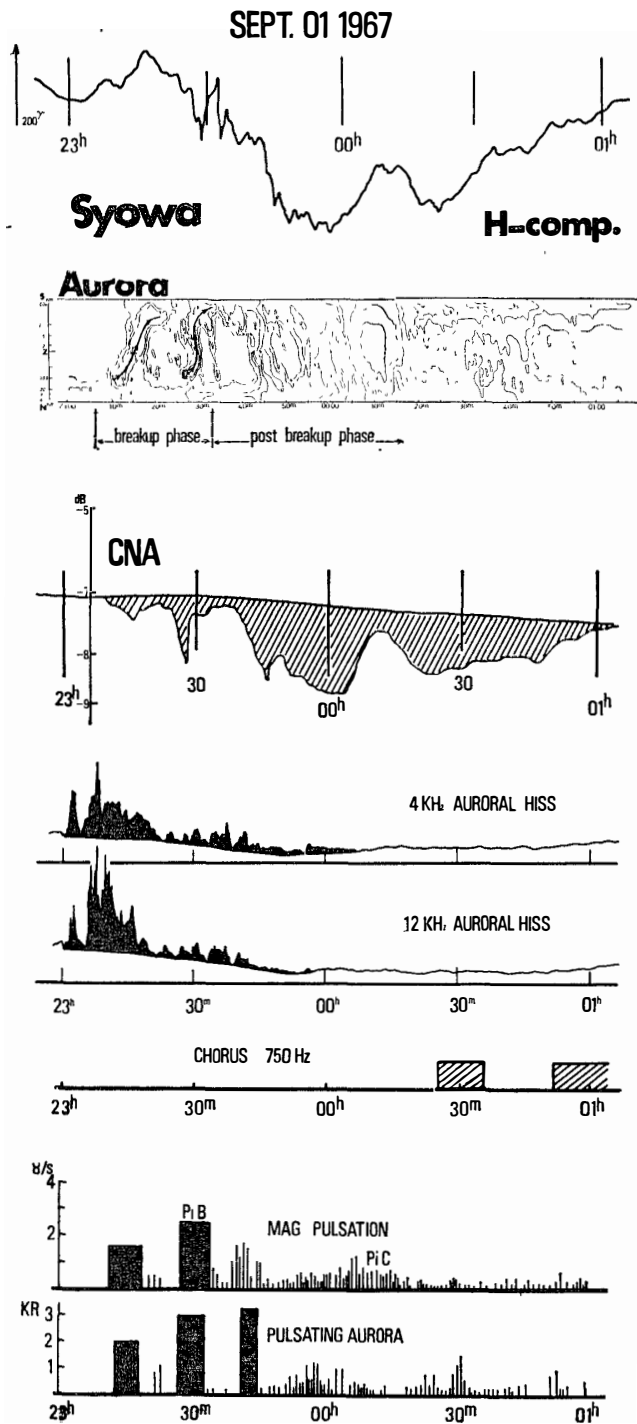


Fig. 49. Example of auroral and magnetic substorm and associated phenomena from top to bottom: (1) Horizontal component of magnetogram. (2) Meridian-time diagram of  $\lambda 4278\text{\AA}$  auroras. (3) CNA. (4) Intensity of VLF hiss emission ( $f=4\text{kHz}$ ). (5) Intensity of VLF hiss emissions ( $f=12\text{kHz}$ ). (6) Intensity of VLF chorus emission ( $f=750\text{Hz}$ ). (7) Amplitude of geomagnetic pulsations. (8) Amplitude of auroral pulsation in the zenith (All observed at Syowa Station).

H-component and CNA, geomagnetic PiB pulsations and the burst intensifications of the zenith auroral luminosity are observed. Auroral VLF hiss is emitted continuously during the breakup phase.

After the breakup type aurora had passed away towards the pole, the post-breakup phase at Syowa Station began and continued till about 03h 00m. During this period, the auroral chorus, the geomagnetic pulsations PiC and the pulsating fluctuations of the zenith auroral luminosity were almost continuously observed, while the auroral hiss disappeared entirely.

Another correlation diagram of the polar geophysical phenomena on Sept. 1, 1967 is given in Fig. 49. The similar occurrence tendencies to those shown in Fig. 48 are detectable in the correlation chart of Fig. 49 also; Namely, the sharp pulsative variations of the magnetic H-component and CNA, auroral hiss, geomagnetic pulsations PiB, burst intensifications of auroral luminosity in zenith during the breakup phase, whereas the gradual variations of magnetic H-component and CNA in association with the activity of the post-breakup type auroras, auroral chorus, geomagnetic pulsation PiC and auroral pulsations.

Judging from the above-mentioned observed facts, it may be concluded that the breakup of auroral and magnetic substorm is simultaneously accompanied by the sharp CNA, the auroral hiss and the PiB type of geomagnetic pulsations. On the other hand, the post-breakup phase is characterized by the gradual variation of CNA, the auroral chorus, the PiC type of geomagnetic pulsations and the pulsating fluctuations of the auroral luminosity.

## 8. Discussion and Summary

### 8.1. Constitution of an auroral substorm

A time sequence of an auroral substorm phenomenon has been divided into three phases, namely (i) the pre-breakup (ii) the breakup and (iii) the post-breakup phases (*e.g.* AKASOFU, 1968). The result of the present studies on the auroral substorm strongly supports the concept of the breakup and the post-breakup phases (*cf.* Section 3). Phenomenologically, the present authors also have noticed a certain kind of auroral agitations precedent to an auroral breakup, but they have not yet been able to conclude whether this apparent pre-breakup aurora is a precursor phenomenon (the indication of the energy storage in the magnetosphere) of an isolated auroral substorm or a part of the post-breakup type aurora of another auroral substorm which broke up previously in a certain higher latitude. Although we could find in the previous section an auroral phenomenon which is very likely due to the growth mechanism of a polar substorm, this question should be regarded still pending, because extensive studies on this problem dependent on time as well as on space have not yet been completed.

### 8.2. Breakup type aurora

In the present study, the following characteristics of the breakup type aurora are noted:

(1) An enhanced auroral arc or band with the discrete structure lying quietly along the geomagnetic east-west direction (pre-stage, B1-stage) for a while precedes the main stage which is characterized by a rapid poleward movement with the increasing brightness (main stage, B2-stage).

(2) The breakup type auroras are most frequently observed around the midnight (from 23–24h, Geomag. LT) at the typical auroral zone station. It is also noted that their occurrences are less frequent in the morning than in the evening hours and no breakup type aurora are observable after 02h LT.

(3) The duration of their B1-stage is shortest around midnight (about 2 min) and longest at the dusk side (about 25 min). This fact may indicate that their poleward movement begins from the midnight sector and propagates towards the dusk.

(4) The duration of the B2-stage ranges from 5 to 30 min, the median value being 10 min or so.

(5) The speed of their poleward movements ranges mostly from 0.5 to 1.5 km/s,

the median value being 1 km/s.

(6) During the course of an auroral substorm, one or more breakup type auroras often appear in the night sector of the auroral oval.

AKASOFU (1964, 1968) has shown the growth and decay of a model auroral substorm based on the extensive investigations of the all-sky camera data obtained at widely distributed polar stations. His concept of the auroral substorm is as follows: the first indication of the substorm is a sudden brightening of one of the quiet arcs lying in the midnight sector of the oval. In most cases, the brightening of an arc is followed by its rapid poleward motion, resulting in an 'auroral buldge' around the midnight sector. As the auroral substorm progresses, the buldge expands in all directions. In the evening side of the expanding buldge, a large-scale fold appears which travels rapidly westward along an arc; namely forming the westward traveling surge.

AKASOFU's concept of the auroral substorm gives a fairly good agreement with our result concerning the breakup type aurora, if we could consider that the breakup type aurora discussed in the present study contains, phenomenologically, AKASOFU's sudden brightening of an arc, its rapid poleward motion resulting in an 'auroral buldge' and the westward traveling surge. OGUTI (1969) has illustrated also the similar poleward shift of the narrow, westward electric current filament associated with the active aurora (the average speed of about 600 m/s), from his analysis of "Magnetic spikes" which appear on the evening side in the region from the auroral zone to 80° geomagnetic latitude.

An attempt is made to draw the schematic diagram to show the space-time development of a breakup type aurora, based on its statistical characteristics ob-

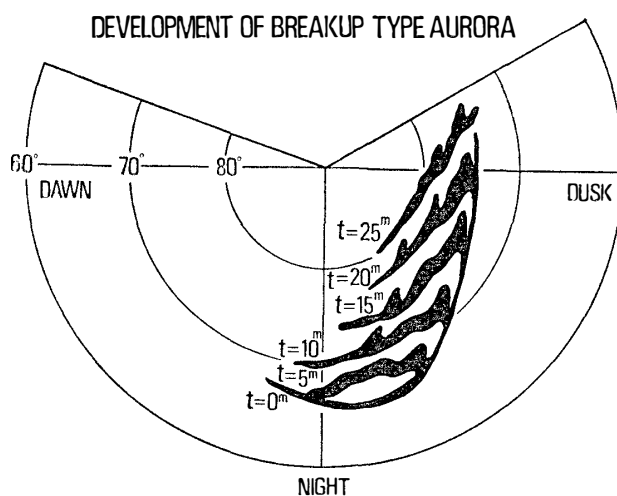


Fig. 50. Schematic diagram showing the space-time development of a breakup type aurora, view from the south geomagnetic pole a few earth radii above the ionosphere.

tained in the present study and referred also to AKASOFU and OGUTI's concepts. Fig. 50 shows the growth and decay of a model breakup type aurora.

**8.3. Elemental auroral substorm**

As is clearly illustrated in Section 5.1., the "breakup" and the "post-breakup type aurora" compose a pair event. We may call the pair of "breakup type aurora" on the poleward side border and the "post-breakup type aurora" expanding equatorwards from the edge of "breakup type aurora" as "an elemental auroral substorm". In actual cases, the so-called auroral substorm consists of the spatial and temporal summation of several "elemental auroral substorms", as schematically illustrated in the bottom of the left figure of Fig. 51.

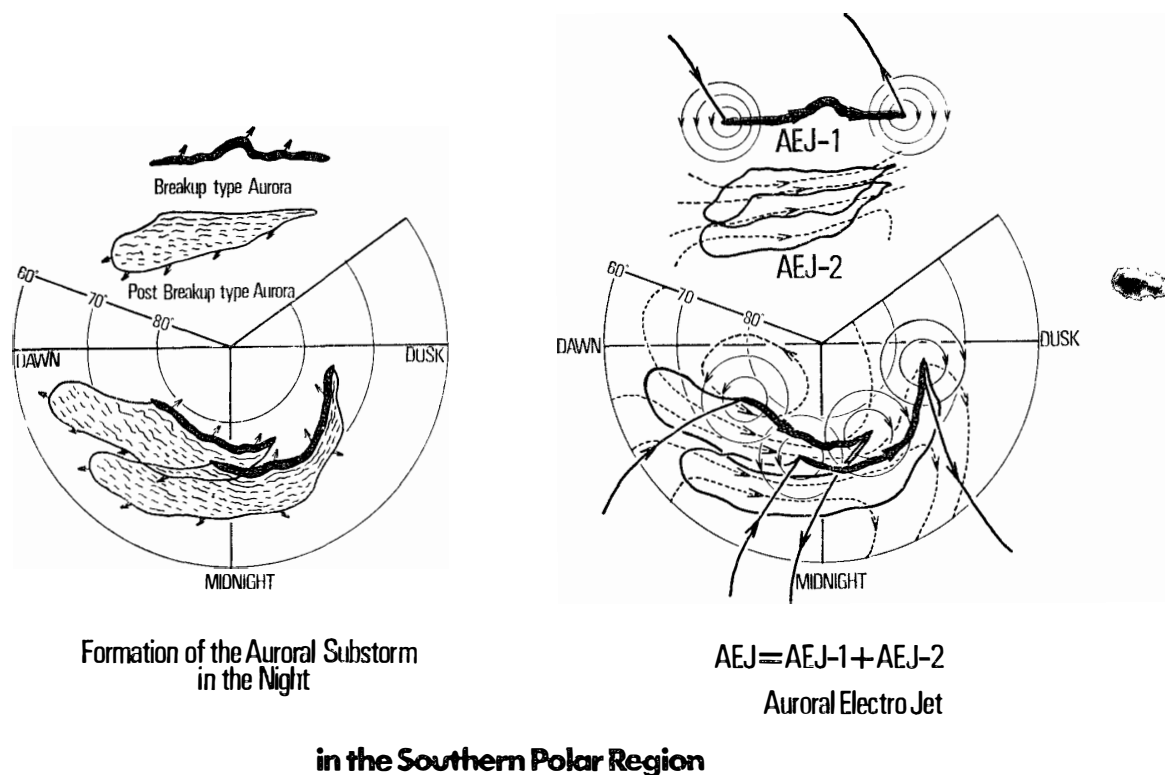


Fig. 51. Schematic representation of the structure of the auroral substorm and of the auroral electrojet.

- Left top: Form and movement of a breakup type aurora.
- Left middle: Form and movement of a post-breakup type aurora.
- Left bottom: Structure of auroras at an instant time in the polar regions (multi-appearance of the elemental auroral substorms).
- Right top: Electric current of AEJ-1 and magnetic field-aligned current.
- Right middle: Electric current of AEJ-2.
- Right bottom: Electric current systems corresponding to the left side structure of auroras.

#### 8.4. Breakup and post-breakup magnetic disturbances

As is discussed in detail in Sections 4 and 5, magnetic variations associated with the auroras can be divided into two types, namely (1) the breakup magnetic disturbance which is originated in the sudden intensification and the rapid poleward movement of the breakup type aurora and shows the transient or the pulsative variation with the duration of about 10-20 min and (2) the post-breakup magnetic disturbance which shows the gradual development and decay in accord with the activities of the post-breakup type auroras.

Some examples of the schematic typical magnetic substorm (H-component) which is frequently observed in the polar observatories are reproduced on the left hand of Fig. 52. In the top of the figure, the magnetic substorm which occurs around the evening hours at the typical auroral zone station is illustrated. In this case, the phenomenological characteristics may be described as follows: a breakup type aurora suddenly brightens near the zenith or at the slightly poleward side of the observing station and shows a rapid poleward motion. This breakup auroral display causes the negative H-component variation at first and then the rapid positive one in association with the auroral poleward movement (breakup

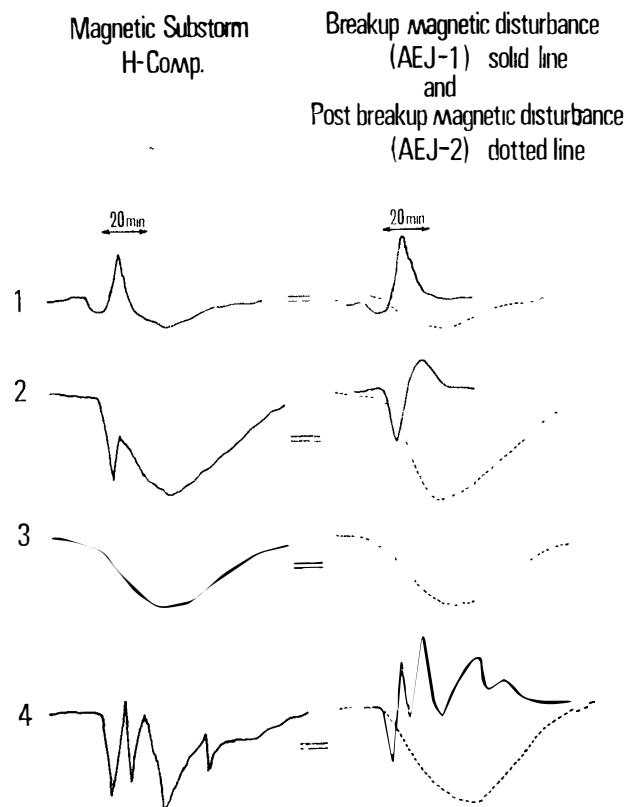


Fig. 52. Schematic illustration of the constitution of the typical magnetic substorm.

magnetic disturbance). Thereafter, the post-breakup type auroras cover gradually over the wide area. The magnetic disturbance develops and decays in accordance with this auroral activity (the post-breakup magnetic disturbance). The bay-shape magnetic substorm shown in the second of the left in Fig. 52 is frequently observable around the midnight sector. In this case, the breakup type aurora starts from the equator side of the observing station, passes over the zenith and propagates away towards the pole. The magnetic variation shows a sharp drop in the H-component at first and then tends towards the positive in association with this breakup auroral display (the breakup magnetic disturbance). Thereafter, the post-breakup magnetic disturbance gradually develops in proportion to the activation of the post-breakup type auroras. The third of Fig. 52 represents an example of the magnetic substorm which is caused mainly by the post-breakup type aurora with a slight effect of the breakup type aurora in the pole side far from the observing point. The magnetic substorms of this type are more frequently observed in the dawn than in the dusk hours. The bottom example in Fig. 52 shows the magnetic substorm during which several breakup type auroras occur successively near the observing area.

As mentioned above, the magnetic substorms shown on the left of Fig. 52 are considered to consist of the “breakup” (solid line) and the “post-breakup magnetic disturbance” (dotted line), such as illustrated in the right. One may express therefore the structure of a magnetic substorm observed at a station in or near the auroral zone by the following diagram :

$$\boxed{\text{Magnetic substorm}} = \boxed{\text{Breakup magnetic disturbance}} + \boxed{\text{Post-breakup magnetic disturbance}}$$

### 8.5. Current flow associated with aurora. Auroral electrojet (AEJ)

As previously described in Section 4.2., the auroral electrojet associated with a breakup type aurora (AEJ-1) would be the three-dimensional current flow, such as shown in the top of the right figure in Fig. 51. The rapid poleward motion of AEJ-1 causes a sharp pulsative magnetic variation (the breakup magnetic disturbance, cf. Section 8.4.).

A number of observed facts seem to suggest a difference in characteristics between the electrojet associated with the breakup type aurora (AEJ-1) and that with the post-breakup type aurora (AEJ-2). Namely, the horizontal magnetic vector ( $\vec{H}$ ) considerably changes its direction during the breakup phase, while it points quietly southward (overhead current westward) during the post-breakup phase. The auroral electrojet during the latter phase is represented mostly by a quasi-steady westward electrojet, which is accompanied by a diffused surface or rays of comparatively weak auroras and which is extended throughout the geomagnetic meridional width of  $10^\circ \sim 20^\circ$ . It seems likely therefore that the post-breakup type auroral electrojet is mostly due to the steady current flow through the high electrical conductive area continuously ionized by the post-breakup auroral particles. The motive electric field for this current would be the large scale

field given over the entire polar region, such as the dawn-dusk electric field; (SP-field or DP-2 field). The middle of the right figure in Fig. 51 is a schematic figure of such a post-breakup type auroral area and the associated auroral electrojet (AEJ-2).

The bottom of the right side of Fig. 51 represents the electric current systems which correspond to the multi-occurrence of the elemental auroral substorms. As

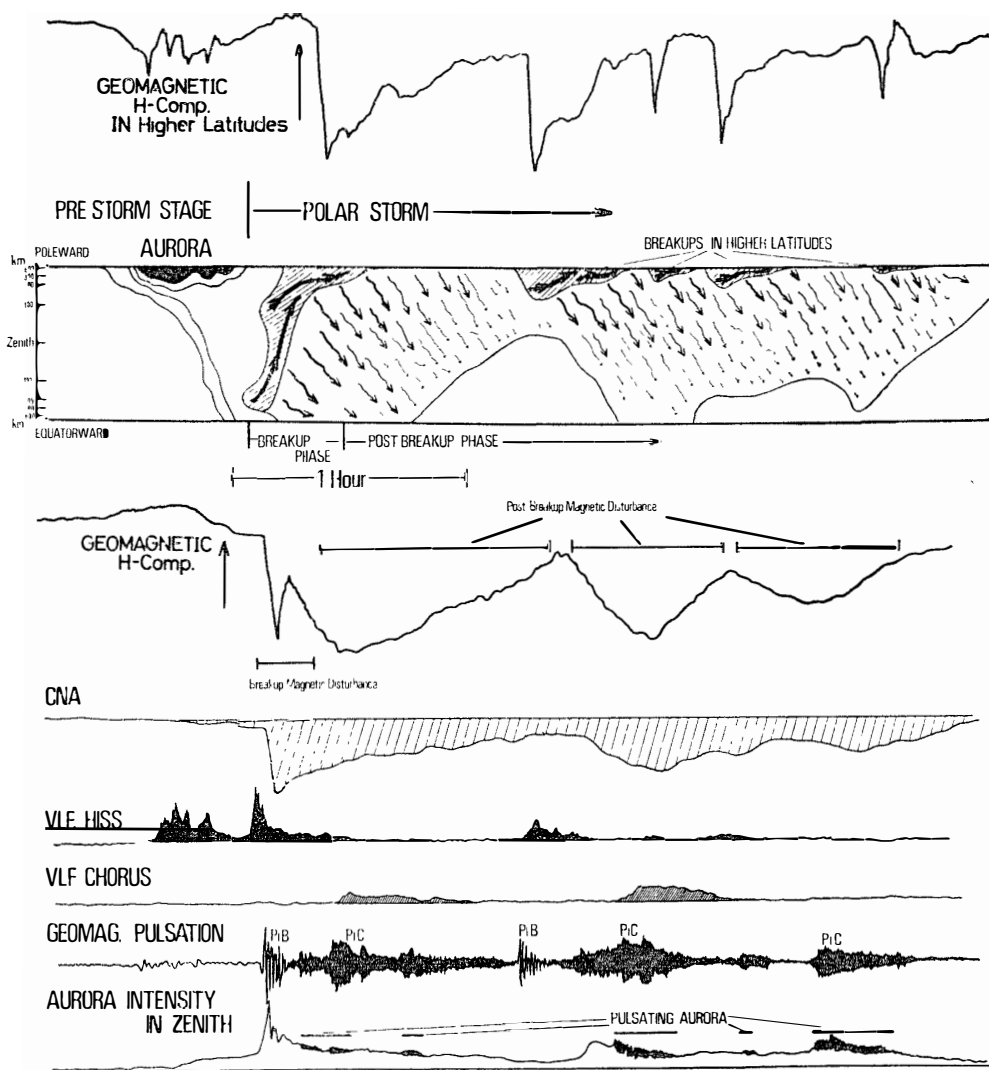


**Fig. 53.** Schematic summary of polar substorms and associated phenomena from top to bottom: (1) Horizontal geomagnetic variation at higher latitudes. (2) Meridian-time diagram of auroras at an auroral zone station. (3) Horizontal geomagnetic variation at a station same as (2). (4) CNA observed at a station same as (2). (5) Intensity of VLF hiss observed at a station same as (2). (6) Intensity of VLF chorus observed at a station same as (2). (7) Geomagnetic pulsations observed at a station same as (2). (8) Intensity of aurora at the zenith of a station same as (2).

illustrated in this figure, the auroral electrojet responsible for the polar substorm may be expressed by the following diagram.

$$\boxed{\begin{array}{c} \text{Westward AEJ} \\ \text{during the magnetic} \\ \text{substorm} \end{array}} = \boxed{\begin{array}{c} \text{AEJ-1} \\ \text{associated with} \\ \text{breakup type auroras} \end{array}} + \boxed{\begin{array}{c} \text{AEJ-2} \\ \text{associated with post-} \\ \text{breakup type auroras} \end{array}}$$

### 8.6. Summary of polar substorm and associated phenomena

The relationships among the polar geophysical phenomena associated with the polar substorm are summarized in the following table, which have been obtained based on the various kinds of the observational facts in the present study.

	Breakup phase of polar substorm	Post-breakup phase of polar substorm
Aurora	Breakup type aurora	Post-breakup type aurora
Geomagnetism	Breakup magnetic disturbance	Post-breakup magnetic disturbance
Auroral electrojet	AEJ-1 (westward)	AEJ-2 (westward)
Geomagnetic pulsations	PiB (auroral zone Pi 2)	PiC (auroral zone Pi 1)
VLF emission	Auroral hiss	Auroral chorus
Cosmic noise absorption	Sharp CNA	Broad CNA

In Fig. 53, a schematic summary of polar substorms and associated phenomena is represented.

### Acknowledgments

The authors wish to express their most hearty gratitude to all member of the 8th wintering party of Japanese Antarctic Research Expedition for their valuable assistance. They also wish to thank Prof. N. FUKUSHIMA and Dr. T. IJIMA for their kind discussions. They are indebted to Prof. T. OGUTI, Dr. T. TOHMATSU, Dr. S. KOKUBUN and Dr. E. KANEDA for their kind encouragement and advice in planning the instrumentations for the observations.

## References

- AKASOFU, S.-I. (1960): Large-scale auroral motions and polar magnetic disturbances, I. *J. Atmos. Terr. Phys.*, **19**, 10-25.
- AKASOFU, S.-I. (1964): The development of the auroral substorm. *Planet. Space Sci.*, **12**, 273-282.
- AKASOFU, S.-I. (1965): Dynamic morphology of auroras. *Space Sci. Rev.*, **4**, 498-540.
- AKASOFU, S.-I. (1968): Polar and magnetospheric substorms. D. Reidel, Dordrecht, 1-280.
- AKASOFU, S.-I. and S. CHAPMAN (1963): The lower limit of latitude (U.S. sector) of northern quiet auroral arcs, and its relation to Dst (H). *J. Atmos. Terr. Phys.*, **25**, 9-12.
- AKASOFU, S.-I. and C.-I. MENG (1969): A study of polar magnetic substorms. *J. Geophys. Res.*, **74**, 293-313.
- ALFVÉN, H. (1939, 1940): A theory of magnetic storms and of the aurorae. *Kungl. Sv. Vetensk.-Akad. Handl., Ser. III*, **18**, (3 and 9).
- ATKINSON, G. (1967): The current system of geomagnetic bays. *J. Geophys. Res.*, **72**, 6063-6067.
- AUBRY, M.P. and R.L. MCPHERRON (1971): Magnetotail changes in relation to the solar wind magnetic field and magnetospheric substorms. *J. Geophys. Res.*, **76**, 4381-4401.
- AUBRY, M.P., C.T. RUSSELL and M.G. KWELSON (1970): On inward motion of the magnetopause before a substorm. *J. Geophys. Res.*, **75**, 7018-7031.
- BIRKELAND, K. (1913): The Norwegian aurora polaris expedition, 1902-1903, Vol. I.
- CAMIDGE, F.P. and G. ROSTORFER (1970): Magnetic field perturbations in the magnetotail associated with polar substorms. *Can. J. Phys.*, **48**, 2002-2010.
- CAMPBELL, W.H. (1960): Magnetic micropulsations, pulsating aurora. *J. Geophys. Res.*, **65**, 784.
- CHAPMAN, S. (1935): The electric current-systems of magnetic storms. *Terr. Magn.*, **40**, 349-370.
- DAVIS, T.N. (1962): The morphology of the aurora display of 1957-1958, I. Statistical analysis of Alaska data. *J. Geophys. Res.*, **67**, 59-74.
- ELLIS, G.R. (1957): Low-frequency radio emission from aurorae. *J. Atmos. Terr. Phys.*, **10**, 302-306 (1957).
- ELLIS, G.R. (1959): Low-frequency electromagnetic radiation associated with magnetic disturbances. *Planet. Space Sci.*, **1**, 253-258.
- FAIRFIELD, D.H. and L.J. CAHILL (1966): Transition region magnetic field and polar magnetic disturbances. *J. Geophys. Res.*, **71**, 155-169.
- FELDSHTEYN, Y.I. (1964): Auroral morphology I. The location of the auroral zone. *Tellus*, **16**, 252-257.
- FUKUSHIMA, N. (1953): Polar magnetic storms and geomagnetic bays. *J. Fac. Sci. Tokyo Univ.*, **8**, 293-412.
- FUKUSHIMA, N. (1971): Electric current-system for polar substorms and their magnetic effect below and above the ionosphere. *Radio Sci.*, **6**, 269-275.
- HAYASHI, K. and S. KOKUBUN (1972): VLF emissions during post breakup phase of polar substorm. *Rep. Ionosph. Space Res. Japan* (in press).
- HEPPNER, J.P. (1954): A study of the relationships between the aurora borealis and the geomagnetic disturbances caused by electric currents in the ionosphere. Thesis, California Institute of Technology.
- HIRASAWA, T. and K. KAMINUMA (1970): Space-time variation of aurora and geomagnetic disturbance—Auroral observations at Syowa Station in Antarctica—1967-1968. *JARE Sci. Rep., Ser. A*, No. 8, 1-29.
- HIRSHBERG, J. and D.S. COLBURN (1969): Interplanetary field and geomagnetic variations—a unified view. *Planet. Space Sci.*, **17**, 1183-1206.

- HOLT, O. and A. OMHOLT (1962): Auroral luminosity and absorption of cosmic radio noise. *J. Atmos. Terr. Phys.*, **24**, 467-474.
- HONES, E.W., S.-I. AKASOFU, P. PERREAULT, S.J. BAME and S. SENJER (1970): Poleward expansion of the auroral oval and associated phenomena in the magnetotail during auroral substorms. *J. Geophys. Res.*, **75**, 7060-7074.
- HONES, E.W., J.R. ASBRIDGE and S.J. BAME (1971): Time variations of the magnetotail plasma sheet at 18 Re determined from concurrent observations by a pair of Vela satellites. *J. Geophys. Res.*, **76**, 4402-4419.
- IJIMA, T. (1968): Comparison of magnetic field variation on the ground, in the magnetosphere and interplanetary space. *Rep. Ionosph. Space Res. Japan*, **22**, 295-300.
- IJIMA, T. and T. NAGATA (1970): The constitution of magnetospheric storms. *Ann. Géophys.*, **26**, 417-426.
- IJIMA, T. and T. NAGATA (1971): Signatures for substorm development of the growth phase and expansion phase. *Planet. Space Sci.* (in press).
- KAMINUMA, K. and T. HIRASAWA (1969): Auroral observation of Syowa Station, 1967-1968. *Antarctic Rec.*, **35**, 22-34.
- KOKUBUN, S. (1971): Polar substorm and interplanetary magnetic field. *Planet. Space Sci.*, **19**, 697-714.
- KOKUBUN, S., K. HAYASHI and T. OGUTI (1969): VLF emission study at Syowa Station Antarctica—Polar chorus emission and worldwide geomagnetic variation. *JARE Sci. Rep.*, Ser. A., No. 6, 1-34.
- LITTLE, C.G. and H. LEINBACH (1958): Some measurements of high-latitude ionospheric absorption using extra terrestrial radio waves. *Proc. Instn Radio Engrs*, **46**, 334-348.
- MOROZUMI, H.M. (1965): Diurnal variation of auroral zone geophysical disturbances. *Rep. Ionosph. Space Res. Japan*, **19**, 286-298.
- MOROZUMI, H.M. (1967): Auroral zone; geophysical phenomena and their relationship to the magnetosphere. *JARE Sci. Rep.*, Special Issue, No. 1, Proc. Symp. Pacific-Antarctic Sci., 53-64.
- MOROZUMI, H.M. and R.A. HELLIWELL (1966): A correlation study of the diurnal variation of upper atmospheric phenomena in the southern auroral zone. *Radio Sci. Lab. Stanford Univ.*, SU-SEL-66-124.
- MCPHERRON, R.L. (1970): Growth phase of magnetospheric substorms. *J. Geophys. Res.*, **75**, 5592-5599.
- MCPHERRON, R.L., G.K. PARKS, F.V. CORONITI and S.H. WARD (1968): Studies of the magnetospheric substorm. 2. Correlated magnetic micropulsations and electron precipitation occurring during auroral substorms. *J. Geophys. Res.*, **73**, 1697-1713.
- OGUTI, T. (1963): Inter-relations among the upper atmosphere disturbance phenomena in the auroral zone. *JARE Sci. Rep.*, Ser. A, No. 1, 1-82.
- OGUTI, T. (1969): Poleward travel of electric current filament in the polar cap region. *Rep. Ionosph. Space Res. Japan*, **23**, 175-184.
- ROSTOKER, C. (1968): Macrostructure of geomagnetic bays. *J. Geophys. Res.*, **73**, 4217-4229.
- RUSSELL, C.T., R.L. MCPHERRON, and P.J. COLEMAN, Jr. (1971): Magnetic field variations in the near geomagnetic tail associated with the weak substorm activity. *J. Geophys. Res.*, **76**, 1823-1829.
- SILSBEE, H.C. and E.H. VESTINE (1942): Geomagnetic bays, their frequency and current-systems. *Terr. Magn.*, **47**, 195-208.
- VASYLIUNAS, V.M. (1968): A survey of low-energy electrons in the evening sector of the mag-

70 Constitution of Polar Substorm and Associated Phenomena in the Southern Polar Region

netosphere with OGO 1 and OGO 3. J. Geophys. Res., **73**, 2839-2884.

VESTINE, E.H. and S. CHAPMAN (1938): The electric current-system of geomagnetic disturbance. Terr. Magn., **43**, 351-382.

WATTS, J.M. (1957): An observation of audio-frequency electromagnetic noise during a period of solar disturbance. J. Geophys. Res., **62**, 199-206.

*(Manuscript received January 5, 1972)*

## APPENDIX

## Correlation Chart of Polar Geophysical Phenomena

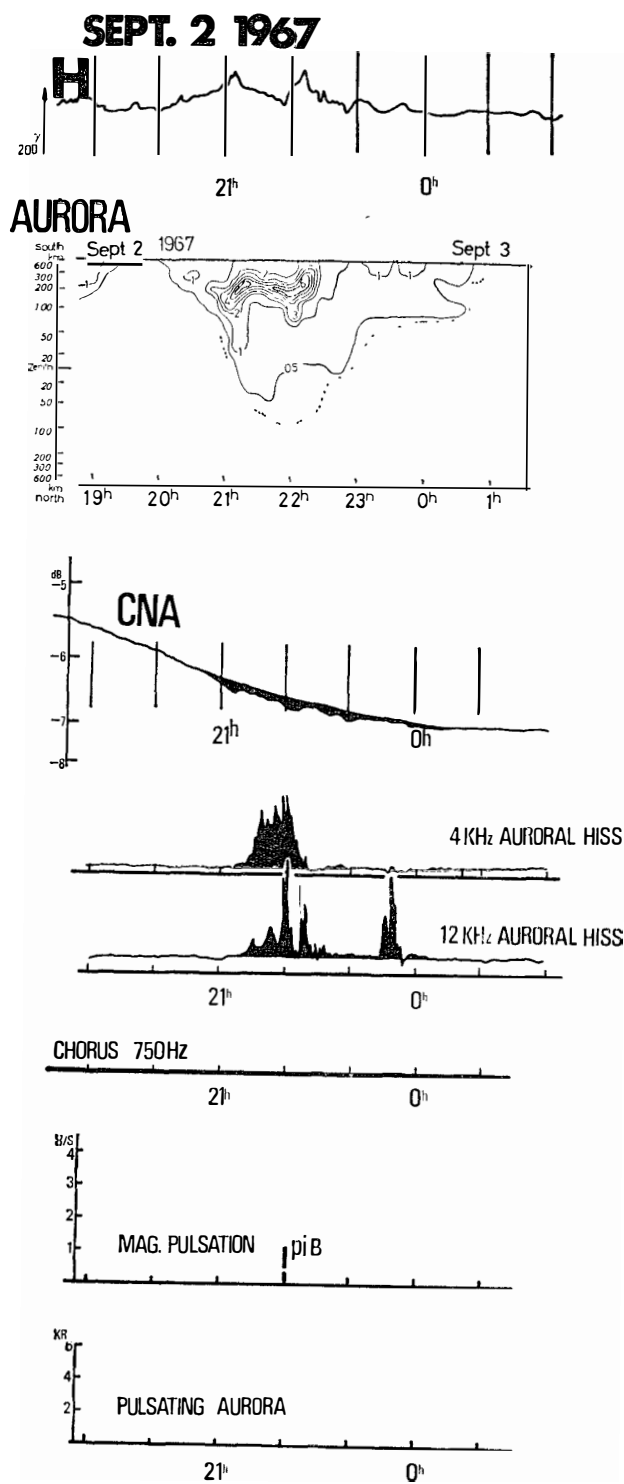


Fig. A-I. Example of auroral and magnetic variations through a night and associated phenomena from top to bottom: (1) Horizontal component of magnetogram. (2) Meridian-time diagram of  $\lambda$  4278Å auroras. Contour; "1" corresponds to 1kR. (3) CNA. (4) Intensity of VLF hiss emissions ( $f=4\text{kHz}$ ). (5) Intensity of VLF emissions ( $f=12\text{kHz}$ ). (6) Approximated intensity of VLF chorus emissions ( $f=750\text{Hz}$ ). (7) Amplitude of geomagnetic pulsations. (8) Amplitude of auroral pulsation in the zenith (All observed at Syowa Station).

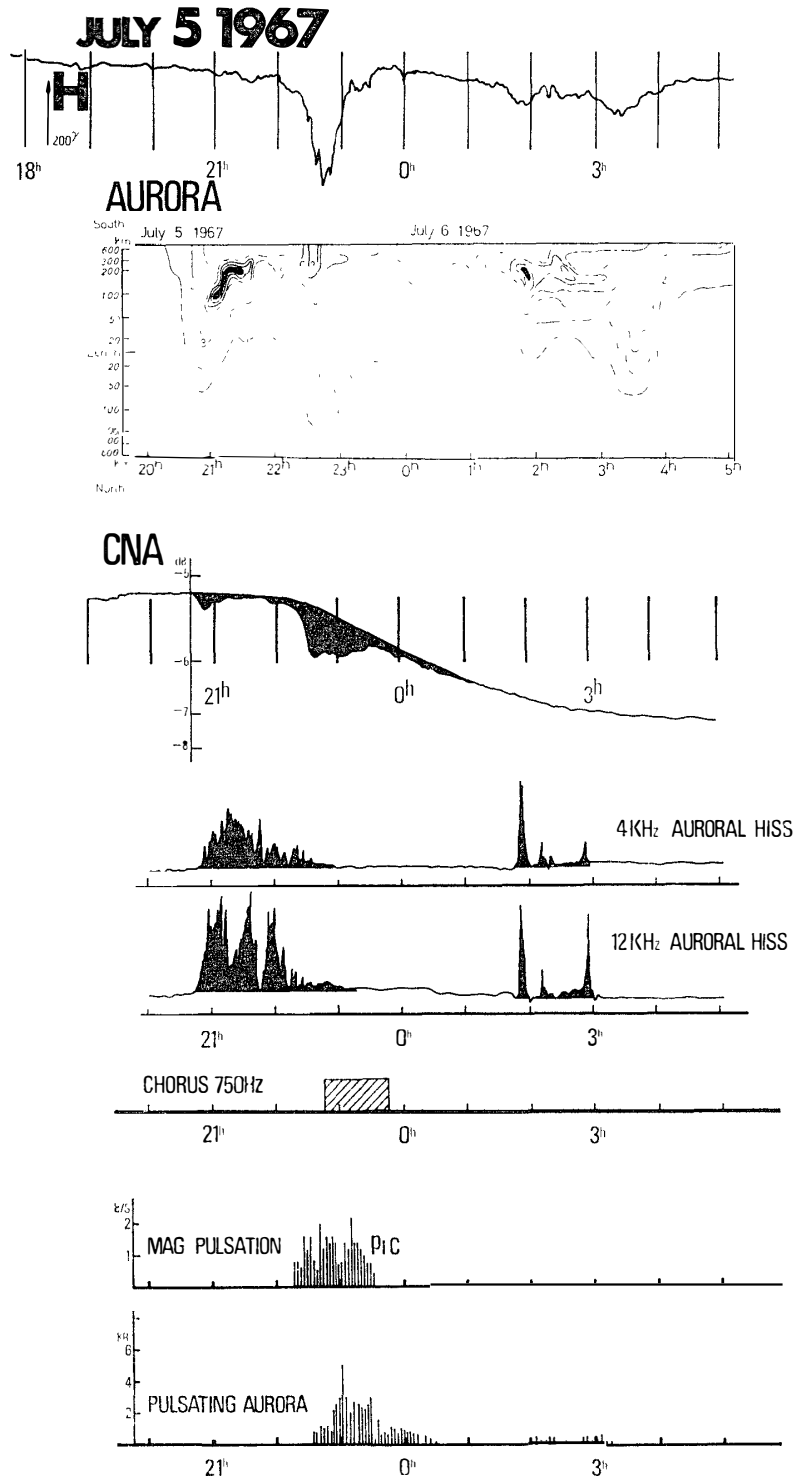


Fig. A-II. The same as that for Fig. A-I.

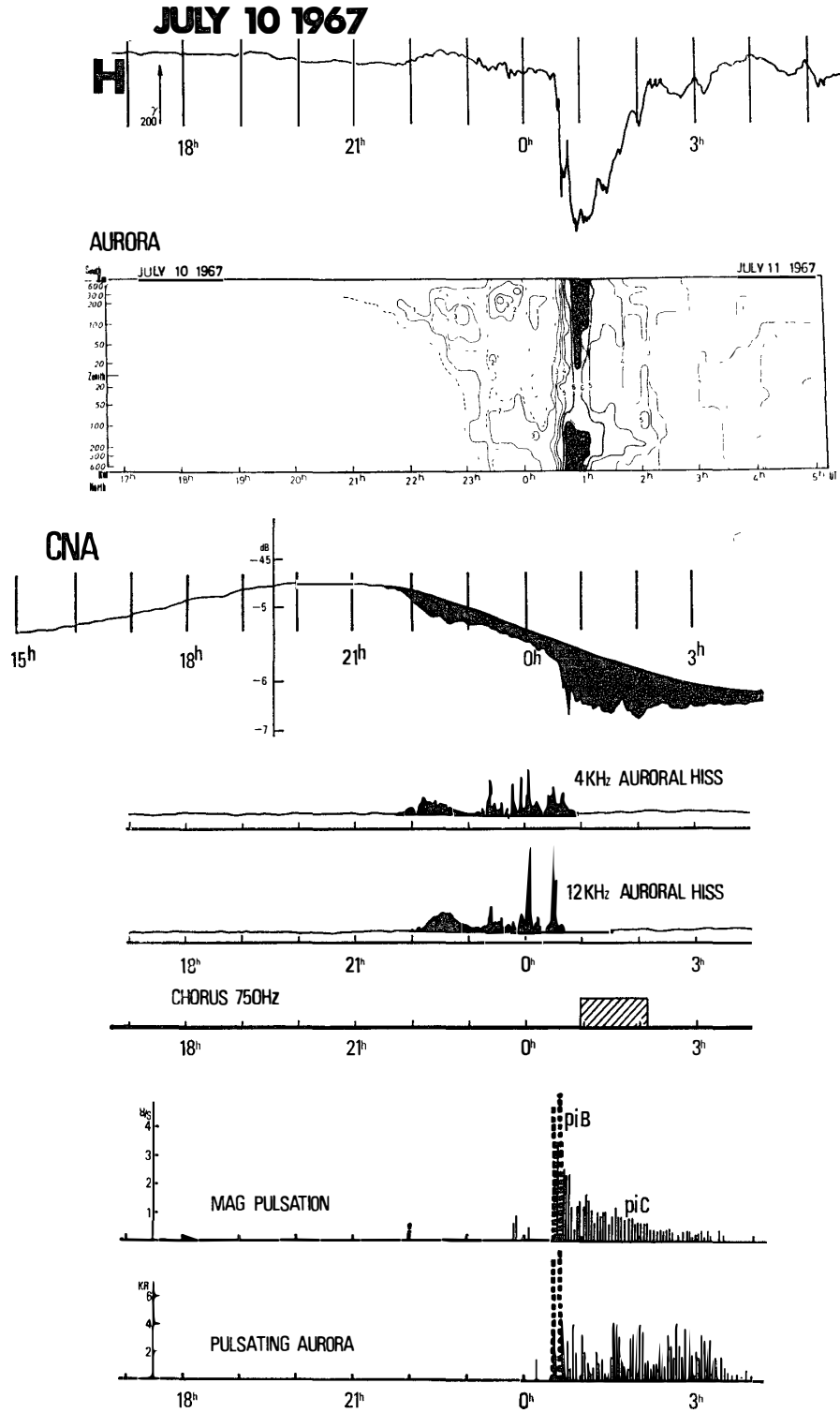


Fig. A-III. The same as that for Fig. A-I.

74 Constitution of Polar Substorm and Associated Phenomena in the Southern Polar Region

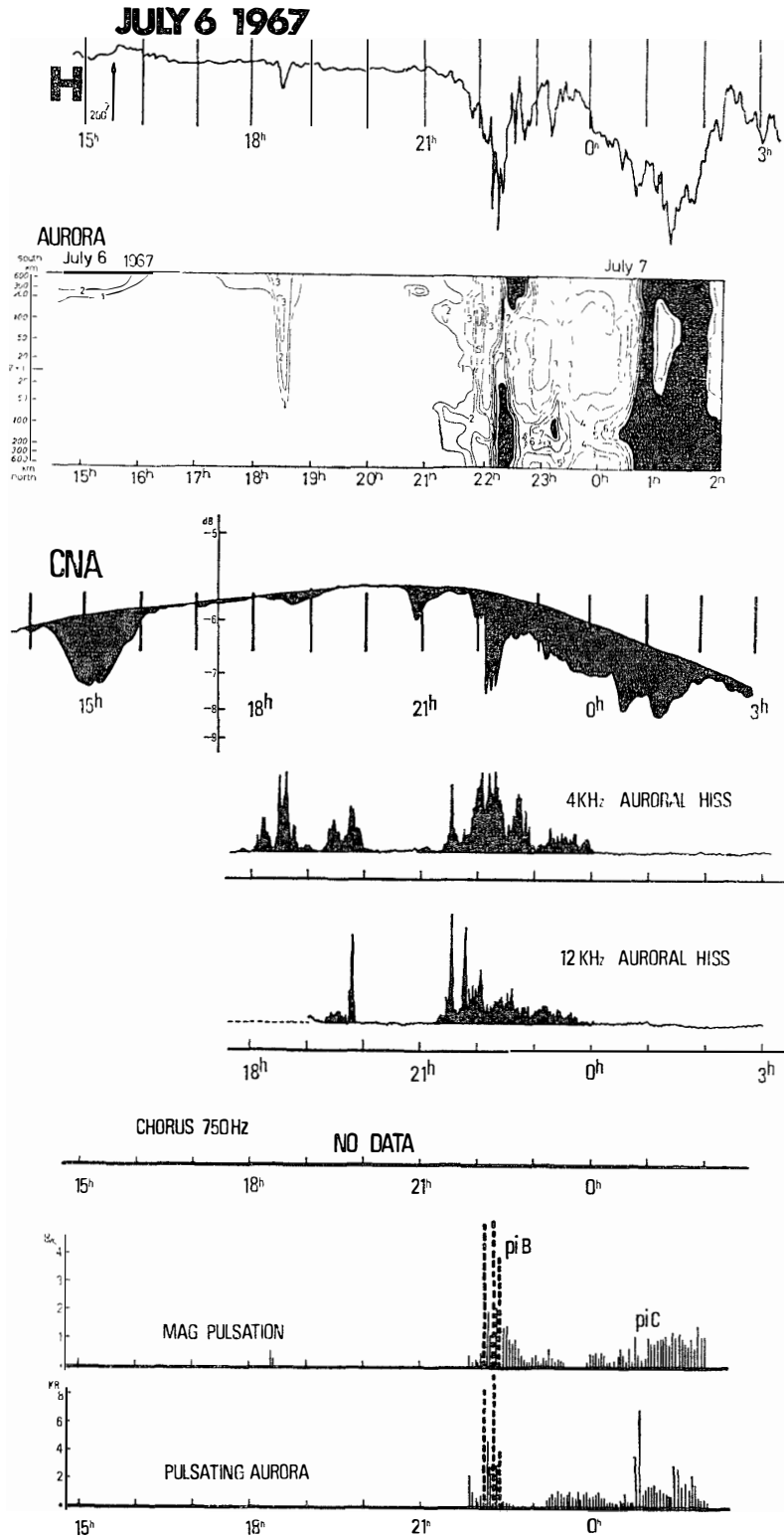


Fig. A-IV. The same as that for Fig. A-I.

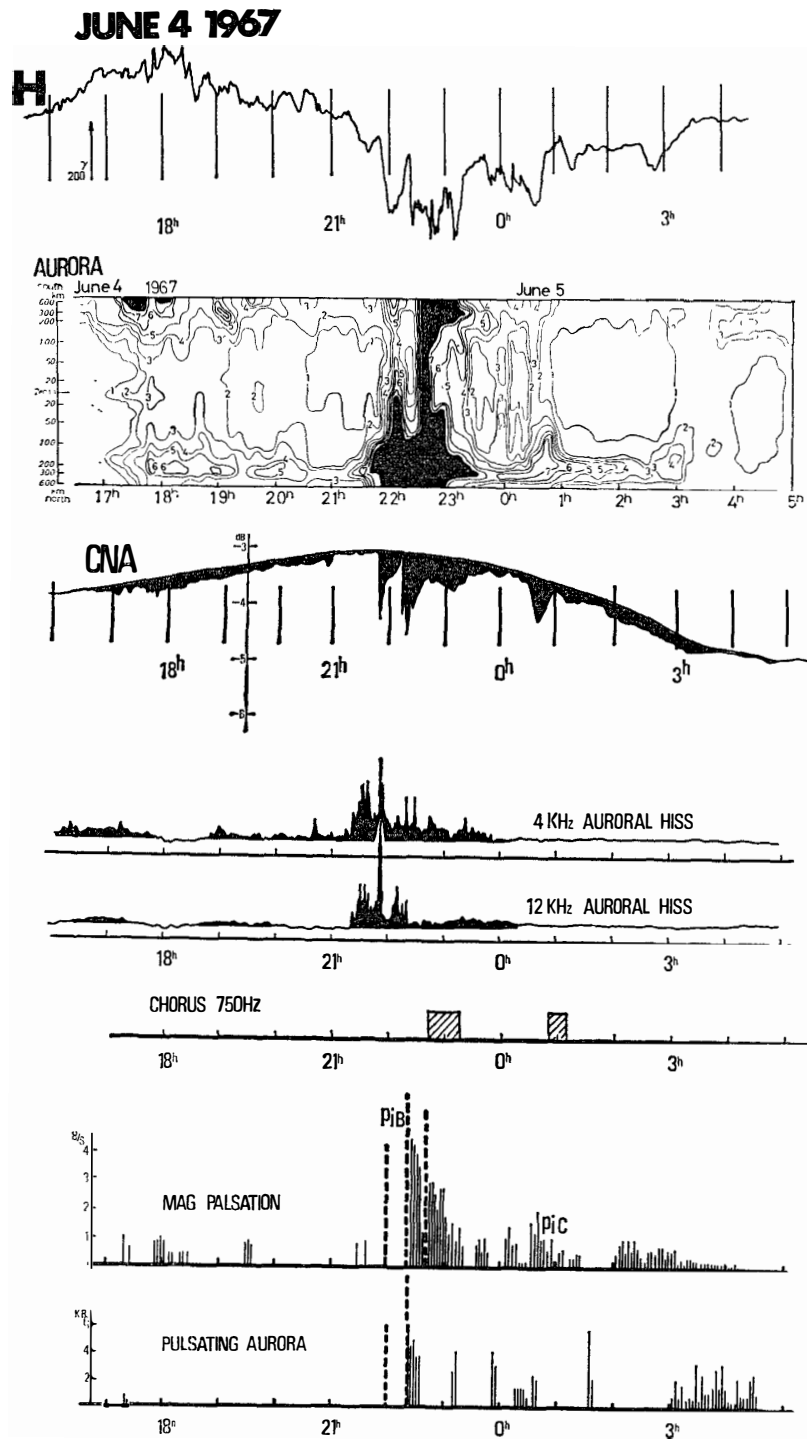


Fig. A-V. The same as that for Fig. A-I.

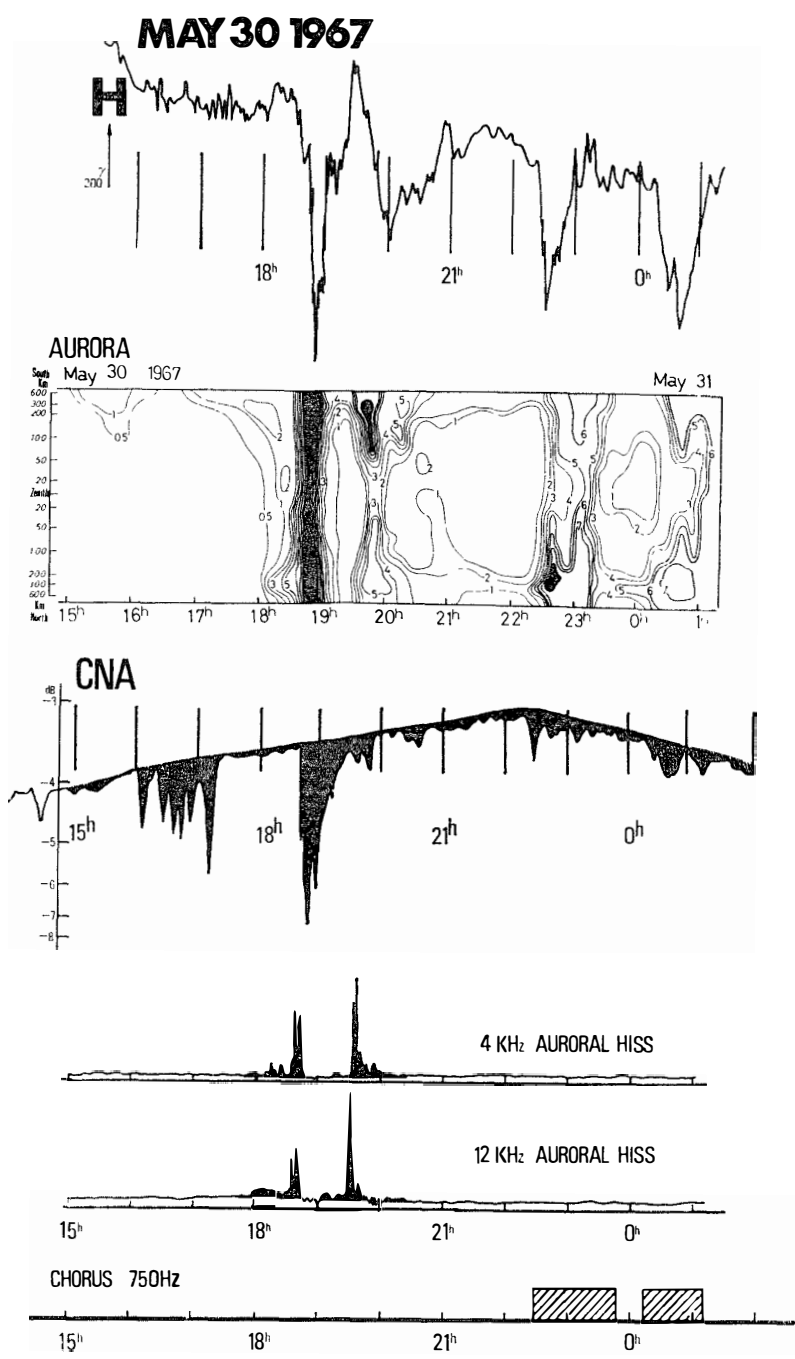


Fig. A-VI. The same as that for Fig. A-I.